ADDITIVE MANUFACTURING PROCESS PARAMETER EFFECTS ON THE MECHANICAL PROPERTIES OF FUSED FILAMENT FABRICATION NYLON

THESIS

Eric S. Holm, Captain, USAF

AFIT-ENV-MS-16-M-159

DEPARTMENT OF THE AIR FORCE
AIR UNIVERSITY

AIR FORCE INSTITUTE OF TECHNOLOGY

Wright-Patterson Air Force Base, Ohio

The views expressed in this thesis are those of the author and do not reflect the official policy or position of the United States Air Force, Department of Defense, or the United States Government

ADDITIVE MANUFACTURING PROCESS PARAMETER EFFECTS ON THE MECHANICAL PROPERTIES OF FUSED FILAMENT FABRICATION NYLON

THESIS

Presented to the Faculty

Department of Systems Engineering and Management

Graduate School of Engineering and Management

Air Force Institute of Technology

Air University

Air Education and Training Command

In Partial Fulfillment of the Requirements for the

Degree of Master of Science in Engineering Management

Eric S. Holm, BS

Captain, USAF

March 2016

AFIT-ENV-MS-16-M-159

ADDITIVE MANUFACTURING PROCESS PARAMETER EFFECTS ON THE MECHANICAL PROPERTIES OF FUSED FILAMENT FABRICATION NYLON

Eric S. Holm, BS

Captain, USAF

Committee Membership:

Maj Vhance V. Valencia, PhD
Chair

Lt Col Chad E. Ryther, PhD
Member

Maj Jason K. Freels, PhD
Member

Craig A. Przybyla, PhD
Member

Abstract

There is much yet to learn regarding how additive manufacturing process parameters affect the mechanical properties of additive manufactured parts. The ability to predict the expected mechanical properties of an additive manufactured part with a high degree of confidence will encourage the use of these materials in more high-performance applications. The purpose of this research was to determine how varying Fused Filament Fabrication (FFF) process parameters affect the mechanical properties of PA6 nylon dog-bone specimens produced on the Mark One 3D Printer. A design of experiment (DOE) was conducted using the factors of layer height and raster angle orientation. The mechanical properties measured in the experiment were tensile modulus, yield stress, percent strain at yield, ultimate tensile strength and percent strain at break. An analysis of variance (ANOVA) was performed to identify which factors were statistically significant in influencing mechanical properties. Results of the ANOVA showed that layer height was significant in influencing tensile modulus, ultimate tensile strength and percent strain at break; raster angle orientation was significant in influencing tensile modulus, yield stress, percent strain at yield, and percent strain at break. Both tensile modulus and ultimate tensile strength increased with decreasing layer height. The optimal condition that maximizes stiffness and strength is a layer height of 0.1 mm and a (±45) raster angle orientation.

Acknowledgments

First, I would like to express my sincere appreciation to my thesis advisor, Major Vhance Valencia, for his unwavering support and encouragement during my thesis. I am thankful for Lieutenant Colonel Chad Ryther from the Materials and Manufacturing Directorate, Air Force Research Lab, for sponsoring my research, being a member of my committee and for the time spent teaching me about material science and composites. I would like to thank my committee members, Major Jason Freels and Dr. Craig Przybyla, for guiding my research and always being available to answer any questions regarding my research. I am thankful for Mr. Andrew Abbot who gave me a head start on using the Mark One 3D printer by teaching me what he had learned about the printer during his own research. I would like to extend my appreciation to Dr. Daniel Felker who helped me produce the scanning electron microscope photographs of the carbon fiber reinforced composites for this thesis. I would like to thank Lieutenant Torin Quick who coordinated my use of the testing machines and Mr. Ronald Trejo who assisted me during the tensile testing. I would like to thank Captain Brad Shields who drew for me a SolidWorks shape file for the nylon dogbone tensile specimens. I am also grateful for the support and encouragement I received from my fellow students in my advising group.

Eric S. Holm

Table of Contents

Page

List of Figures

Page

List of Tables

Page

ADDITIVE MANUFACTURING PROCESS PARAMETER EFFECTS ON THE MECHANICAL PROPERTIES OF FUSED FILAMENT FABRICATION NYLON

I. Introduction

Topic Overview

Humans are gifted with the ability to create. Before the Industrial Revolution, nearly all manufactured goods were made by hand. A craftsman could create an object to fit their own unique requirements or could custom make a product to satisfy their client's unique wishes. Craftsmen used a combination of technical skill and creative artistry to create hand-crafted objects that took hours to complete.

The Industrial Revolution moved manufacturing from the craftsman's workshop to the factory. Factories produced goods using assembly lines made up of many workers. Each worker along the line was responsible for a single task in making a finished product. This method of dividing individual steps to produce a finished product among assembly line workers is known as mass production. With mass production, goods could be made both in large quantities and inexpensively. However, mass production was usually at the expense of one-of-a-kind goods customized to a user's unique needs.

In traditional manufacturing, craftsman machine or cast materials to achieve the desired shape. Machining is a form of "subtractive" manufacturing. A block of material is formed into the desired shape by cutting or grinding away unwanted material. Material

that is removed is discarded as waste. Traditional manufacturing also includes standardized assembly line processes that makes one-time changes to the object being made more difficult.

An alternative manufacturing method that allows one-of-a-kind objects to be made more efficiently compared to traditional manufacturing methods is called additive manufacturing. This process uses a machine to add materials selectively together to create an object, which is modeled from a three-dimensional computer-aided design (CAD) drawing. Unlike traditional manufacturing, additive manufacturing allows for the creation of new shapes with complex geometries (Lipson and Kurman, 2013). Shapes can be easily customized by editing or drawing a new CAD drawing. Additive manufacturing is also synonymously referred to as "3D printing," and a machine used in the additive manufacturing process is called a 3D printer. Before the 3D printer can make the object, the CAD software must first convert the digital model to a stereolithography (STL) file format (Grimm, 2004). In additive manufacturing, STL is the industry standard file format for three-dimensional model data, which is used by additive manufacturing machines (ASTM Standard F2792, 2012).

Two classes of additive manufacturing technology are selective deposition printers and selective binding printers (Lipson and Kurman, 2013). Selective deposition printers selectively deposit raw materials into layers. The machine extrudes material through a nozzle and deposits it on a build plate or previous build layer. The material is sequentially applied in layers until the desired object is formed. In selective binding printers, heat or light solidifies a powder or light sensitive photopolymer. After a layer

has been cured by heat or light, the machine adds another layer of powder or photopolymer. Next, the machine selectively cures the portion of the layer that will become a solid object. This process is repeated until a complete object is formed. Post processing removes excess powder or photopolymer liquid from the object.

A common subset of selective deposition printing is fused deposition modeling (FDM). In FDM, a thermoplastic filament is pushed through a computer-controlled extrusion head and deposited on a build plate as a series of layers to form a three-dimensional object. FDM is a trademark of Stratasys, a 3D printing company, which invented the process (Barnatt, 2013). Other terms used to describe FDM include plastic jet printing (PJP), fused filament modeling (FFM), and fused filament fabrication (FFF). FFF was conceived by the RepRap project to avoid legal constraints with using FDM. The RepRap project is an open source additive manufacturing consortium that shares freely available 3D printer designs. The term used in this thesis will be FFF.

In FFF, the extrusion nozzle moves in a plane, parallel with the build surface or build plate. The literature refers to this plane as the x-y plane (Ahn, Montero, Odell, Roundy, and Wright, 2002). The heated extrusion head melts the thermoplastic filament before it passes through the extrusion nozzle. Next, the 3D printer deposits the viscous thermoplastic onto the build surface as a series of rows. These rows are called rasters or roads. After the 3D printer deposits a layer of material on the build plate, the build plate lowers, and the machine deposits another layer of thermoplastic. This process repeats itself until the desired shape is complete (Gibson, Rosen, and Stucker, 2010). Figure 1 shows a schematic of the FFF process.

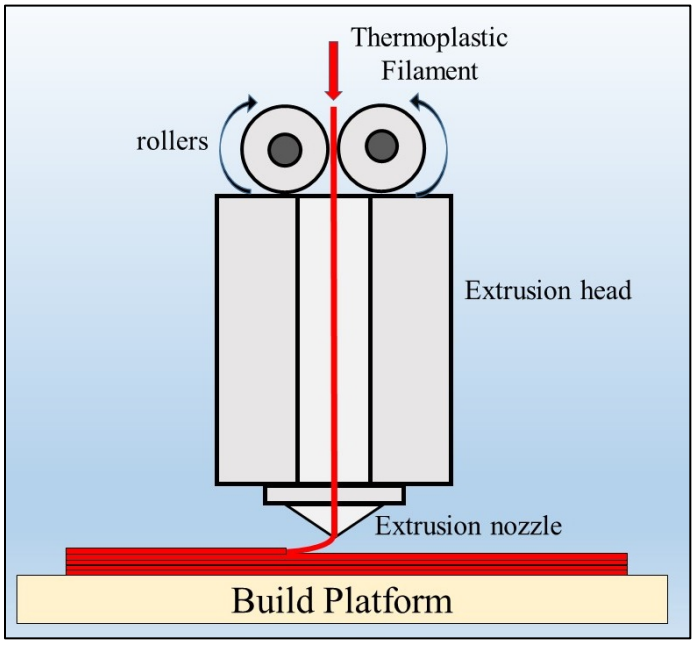

Figure 1. Schematic of the FFF Process (drawn by author), (Ziemian, Sharma, and Ziemian, 2012)

FFF machines may also include an additional extrusion nozzle for support material. The machine will deposit support material underneath objects that have overhangs or bridges. After the machine finishes printing the object, mechanical or chemical methods are used to remove the support material (Ahn, Montero, Odell, Roundy, and Wright, 2002).

A strength of additive manufacturing (AM) or 3D printing, is the ability to produce unique objects from imagination to reality quickly. An application of quickly creating unique objects is rapid prototyping. Rapid prototyping is the process of creating prototypes through additive manufacturing. Before an object, part, or tool can be manufactured for functional use it must be tested to ensure that the object will work for its intended purpose. Prototypes are created to test the object before full-scale

manufacturing. Creating prototypes with traditional manufacturing methods requires many hours of skilled labor. With additive manufacturing, prototypes can be designed and tested within hours.

Military Applications for Additive Manufacturing

Additive manufacturing could revolutionize the military supply chain. A 3D printer can print needed components or tools in austere areas that are either far removed from supply lines or on the frontlines of the battlefield. Designs can be made anywhere in the world and sent electronically to a strategically placed 3D printing center on the battlefield.

In an austere fiscal environment, the military will continue to maintain legacy systems for lifespans longer than expected. Maintaining a supply inventory of spare parts for multiple weapon systems is a challenge for the United States military (Brown, Davis, Dobson, and Mallicoat, 2014). As legacy weapon systems continue to age, repair parts needed to maintain the systems become increasingly difficult to obtain. Additive manufacturing can create replacement parts for legacy systems that may not have the availability of repair parts compared to newer systems. Instead of going through a lengthy acquisition process to acquire a critical replacement part that has since gone out of production, additive manufacturing can print parts on-demand (Brown, Davis, Dobson, and Mallicoat, 2014). On-demand production could eliminate the need for maintaining costly supply warehouses.

The Navy has introduced 3D printers on some ships in a program called "Print the Fleet" (Tadjdeh, 2014). The program seeks to introduce sailors to additive manufacturing and investigate the applicability of additive manufacturing for the Navy. The Navy is currently using additive manufacturing for tooling, modeling, and prototyping. Jim Lambeth, Vice Admiral and Phil Cullom, Deputy Chief of Naval Operations for fleet readiness and logistics believe "that 3D printing and advance manufacturing are breakthrough technologies for our maintenance and logistics functions in the future" (Tadjdeh, 2014). Cullom emphasized some of the advantages of additive manufacturing for the Navy are rapid repairs, print tools, reduction in inventory spares, and the immediate availability of parts.

The Rapid Equipping Force is an Army organization which quickly provides deployed Army units with advanced government and commercially available solutions that meet urgent requirements. The Rapid Equipping Force has deployed the Expeditionary Lab Mobile, or ELM for short (Parsons, 2013). The outside of the ELM resembles a metal shipping container. Inside, the ELM contains 3D printers, computers, and milling machines. Two engineers are needed to operate one ELM. The engineers use the ELM 3D printers and milling machines to create parts from plastic, steel, or aluminum. Satellite communications allow the ELM engineers to communicate with colleagues anywhere in the world. Westley Brin, a member of the Army's Rapid Engineering Force, states "the technology has allowed troops to modify systems with proprietary designs to better fit their needs or make them more efficient in the field" (Parsons, 2013). One result of the ELM was the modification of a flashlight used by

soldiers in Afghanistan that would accidently turn on, which could give away the patrol's position at night. ELM additive manufactured a part, which prevented the flashlight from turning on by accident. Using the traditional defense acquisition process to field a new flashlight would have taken months, if not years. Additive manufacturing allows a solution to be tested and fielded quickly on the battlefield (Parsons, 2013).

Limitations of Current FFF Materials

Thermoplastics are the most widely used feedstock material in the FFF processes. The most common thermoplastic feedstock material includes acrylonitrile butadiene styrene (ABS), polycarbonate (PC), polylactide (PLA) and polyamide (PA). The mechanical properties of thermoplastics limit their use in more high-performance applications such as aerospace, automotive industry, and infrastructure replacement parts. Thermoplastics are low in strength compared to metals. The maximum tensile strength for polymers is about 100 MPa (15,000 psi), whereas some metal alloys have tensile strengths of 4,100 MPa (600,000 psi) (Callister and Rethwisch, 2012). Because of the strength limitations of FFF, a need exists to improve the strength of FFF made thermoplastic parts.

Incorporating carbon fibers into the plastic creates a composite material called carbon fiber reinforced plastic. The method increases the strength of FFF materials (Love, Kunc, Elliot, and Blue, 2014). A composite is made up of two or more materials which exhibits a better combination of material properties then the materials which make up the composite (Daniel and Ishai, 2003). Table 1 shows the tensile yield strength of

ABS plastic, nylon-12, carbon fiber reinforced polymer and carbon fiber. Table 1 does not consider materials made by additive manufacturing. Even though carbon fibers have a high tensile strength, they are weak in shear and exhibit brittle behavior. Combining carbon fibers with a plastic allows for a more durable material.

Table 1. Tensile Yield Strength for Various Materials (MatWeb, LLC, 2015), (Daniel and Ishai, 2003), (Callister and Rethwisch, 2012)

Material	**Tensile Strength, Yield (Mpa)**	**Tensile Strength, Yield (psi)**
ABS	42.5 - 44.8	6,160 - 6,500
Nylon-12	9.50 - 170	1,380 - 24,600
Carbon/Epoxy (AS4/3501-6)	2,280	330,000
Carbon Fiber (AS4)	3,700	535,000

New materials require thorough analysis to gain greater understanding of the material's behavior and mechanical properties. With this understanding, engineers can predict how the material will perform under certain environments and life-cycle loads. The ability to know the expected material properties of a part produced through FFF with a high degree of confidence, will encourage the use of these materials in more high-performance applications.

Additive Manufacturing Process Parameters

Additive manufacturing gives new ways to influence and change the processing and structure of materials to create materials with desired properties. The processes used

during the manufacturing phase of materials play a role in influencing the properties of materials. The most important property for high-performance applications is material strength. There is much yet to learn regarding how additive manufacturing process parameters affect the mechanical properties of additive manufactured parts (Lanzotti, Grasso, Stainano, and Martorelli, 2015).

Research Purpose

The purpose of this research is to determine how varying FFF process parameters affect the mechanical properties of PA6 nylon and carbon fiber reinforced PA6 nylon composite specimens produced by the Mark One 3D Printer. This research is a stepping-stone for further research to develop AM composite technology and encourage the use of FFF parts in high-performance applications. The long term goal is the ability to produce aerospace parts through AM that meet the same service specifications as traditionally manufactured aerospace parts. This research will attempt to answer the following questions:

- What are the range and confidence intervals for material properties of FFF parts made with varying process parameters?
- Can certain FFF process factors be used to optimize the mechanical properties of FFF parts?
- How do nylon parts produced by FFF compare with compression molded nylon parts?
- What are the mechanical properties of carbon fiber reinforced thermoplastic composites made by FFF?

Document Overview

This study is organized into five chapters. Following this introduction, Chapter II will further explain several technical concepts in this report: stress, stress, polymers, plastics, carbon fibers, composites and carbon-fiber reinforced polymer composites. Chapter II also contains a literature review of relevant articles related to AM and FFF, as well as a survey of mechanical characterization studies on materials made through FFF. Chapter II will also include a review of research that investigates the incorporation of carbon fibers into FFF plastic materials.

Chapter III explains the methodology used in this research. A Design of Experiment (DOE) was conducted using the Taguchi method to determine how changing FFF process parameters affect the mechanical properties of PA6 nylon and determine what process parameters are significant in influencing mechanical properties. Sample carbon-fiber reinforced polymer composites were made using the Mark One. The samples were tensile tested to record the tensile strength and Young's modulus.

Chapter IV will present the results of the DOE. Mechanical properties for PA6 nylon and carbon-fiber reinforced composites produced by the Mark One with varied process parameters will be compared. Results from an analysis of variance (ANOVA) is explained to show which FFF process parameters are significant in affecting the mechanical properties of FFF produced specimens.

Chapter V summarizes the research results and discusses the implications for the material science community. Chapter V will also present recommendations for future

research and discuss lessons learned during the course of this research, which will help future materials scientists and engineers.

II. Literature Review

Chapter Overview

This chapter will review research on significant process parameters affecting FFF material properties. A summary of significant process parameters for polymer materials was reviewed. As FFF techniques become more sophisticated researchers are beginning to experiment with short-fiber carbon reinforcement. However, at the time of this writing, only one study was found on material properties of continuous carbon fiber reinforced polymer composites made through FFF (Namiki, Ueda, Todoroki, Hirano, and Matsuzaki, 2014).

Material science and engineering can be broken down into two sub-disciplines: *materials science* and *materials engineering*. Material scientists work to understand how the structure of a material affects the physical properties of the material; while a materials engineer designs the material structure to achieve desired material properties. Materials science and materials engineering can be described by four components: processing, structure, properties and performance.

The structure of a material relates to how the internal material components are arranged. The smallest structural level is the atomic level, which encompasses the organization of atoms or molecules relative to one another. The next larger structural level is the microscopic level. The microscopic level is everything that can be seen by a microscopic. The structure that can be observed by the naked eye is called the macroscopic level (Callister and Rethwisch, 2012).

The properties of solid materials can be grouped into six different categories: mechanical, electrical, thermal, magnetic, optical, and deteriorative. Each property includes stimuli that create a certain response. The focus for this research is the mechanical properties of FFF made materials. Mechanical properties describe how a material behaves under an applied load. Examples of mechanical properties include elastic modulus, yield strength, and ultimate strength.

Stress-Strain Behavior of Thermoplastics

The way a material responds to the forces exerted on it are of interest to engineers. Understanding how a material behaves under different kinds of forces helps engineers design materials that are strong. When a material is stretched or pulled, forces are being exerted on it. Forces are also exerted when a material is compressed. An example of compressive forces acting on a material would be if a hand were used to compress a ball of clay into a thin sheet of clay. The hand exerts compressive forces on the ball of clay. The amount of force which acts over a given area is called stress. Stress is equal to the force applied on an object divided by the area over which the force acts, which is defined by the following equation:

$$\sigma = \frac{F}{A} \tag{1}$$

Where

F = applied force (lb-force)

A = area over which the force is applied (in^2)

Stress may deform or change the shape of the area that the force was acting on. Because of this, engineers use *engineering stress* to provide consistency when comparing stress measurements. Engineering stress is calculated by using the original area for which the force is acting.

The amount a material stretches or compresses due to a given stress is called strain. Engineering strain, ε, is defined as:

$$\varepsilon = (\Delta L)/L = (L - L_0)/L_0 \quad (2)$$

Where

$L - L_0$ = *Change in length*

L_0 = *Original length*

How much a material strains depends on the magnitude of stress that is applied. For most materials that are stressed at low levels, stress and strain are proportional to each other through the relationship:

$$\sigma = E\varepsilon \quad (3)$$

This is known as Hooke's law, and the constant of proportionality E (GPa or psi) is the modulus of elasticity, or Young's modulus (Callister and Rethwisch, 2012). Modulus is also related to the stiffness of a material. Stiffness increases with increasing Young's modulus. Stiffness is the ability of a material to withstand deflection from an applied stress (Callister and Rethwisch, 2012). When stress and strain are plotted on a graph, Young's modulus is the slope of the linear portion of the stress-strain curve. Figure 2 illustrates the linear portion of a stress-strain curve. A steep linear portion of the stress-strain curve indicates a stiff material.

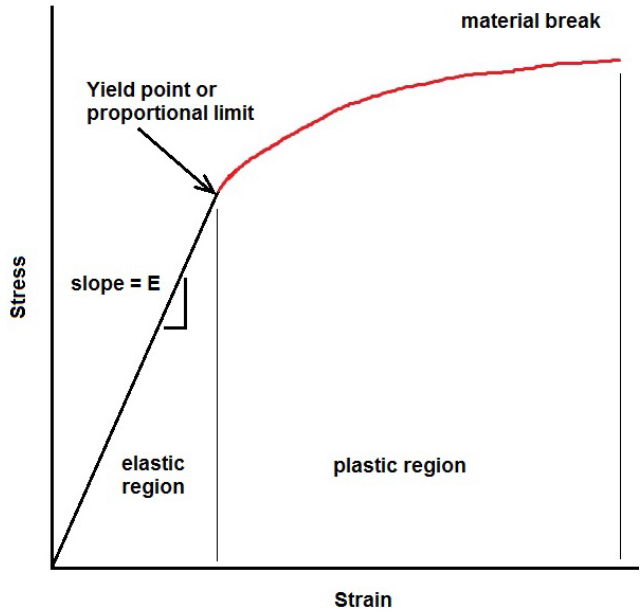

Figure 2. Stress-Strain Curve Illustrating the Elastic and Plastic Regions (drawn by author)

Thermoplastics are viscoelastic materials. This means thermoplastics respond to stress in two ways: elastic deformation and viscous flow. Elastic deformation stores mechanical energy as recoverable material deformation. Elastic deformation can be compared to pulling a spring; when the pulling force on the spring is released the spring returns to its original length. Viscous flow is the realignment of molecules due to the applied load and results in permanent deformation. This can be compared with a spring that is stretched so much that it does not return to its original length when the stretching force is stopped. During viscous flow mechanical energy is converted to frictional heat by molecules realigning themselves within the material (Rubin, 1990).

Studying the stress-strain curve for a material helps to better understand the mechanical behavior of the material. For most materials under low strains the curve is a

straight line. The linear portion of the stress-strain curve is the elastic region. In the elastic region stress is proportional to strain and only elastic deformation occurs. Some materials may exhibit non-linear elastic behavior. As shown in Figure 2, when the stress and strain increase to a certain point, the shape of the curve becomes nonlinear. The point on the curve that transitions between linear and non-linear behavior is the yield point or proportional limit (SPI, 1991). The corresponding stress at the yield point is called the yield stress or yield strength (Callister and Rethwisch, 2012).

A study of stress-strain curves for thermoplastics has shown that there is no linear elastic region, but rather a deviation from linearity that increases from the origin. The deviation is small below 0.5% strain, and most published figures of the elastic modulus, E, are the slope of a line tangent to the low-strain portion of the stress-strain curve (SPI, 1991). For this research the elastic modulus is defined as the secant modulus at 0.5% strain.

Thermoplastics have no definite proportional limit, which makes it difficult to accurately define the yield point exactly (SPI, 1991). A convention has been established where a straight line is drawn parallel to the linear or near linear portion of the stress-strain curve at some specified strain offset. This strain offset is usually set as 0.2%. The stress corresponding to the intersection of this line and the stress-strain curve is defined as the yield stress (Callister and Rethwisch, 2012). For this research a 0.2% strain offset was used to measure the yield stress. The 0.2% strain offset line is shown in Figure 3.

The stress-strain behavior for thermoplastics is influenced by the rate of deformation, the temperature, and the environment. The rate at which a material is

deformed is called the strain rate. With increasing strain rate thermoplastics behave more rigid and have higher elastic moduli. With decreasing strain rate thermoplastics behave more ductile (Callister and Rethwisch, 2012). Temperature also greatly affects the mechanical properties of thermoplastics. With increasing temperatures, thermoplastics show a decrease in elastic modulus, reduction in tensile strength and greater ductility. Under cold temperatures near freezing thermoplastics may show brittle characteristics. A brittle material allows for little deformation before breaking.

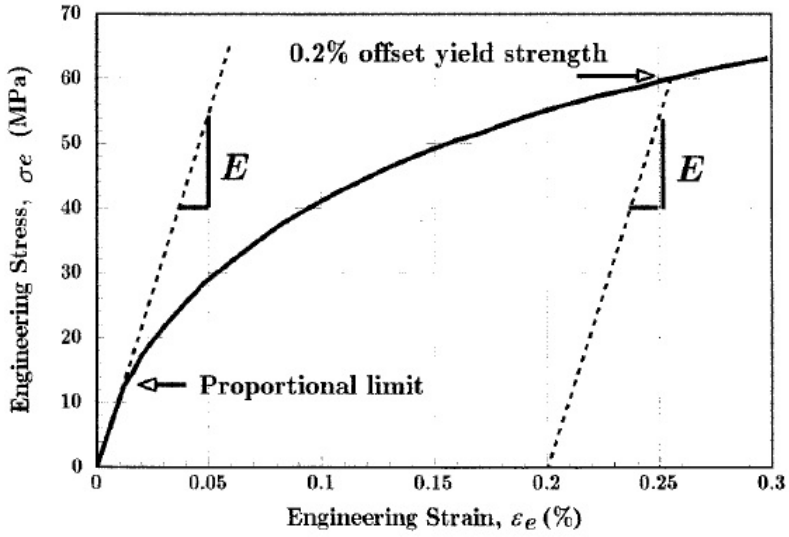

Figure 3. Stress-Strain Curve for Annealed Polycrystalline Copper Illustrating the 0.2% Strain Offset Method for Determining the Yield Stress (Roylance, 2001)

Process Effects on Materials

Two other areas of interest to materials scientists and materials engineers is process and performance. Nearly all modern materials are processed in some way. The

method of processing influences the structure of the material, which in turns affects the material's properties. A material's performance is a function of its material properties. Finding new ways to process materials can lead to new ways to design materials with desired properties. Additive manufacturing gives us new ways to process materials to selectively design the materials structure to achieve desired properties. Improved properties can lead to high performance materials.

The additive manufacturing process has many process parameters that can be used to influence the material structure. A process parameter is a variable in a process that can be altered or changed in order to influence the outcome of the process. For the FFF process that outcome is the material itself. Figure 4 visually depicts several additive manufacturing process parameters. The properties of the FFF material will determine the type of applications the material can be used for. Below is a list of process parameters specific to FFF:

- Layer height
- Raster fill
- Print orientation
- Temperature of the extrusion head
- Environmental factors: temperature, humidity, etc.
- FFF Material selection
- Gap spacing between rasters
- Part spacing

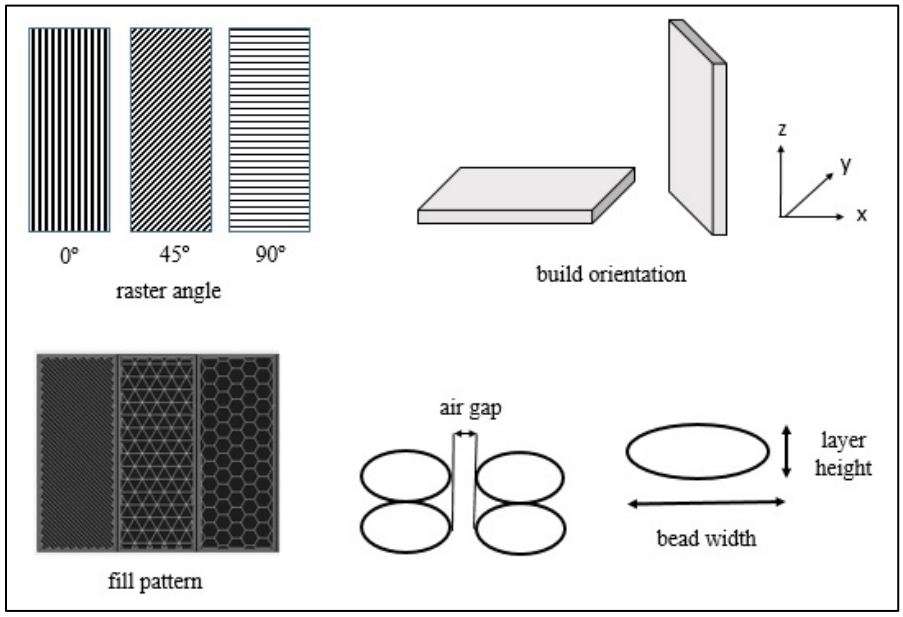

Figure 4. Graphical Representation of Several Additive Manufacturing Process Parameters (drawn by author), (Forster, 2015)

FFF technology allows both the choice of material and its specific location to be chosen in a three dimensional space. An object made by FFF can be made up of more than one type of material. A composite material is made up of two or more materials and exhibits a combination of properties from its constituent materials. Creating composites through FFF can be a way to improve the material properties of FFF parts. Research on carbon fiber reinforced thermoplastics made by FFF is discussed later in this chapter.

Optimizing process parameters is a method to improve the mechanical properties of FFF materials. An understanding of the relationship between process parameters and a desired process output is necessary before optimizing the system. The systematic method to determine the relationship between factors affecting a process and the output of that process is called design of experiments. Design of experiments is a way to understand which process parameters are significant in influencing a desired property of the material

and how varying the parameter changes the desired property. Many researchers have used design of experiments to get a greater understanding on how FFF process parameters influence material properties.

Air gap is a process parameter found to be significant in influencing mechanical properties of FFF materials. Air gap is the amount of space between deposited rasters or roads. A zero air gap means the roads are touching. A negative air gap means the roads overlap each other. A positive air gap means a space exists between roads. Ahn and others (2002) found that decreasing air gap results in greater ABS tensile strength. Air gap has also been found to be significant in influencing the compressive strength of porous FFF structures (Ang, Leong, and Chua, 2006). A decrease in air gap also increases the build time for a part by increasing the number of roads required to be deposited to complete a layer.

Researchers have also found raster angle orientation to influence the strength of a part. Raster angle is defined as the angle between the raster and the axis of the test specimen. A raster angle of 0° means the roads are aligned with the axis of the test specimen. Loads are applied along the axis of the test specimen. Greater tensile strength was found in ABS when the raster angle was aligned with the tensile load (Durgun and Ertan, 2014). This was also observed by both Ahn and others (2002) and Martínez and others (2012).

Unlike the previous studies that looked at raster angle orientation being the same for each layer Tymrak, Kreiger and Pearce (2014) looked at alternating raster angles between layers. The raster angle parameter had two levels: (0/90) and (±45). The

researchers also looked at layer height using three levels: 0.4mm, 0.3mm, and 0.2mm; and material type with two levels: ABS, and PLA. The average tensile strength, strain at tensile strength and elastic modulus for RepRap printed specimens is shown in Table 2. The 0.2 mm layer height had higher tensile strength on average for both ABS and PLA specimens. This possibly shows that tensile strength increases with decreasing layer height. There was not a large difference in tensile strength or elastic modulus between the raster angle orientations (0/90) and (±45). Unfortunately, the study did not investigate to see if layer height or alternating raster angle orientation were statistically significant in influencing the mechanical properties of the printed specimens.

Table 2. Average Tensile Strength, Strain at Tensile Strength and Elastic Modulus for RepRap Printed Specimens (Tymrak, Kreiger, and Pearce, 2014)

	Specimens Tested	Specimens considered	Average tensile strength (Mpa)	Average strain at tensile strength (mm/mm)	Average elastic modulus (Mpa)
ABS					
0.4 mm Layer height	30	24	28.2	0.0197	1875
0.3 mm Layer height	40	39	27.6	0.0231	1736
0.2 mm Layer height	40	35	29.7	0.0201	1839
0/90 orientation	60	52	27.7	0.0192	1867
±45 orientation	50	46	29.5	0.0233	1739
Total	110	98	28.5	0.0212	1807
PLA					
0.4 mm Layer height	30	17	54.9	0.0194	3286
0.3 mm Layer height	40	31	48.5	0.0171	3340
0.2 mm Layer height	20	18	60.4	0.0196	3480
0/90 orientation	50	27	54.9	0.0188	3336
±45 orientation	40	39	52.3	0.0181	3384
Total	90	66	56.6	0.0193	3368

Print orientation is also a significant factor in determining part strength. Print orientation refers to how an object being printed is oriented with regards to the build

space. Explained further, the plane that is parallel with the build surface is usually referred to as the x-y plane, while the z-axis is perpendicular to the x-y plane. FFF layers are oriented in the x-y plane. Parts built in the z-axis exhibit lower tensile strength versus parts built in the x-y plane. The reason is that the bond between layers are weak and defects are usually present between the layers. A part will exhibit weakness for forces orthogonal to the build layers (Bertoldi, Yardimci, Pistor, Guceri, and Sala, 1998). Hoekstra and others (2001) found that an increase in the number of roads aligned with the tensile force resulted in higher tensile strength. Parts printed with an x-y plane orientation had the greatest number of roads aligned with the tensile force (Hoekstra, Kraft, and Newcomer, 2001).

A review of the literature reveals that FFF materials are highly anisotropic (Ahn, Montero, Odell, Roundy, and Wright, 2002), (Ziemian, Sharma, and Ziemian, 2012). An anisotropic material means that the properties of the material are directionally dependent, as opposed to isotopic, which means the material has the same properties in all directions. This is the result of materials being deposited by rows and layers.

Mechanical Properties of FFF Plastics Reinforced with Short Carbon Fiber

Only within the last few years has there been research investigating the material properties of FFF fabricated parts with short carbon fiber reinforcement. Ning, Cong, Qiu and Wang (2015) investigated how adding short carbon fibers to ABS plastic can improve the mechanical properties of FFF parts. ASTM D638-10 and ASTM D790-10 standards were followed for tensile test and flexural test, respectively. Carbon fiber

powders were blended with ABS thermoplastic pellets. A plastic extruder was used to blend the short carbon fibers and ABS pellets together to create carbon fiber filled filaments. Parameters included: carbon fiber content, carbon fiber length and porosity of fabricated parts. The results of the study showed that adding carbon fiber reinforcement into plastic materials can increase ultimate tensile strength and Young's modulus, but may decrease toughness, yield strength and ductility. The largest average ultimate tensile strength (42 MPa) occurred with five percent carbon fiber (by weight) content. The lowest average tensile strength (34 MPa) occurred when the carbon fiber content was 10 weight percent. The largest mean Young's modulus (2.5 GPa) occurred at 7.5 weight percent carbon fiber content, while the smallest mean value (1.9 GPa) occurred in a pure plastic specimen.

A similar study by Love, Kunc, Elliot and Blue (2014) investigated the material properties of short carbon fiber reinforced ABS polymers. The researchers measured the tensile yield strength and stiffness from samples made from several different desktop 3D printer platforms. ASTM D638-03: Standard Test Method for Tensile Properties of Plastics was the test method used. Five sets of ASTM D638 Type V specimens populated on the corners and the center of the build platform were made at a time. Specimen sets were made in both in-plane and vertical (z-axis) direction. The desktop platforms utilized acrylonitrile butadiene styrene (ABS). The carbon fiber reinforced ABS samples were prepared by combining ABS pellets (GPS35-ABS-NT from M Holland Co, Il) with Chopped Hexcel AS4 CFs (epoxy sizing, 3.2 mm long) in a Brabender high-shear mixer at a temperature of 220°C at 60 rpm until the torque

remained constant. The combined material was then extruded through a cylindrical die (1.75 mm diameter) at 220°C using a batch extrusion unit, composed of a steel barrel and a cylindrical rod. A cylindrical die is used in manufacturing to shape material into long strands of wire or filament. Five sets of the ABS and carbon fiber test specimens were manufactured on the Solidoodle S3, a type of 3D printer.

The results of the study by Love and others showed that the strength and stiffness of AM parts can be increased with the introduction of carbon fibers into the polymer matrix. ABS with 13% carbon fiber had an approximately 200% increase in strength and an approximately 400% increase in modulus of elasticity for in-plane samples compared to samples made without carbon fiber. Specimens that were made along the Z-axis showed a decrease in tensile strength. The author speculates that the decrease was because the ABS filament did not conform to the underlying substrate as it was deposited, reducing the contact area between layers.

Tekinalp and others (2014) investigated how changing the percent weight of short carbon fibers in ABS filaments affected material strength. The researchers created short carbon fiber reinforced ABS filaments similar to Ning and others (2014) and Love and others (2014) ABS filaments with mixtures of 10, 20, 30, and 40 weight percent carbon fiber were used. Five ASTM D638 standard type-V dog-bone samples of each carbon fiber weight percentage were tensile tested. Results showed that tensile strength increased to 52.9 kN m/kg), which is higher than Aluminum 6061-0 (45.9 kN m/kg). Tensile strengths increased linearly with increasing carbon fiber content.

Mechanical Properties of FFF Plastics Reinforced with Continuous Carbon Fiber

Only one article could be found that investigated the material properties of FFF fabricated parts with continuous carbon fiber reinforcement. Namiki, Ueda, Todoroki, Hirano and Matsuzaki (2014) measured the tensile strength and tensile modulus for poly-lactic acid (PLA) specimens reinforced with continuous carbon fibers. The carbon fiber reinforcement was a PAN based carbon fiber (T800S-10E, Toray). The researchers referred to these specimens as continuous carbon fiber reinforced thermoplastic (CFRTP). The researchers themselves modified a commercially available FFF printer to create the specimens. Figure 5 shows a schematic of the printer used by Namiki and others (2014). During the FFF process, melted PLA was impregnated with the carbon fiber inside the extrusion head and both the PLA and fiber were deposited on the print bed together. The carbon fiber was aligned in the longitudinal direction of the dog bone specimens. The carbon fiber fraction was 1.0%, which was determined by the supplied amount of carbon fiber and PLA. Figure 6 shows a picture of the tensile specimen that was used for the experiment with dimensions.

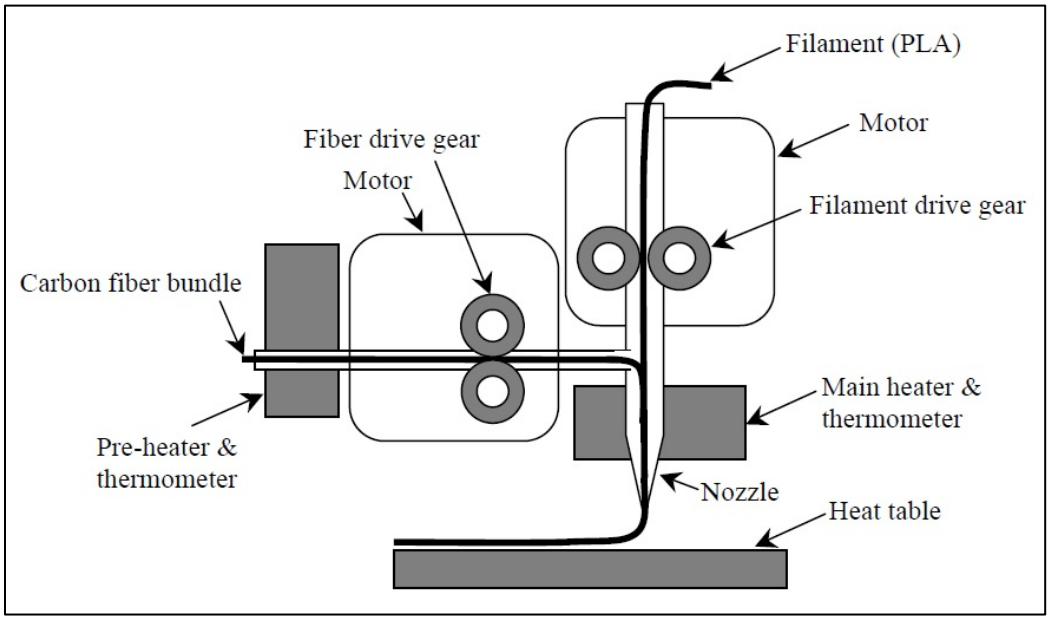

Figure 5. Schematic of Printer Head Used by Namiki and Others (2014)

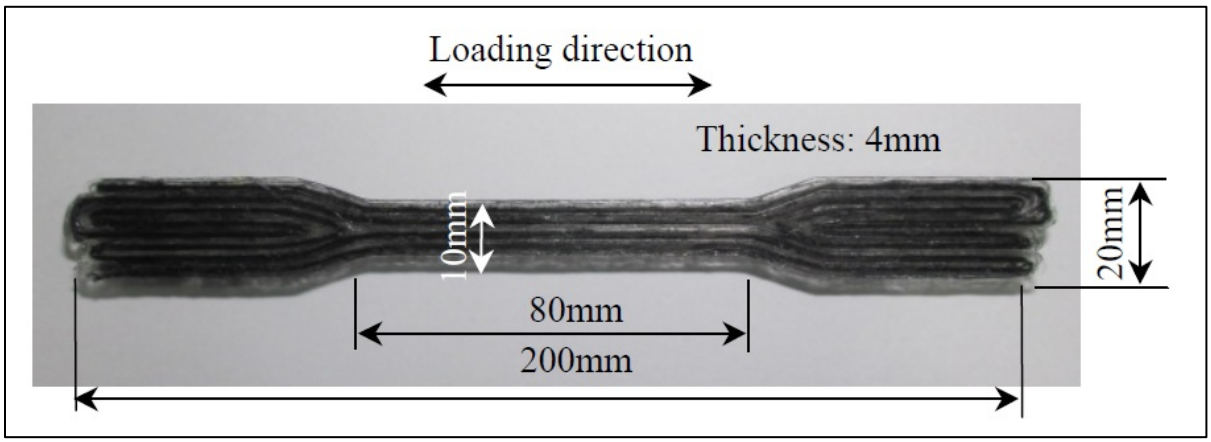

Figure 6. Carbon Fiber Reinforced Thermoplastic Specimen Dimensions (Namiki, Ueda, Todoroki, Hirano, and Matsuzaki, 2014)

Namiki and others (2014) conducted tensile tests of both PLA specimens reinforced with continuous carbon fiber. The average tensile strength of the carbon fiber reinforced PLA was 90.0 MPA while the tensile strength of the PLA without carbon fiber was 57.1 MPA. The researchers used the rule of mixture to predict both Young's

Modulus and tensile strength. The observed averages for Young's modulus and tensile strength were approximately 10% and 20% lower respectively than estimated measurements using the rule of mixture equation.

Mark One Printer

In 2014, MarkForged Inc. introduced the first commercially available 3D printer to create continuous carbon fiber reinforced polymer composites (Black, 2014). MarkForged Inc. is a company started by Greg Mark in early 2013 that makes 3D printers (Black, 2014). Mark explains the company's goal was to manufacture "end-use parts," but make them "a lot more efficiently" and "use the mechanics of a 3-D printer to automate carbon fiber composite layup" (Black, 2014).

During the time of this research, the matrix material for the Mark One 3D printer was a proprietary blend PA6 co-polymer nylon with three types of fiber reinforcement: Kevlar, carbon fiber, and fiberglass (T. Nutile, personal communication, February 8, 2016). The Mark One has two extrusion nozzles; one for the nylon filament, and the second for the continuous fiber towpreg. A carbon fiber towpreg is a bundle of carbon fibers coated with a thermoplastic resin to create a filament. When the carbon fiber towpreg passes through the heated extrusion nozzle the thermoplastic resin melts and the towpreg is deposited on a nylon layer. This is different compared to the modified machine used by Namiki and others (2014) which impregnated the nylon with a carbon fiber towpreg inside the extrusion head, as discussed earlier.

The Mark One's slicing software is called Eiger. The Eiger software allows several printing factors to be modified by the end user. The printing factors that can be modified are layer height, nylon fill pattern, nylon fill density, number of nylon layers, and fiber fill pattern. These factors are discussed below. First, the layer height for nylon can be adjusted between 0.1 mm and 0.2 mm in 0.01 mm increments. If a part is built with fiber, the layer height defaults to a value specific to the type of fiber used. The default layer height for fiber are as follows; carbon fiber, 0.125 mm; Kevlar, 0.1 mm and, fiberglass, 0.1 mm.

Second, three types of fill patterns can be selected for the nylon layers: hexagonal, triangular, and rectangular. Figure 7 depicts the three nylon fill patterns available. The

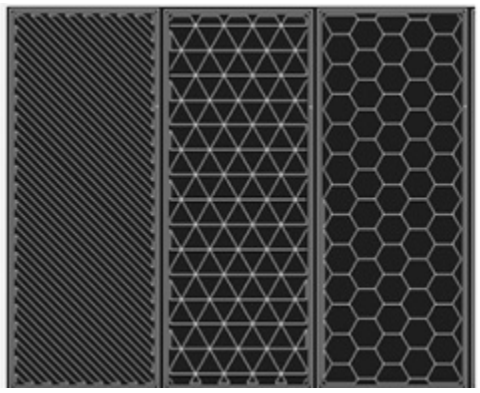

Figure 7. A Depiction of the Rectangular, Triangular, and Hexagonal Nylon Fill Patterns

fill pattern is the manner the nylon roads are deposited on each layer. The hexagonal and triangular fill patterns are laid down as geometric patterns that mimic their name. The rectangular fill pattern lays down nylon roads using a (±45) placement in relation to the print bed. To create a sample that has a (0/90) placement, the specimen can be orientated

to a 45-degree angle from either the x or y-axis of the print bed. In conjunction with the fill patterns, the fill density for each fill pattern can also be adjusted up to 100 percent. Each fill pattern may have minimum and maximum fill densities. The rectangular fill pattern allows for a 100 percent fill density. A 100 percent fill density creates a near completely solid plastic part.

Third, the number of layers around each part can also be specified. These parameters are called wall layers, and roof and floor layers. Wall layers are beads of nylon road that surrounds the perimeter of the part geometry for each layer of the part. The number of wall layers can be specified between one and four. Roof and floor layers are solid plastic layers at the top and bottom of the part. The number of roof and floor layers can be adjusted between one and ten.

Finally, the fiber fill pattern can be specified by layer. Figure 8 shows the three fiber fill patterns available. The angle of orientation for the isotropic fill can also be specified, which is shown as a 45-degree angle in Figure 8. Of note, carbon fiber is limited to the concentric circle fill pattern, while Kevlar and fiberglass do not have this limitation.

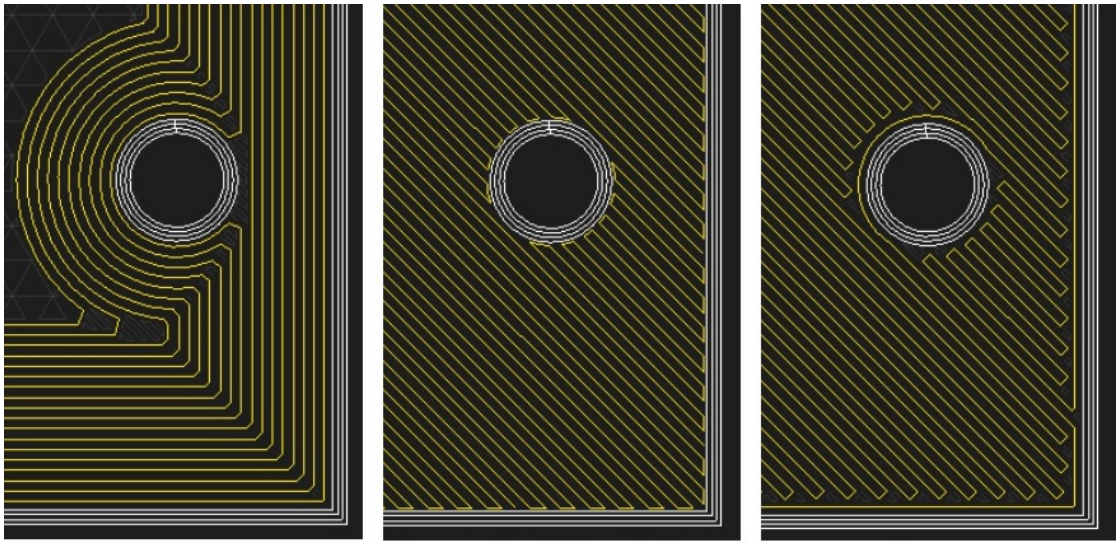

Figure 8. Screen Captures from Eiger Illustrating the Different Fiber Fill Patterns

III. Methodology

Chapter Overview

A Design of Experiment (DOE) was conducted using the Taguchi method to determine how process parameters affect the mechanical properties of PA6 nylon and carbon fiber reinforced PA6 nylon composite specimens produced on the Mark One. The Mark One was chosen because it is the only commercially available printer on the market that creates continuous carbon fiber polymer composites by FFF and for its ease of use. A DOE is a systematic method of conducting controlled tests to evaluate how varying different factors affect a response of interest. Test specimens were made using the Mark One, which is manufactured by MarkForged Inc. Test specimens were tested in accordance with ASTM D638, Standard Test Method for Tensile Properties of Plastics, and ASTM D3039, Standard Test Method for Tensile Properties of Polymer Matrix Composite Materials.

The Taguchi Method

For any system that has an output, there are factors that influence the characteristics of the output. For example, the yield from a farmer's field may be dependent on the amount of rain for the season, the number of sunny days, daily temperature, soil type, plant spacing and date of planting to name a few. It would be beneficial for the farmer to know how each of the variables influence crop yield and if any of the variables interact with each other.

A technique the famer can use to understand how each of the factors influence crop yield is through design of experiments (DOE). A type of DOE is the Taguchi method. The steps in the Taguchi method are listed (Perry Johnson, Inc., 1987):

1. Identify the quality characteristic
2. Identify the factors that will be tested along with each of their levels
3. Create an orthogonal array for the factors and levels selected
4. Conduct the experiment (Run trials and record the observations)
5. Perform an analysis of variance (ANOVA)
6. Identify the significant factors
7. Determine the optimal condition

Quality Characteristics

A quality characteristic is something that can be measured that is of interest to the experimenter. In the previous example with the farmer, the quality characteristic would be crop yield. In this research paper the quality characteristics are the following mechanical properties: tensile modulus, yield stress, percent strain at yield, ultimate tensile strength and percent strain at break. These are the properties that engineers are most interested in knowing when designing parts for functional applications.

Experimental Factors

The factors chosen for this experiment were layer height and raster angle orientation. Most of the process parameters on the Mark One are fixed, which limited the number of factors to choose from for the experiment. Table 3 shows the factors with levels for each of the six treatments. Printing orientation was not selected because a review of the literature showed that the strength of parts with a print orientation along the

z-axis showed less strength than parts printed in the x-y plane. Because only two factors were selected for testing it was easy to conduct a full factorial design. In a full factorial design every combination of factors and levels is tested. A specific combination of factors and levels is called a treatment. This experiment had six different treatments. Three runs were performed for each treatment for a total of 18 specimens.

Table 3. Raster Angle Orientation and Layer Height for Each Treatment

Treatment	Raster Angle Orientation(°)	Layer height (mm)
1	0/90	0.1
2	0/90	0.15
3	0/90	0.2
4	±45	0.1
5	±45	0.15
6	±45	0.2

In order to simplify the experiment, the following parameters were fixed for this experiment:

- The nylon fill density was set to 100 percent
- The number of “Roof”, “Floor”, and “Wall” layers were set to one
- The rectangular fill pattern was used

Specimen Printing

A STL file of the tensile test specimen was created in SolidWorks. SolidWorks is a computer aided design (CAD) software program. Figure 9 shows the CAD dimensions for the nylon tensile specimens according to ASMT D638, Type 1, with a thickness of 4 mm. Next, the STL file was imported into the Eiger software. The Eiger software is the

slicing software specific to the Mark One 3D printer. Eiger was used to specify the printing process parameters for each of the different treatments. After the process

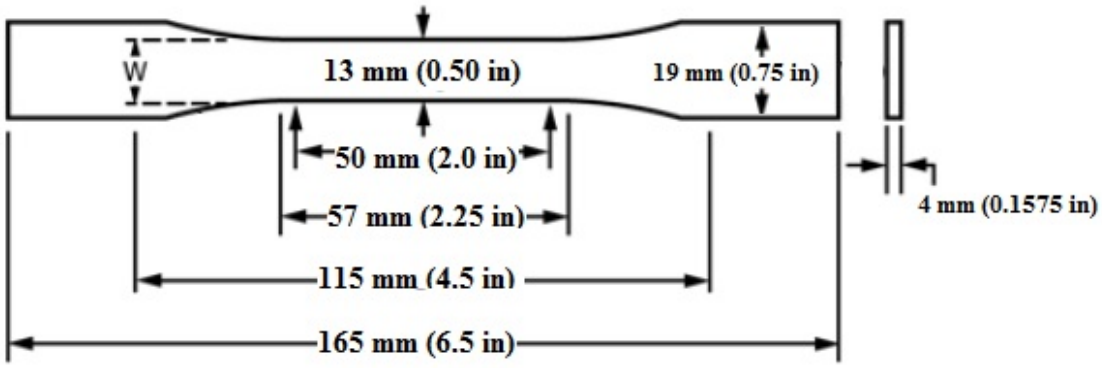

Figure 9. Drawing of Nylon Dog-Bone Tensile Specimen with Dimensions

parameters were selected based on the specific treatment, Eiger makes an electronic file that is transferred to the Mark One by a USB drive. The electronic file provides the information necessary for the Mark One to create the print. In order to reduce the effects of error on the statistical results, the printing order for each treatment specimen was randomized. The print bed was leveled prior to printing. After printing each specimen, the specimen was placed in a plastic bag labeled with the specimen's treatment number and printing order number. All specimens were stored in a desiccant box until testing. Anhydrous calcium sulfate was the chemical desiccant provided for the desiccant box storing the specimens and inside the nylon filament storage box for the Mark One.

Tensile Testing

Tensile testing was conducted on a MTS model 204.52 load cell with a 5.5 kip capacity using a MTS 632.13B-20 clip gage extensometer with a 0.5 inch gage length. Grip pressure was set to 1000 pounds. The temperature of the room was measured at 72.3 degrees Fahrenheit with a relative humidity of 45 percent. Prior to testing the average width and thickness of the gage section of the specimen was recorded by taking the average of three measurements. The average width and thickness of each specimen was later used to calculate the engineering stress and engineering strain. Tensile testing was performed on the specimens in order to measure the engineering strain and engineering stress. The specimens were tested under stress control until failure. Stress control means that the rate of increasing stress applied to each specimen was the same. The desired load rate applied to each specimen was based on the cross sectional area of the gage section for each specimen. Equation 4 shows how the desired load rate for each specimen was calculated.

$$L_{rate} = \frac{11{,}000\ psi \times A_{gage}}{300\ sec} \tag{4}$$

Where

L_{rate} = *desired load rate for each specimen (lb-f/sec)*

A_{gage} = *area of gage section* (in^2)

Equation 4 equals a load rate that will result in a tensile stress of 11,000 psi within 300 seconds from starting the tensile test. A load rate large enough for the specimen to reach failure within five minutes was desired. This is why 300 seconds is in the denominator for equation 4. By using equation 4, the load rate was adjusted for each

specimen based on the average cross-sectional area of the specimen's gage section. The measured mean gage dimension, testing load rate, mass, and density for each tensile specimen is listed in Table 9 of Appendix A.

An extensometer was used to record the elongation of the gage section due to the applied load. The tensile testing machine recorded time, commanded load, actual load, frame displacement, and extensometer displacement. The actual load was divided by the average area of the gauge specimen to calculate the engineering stress. From this data engineering stress and engineering strain was measured to create a stress-strain curve for each specimen. Appendix D contains the stress-strain curves for each nylon tensile specimen.

The change in gage length is recorded by the extensometer. The original gage length used in the experiment is the extensometer length, which was 0.5 in. Strain was calculated by dividing the extensometer reading by 0.5 in. The strain was then multiplied by 100 to get the percent strain. The engineering stress was plotted versus engineering strain to create a stress-strain curve. Figure 10 is an example of a stress-strain curve for treatment 1. From this stress-strain curve the following information was determined: tensile modulus, yield stress, percent strain at yield, and ultimate tensile strength. Table 10 in Appendix B lists the recorded mechanical properties for each tensile specimen.

Tensile Elastic Modulus Measurement.

For this research, the elastic modulus was calculated as the secant modulus at 0.5% strain. The secant modulus is the slope of a line from the point corresponding to 0.5% strain to the origin. This line is shown on Figure 10 as 0.5% secant modulus.

Yield-Stress Measurement.

For this research, a 0.2% strain offset was used to measure the yield stress. A line was drawn parallel to the 0.5% secant modulus at a 0.2% strain offset. The intersection of this line with the stress-strain curve was recorded as the yield stress. The 0.2% strain offset line is shown in Figure 10. Here, the yield stress is recorded as 13.976 MPa.

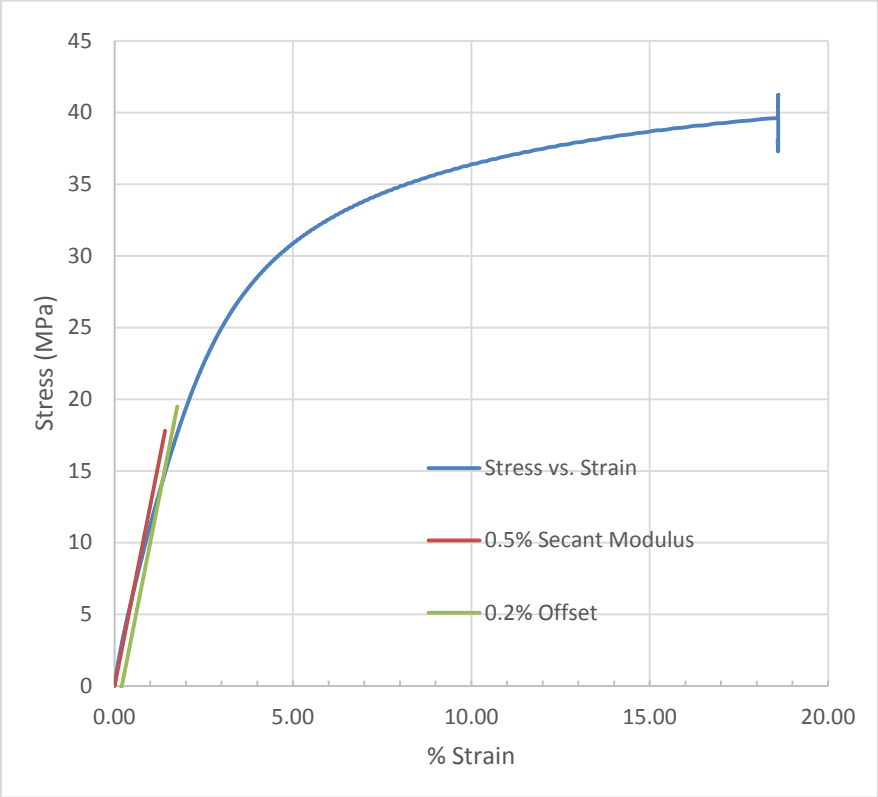

Figure 10. Stress-Strain Curve FFF PA6 Nylon, Treatment 1; Printing Order, 17; Test Order, 1; Gage Area, 0.0830 in2; Load Rate, 3.044 lb-force/sec; Testing Room Temperature, 72.3 Degrees Fahrenheit; Testing Room Relative Humidity, 45%

Tensile Strength Measurement.

Tensile strength is the greatest stress a material can withstand before failure. Failure can be either breaking or substantial plastic deformation, which results in necking. Tensile strength was measured as the greatest stress achieved before substantial necking of the tensile specimen. Figure 10 shows substantial necking at the vertical line at the end of the stress-strain curve.

Percent Strain at Break Measurement.

The percent strain at break was estimated by using the crosshead displacement data recorded by the MTS machine and calculated using Equation 5 below.

$$\varepsilon_{break} = \frac{L_{max} - L_{gage}}{L_{gage}} \quad (5)$$

Where

ε_{break} = *strain at break*

L_{max} = *greatest crosshead displacement before specimen break*

L_{gage} = *length of gage section (2.25 in)*

Specimen Density

After tensile testing, the density of each specimen was determined. The density was determined by dividing the specimen's mass by its density. The mass of each specimen was measured using a digital scale. The volume of each specimen was measured using the Archimedes' principle, which states that the volume of an object is equal to the volume of water displaced by the submerged object. This was done by first placing enough water in a graduated cylinder to allow the specimen to be completely submerged. Next, the volume of water in the graduated cylinder was measured. Next, the specimen was submerged in the graduated cylinder and the new volume reading from the graduated cylinder was recorded. The difference between the volume reading with the submerged specimen and without the submerged specimen was recorded as the

volume of the specimen. The mass and density for each specimen is listed in Table 9 of Appendix A.

After testing, photos were taken of the broken nylon tensile specimens. Photographs of the tensile specimens organized by treatment can be found in Appendix C.

Statistical Analysis

Following the material tests, the collected data was analyzed. The mean, range, and variance of each response due to each factor level was calculated. An analysis of variance (ANOVA) was performed to determine which process parameters are significant in affecting the material properties of the FFF nylon test specimens. Results will be compared to the mechanical properties of compression molded nylon-12 and traditional manufactured carbon-fiber reinforced polymer composites. A discussion of the results is provided in Chapter IV.

An ANOVA was performed to see if either layer height, raster angle orientation, or an interaction of the two factors significantly influenced the responses measured. The statistical software program used to perform the ANOVA was JMP® (John's Macintosh Program) Pro, version 11.2.0, by SAS Institute Inc. (Shipp and Lafler, 2012). An ANOVA was performed twice for each response; once with only the two factors; and again with the two factors and interaction. The factors were layer height and raster angle orientation. The Shapiro-Wilk test was performed for each response to check to see if the

residual of the responses were normally distributed. This was to test the ANOVA assumption that the responses are normally distributed.

Additionally, a statistical analysis was performed to determine if layer height affects material density. This was done by using JMP to determine the Pearson correlation coefficient for density by layer height and performing a one-way ANOVA on density by layer height.

Composite Specimens

Composite specimens were printed with carbon fiber and then tested in accordance with ASTM D3039, Standard Test Method for Tensile Properties of Polymer Matrix Composite Materials. The dimensions of the CAD model for the composite specimen were: length, 254 mm (10 in); width, 12.7mm (0.5 in); and thickness, 2.5 mm (0.098 in).

Tensile testing was conducted on a MTS model 204.52 load cell with a 5.5 kip capacity using a MTS 632.13B-20 clip gage extensometer with a 0.5 inch gage length. Grip pressure was set to 2000 pounds. Figure 11 shows one of the composite specimens during testing. Prior to testing the average width and thickness of the gage section of the specimen was recorded by taking the average of three measurements. The average width and thickness of each specimen was later used to calculate the engineering stress and engineering strain. Tensile testing was performed on the specimens in order to measure the engineering strain and engineering stress. Testing was conducted by strain control

with a strain rate of 0.0208 mm/sec. The temperature of the room was measured at 71.6 degrees Fahrenheit with a relative humidity of 41 percent.

Figure 11. Composite Specimen During Testing

IV. Analysis and Results

Chapter Overview

This chapter will present the Design of Experiment (DOE) results for the PA6 nylon tensile specimens. The statistical analysis of the measured responses for each factor and level will be presented. A discussion will follow on how each factor influences the selected quality characteristics. Next, this chapter will present results from the continuous carbon fiber composite (CCFC) testing to include a stress-strain curve and scanning electron microscope (SEM) photographs of the CCFC failure surface.

Statistical Analysis Results

Table 4 shows the mean of each mechanical characteristic measured by the level of each factor. The upper and lower 95% confidence intervals of the mean are shown below the means. This table can give insight into how each factor and the individual levels within the factors influence the mechanical properties.

Table 4. Mean and Confidence Intervals of Measured Mechanical Properties by Factor and Level

	Layer Height (mm)			Raster Angle Orientation	
	0.1	0.15	0.20	±45	0/90
Mean Tensile Modulus (GPa)	1.1899	1.1835	1.0695	1.1857	1.1096
Upper 95% Mean	1.2478	1.2519	1.164	1.2383	1.1808
Lower 95% Mean	1.132	1.1151	0.9749	1.1331	1.0384
Mean Yield Stress (MPa)	12.744	12.302	11.917	11.961	12.681
Upper 95% Mean	13.721	12.628	12.602	12.408	13.222
Lower 95% Mean	11.767	11.975	11.231	11.513	12.140
Mean Percent Strain at Yield Stress (MPa)	1.271	1.242	1.323	1.211	1.347
Upper 95% Mean	1.361	1.292	1.459	1.241	1.412
Lower 95% Mean	1.182	1.190	1.188	1.181	1.282
Mean Ultimate Tensile Strength (MPa)	37.735	36.564	35.104	36.519	36.416
Upper 95% Mean	38.618	37.676	35.808	37.577	37.539
Lower 95% Mean	36.852	35.452	34.400	35.462	35.293
Percent Strain at Break	116.762	78.172	35.840	113.231	40.618
Upper 95% Mean	199.489	117.319	83.213	158.973	74.799
Lower 95% Mean	34.034	39.025	-11.533	67.489	6.436

The statistical analysis software JMP was used to perform an analysis of variance (ANOVA) and Fit Analysis for each response by the factors layer height and angle orientation. An ANOVA was also performed to test for possible factor interactions. Table 5 shows the ANOVA results for each factor and response along with the interaction.

Table 5 includes the R squared and F-test values from the ANOVA. The R squared values can range from 0 to 1. The higher the R squared value the better the factors explain the variability in the data. A higher R squared value also means that differences between factors is less due to randomness. An overall alpha value of $\alpha = 0.05$ was used for the overall F-test. F-test values less than 0.05 indicate that at least one of the factors is statistically significant in influencing the variability of the response.

This means that at least one of the factors influence the mechanical properties. The overall F-test was less than 0.05 for each response, which means that at least one of the two factors can explain the variability in the data. The F-test values for each factor are shown to the right of the overall F-test values in Table 5. The F-test on the factors determines if the difference in the mean responses are the same or statistically different. Because there were two factors being tested the critical p-value was 0.05 divided by 2, or 0.025. F-test values less than 0.025 indicate that the factor is statistically significant in influencing the desired response. Values less than the critical p-value are highlighted green in Table 5 to indicate statistical significance. The critical p-value for the interaction F-test was 0.05 divided by 3, or 0.0167. Only the interaction of layer height and raster angle orientation on yield stress was found to be statistically significant.

Table 5. R Squared and p Values from ANOVA Results for Each Factor with and without Interaction

	Response	R Squared	F-test	F-test, Layer height	F-test, Raster Angle Orieintation	F-test, interaction
Without Interaction	Tensile Modulus	0.6142	0.0033	0.0059	0.0181	
	Yield Stress	0.4874	0.0217	0.0759	0.0186	
	Percent Strain at yield	0.6788	0.0009	0.0861	0.0002	
	Ultimate Tensile Strength	0.6480	0.0018	0.0007	0.8106	
	Percent Strain at Break	0.6392	0.0021	0.0162	0.0025	
With Interaction	Tensile Modulus	0.7522	0.0024	0.0027	0.0093	0.0702
	Yield Stress	0.7765	0.0013	0.0147	0.0029	0.0069
	Percent Strain at yield	0.7951	0.0008	0.0482	0.0001	0.0673
	Ultimate Tensile Strength	0.7858	0.0010	0.0002	0.7769	0.0508
	Percent Strain at Break	0.6994	0.0069	0.0175	0.0052	0.3344

Table 6 provides a summary of the statistical significance of each factor and interaction influencing a certain response based on the ANOVA results.

Table 6. Statistical Significance of Factors for each Response

	Statistically Significance		
Response	**Layer height**	**Raster angle orientation**	**Interaction of raster angle and layer height**
Tensile Modulus (GPa)	Yes	Yes	No
Yield Stress (MPa)	No	Yes	Yes
Percent Strain at Yield	No	Yes	No
Ultimate Tensile Strength	Yes	No	No
Percent Strain at Break	Yes	Yes	No

A discussion of how each factor influences each response measured follows. Layer height was only significant in influencing tensile modulus and ultimate tensile strength. Figure 12 below shows that the mean yield stress increased with decreasing layer height. Both tensile modulus and ultimate tensile strength increased with decreasing layer height as seen in Figure 13. Both tensile modulus and tensile strength are greatly influenced by a material's density. As a material's density increases so does stiffness (modulus) and strength. It could be that the layer height was influencing the density of each specimen.

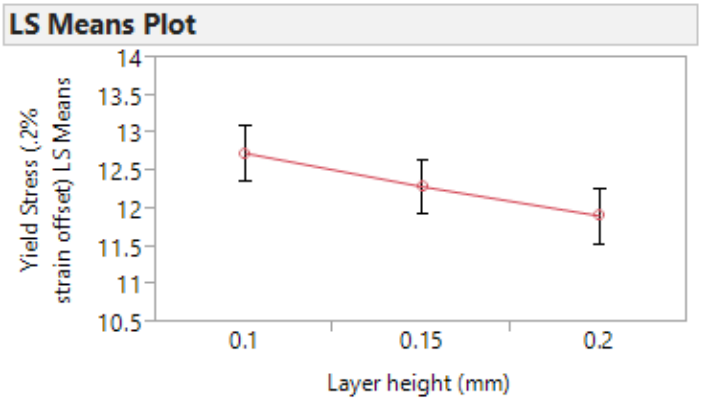

Figure 12. LS Means Plot of Yield Stress versus Layer Height

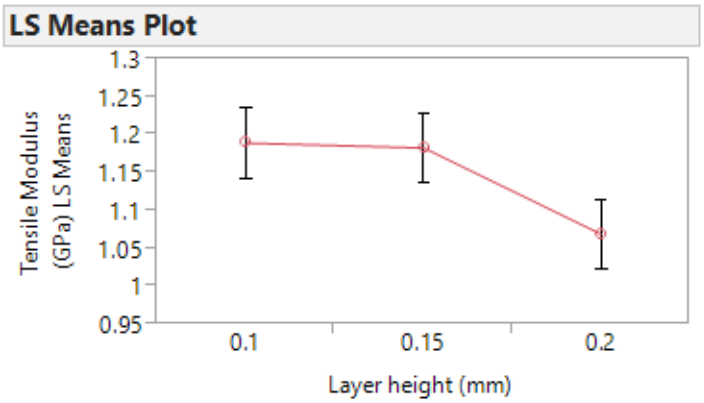

Figure 13. LS Means Plot of Tensile Modulus versus Layer Height

The raster angle orientation was significant in influencing tensile modulus, yield stress, percent strain at yield, and percent strain at break. Figure 14 shows that stiffness was greatest in the ±45 angle orientation versus the 0/90 orientation. Even though the ±45 angle orientation is not directly aligned along the tensile direction, it still has more layers resisting in the tensile direction compared to the 0/90 orientation, which has only half of its layers resisting the force. As discussed in the literature review, layers with raster angles orthogonal to the tensile force do not contribute greatly to stiffness or

strength. Only half of the layers in the 0/90 orientation are aligned with the tensile direction. This may possibly explain why the 0/90 orientation is less stiff then the ±45 angle orientation.

The only response that the raster angle orientation was not significant in influencing was the ultimate tensile strength. Table 4 shows the mean tensile strength of angle orientation ±45 and 0/90 was 1.1857 GPa and 1.1096 GPa respectively.

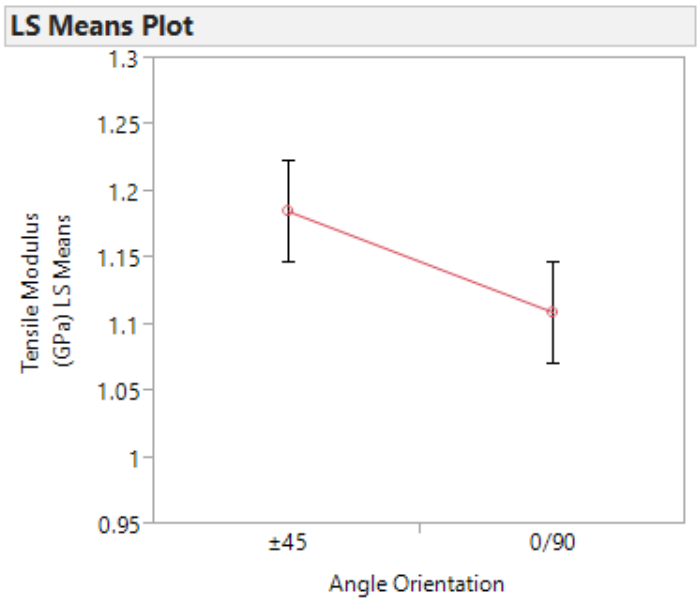

Figure 14. LS Means Plot of Tensile Modulus versus Angle Orientation

Table 7 compares the average results from the DOE with injection grade nylon-12, and nylon-12 made from selective laser sintering (SLS). The values for the injection grade nylon and SLS were taken from MatWeb.com, a website that provides material data provided by manufactures. Nylon-12 measurements made by Griehl and Ruestem (1970) are also listed in Table 7. Griehl and Ruestem measured tensile strength at 63

MPa. This is nearly double the average tensile strength measured in the DOE. The Tensile modulus measured by Griehl and Ruestem at 1.172 GPa is more comparable to DOE results, which were 1.148 GPa. For injection-molded nylon-12, tensile strength at yield ranged from 35 MPa to 42 MPa. It is important to note that tensile strength at yield can vary widely depending on what percent strain is considered "yield". Thermoplastics do not exhibit a clearly defined yield point on stress-strain curves and yield strength is taken to be the stress at a specified percent strain. The Arkema Group Injection Grade nylon-12 use 8% and 10% strain to determine yield stress. From the experimental data for each specimen, the stress at 10% strain was around 36 MPa. The injection grade nylon has greater strength and higher elastic modulus compared to experimental values measured from the DOE of the nylon tensile specimens discussed earlier.

Table 7. Comparisons of Mechanical Properties for Several Different Nylon-12 with Experimental Results (MatWeb, LLC, 2015), (Griehl and Ruestem, 1970)

	Tensile Strength, Yield (MPa)	Ultimate Tensile Strength (MPa)	Strain at Break (%)	Strain at Yield (%)	Tensile Modulus (GPa)
Arkema Group Rilsan® AMN D Nylon-12, Rigid, Injection Grade (Dry)	42.00	not listed	>=50	8.0	1.45
Arkema Group Rilsan® AMN Nylon-12, Rigid, Injection Grade (Conditioned)	39	not listed	>=50	10.0	1.17
Polyram PlusTek PD104 Nylon-12, Injection Molding	35	not listed	300	not listed	0.70
ALM PA 650 Nylon-12 Selective Laser Sintering (SLS) Prototyping Polymer	not listed	48.0	24	not listed	1.70
Nylon-12 measured by Griehl and Ruestem (1970)	not listed	63	not listed	not listed	1.172
Average measurements from all DOE data	12.32**	36.5***	71	1.28**	1.148*
Average tensile strength at 10% strain from DOE data	31.2	n/a	n/a	10	n/a

* Tensile Modulus recorded at .5% strain

**Yield stress defined using the .2% strain offset method

*** Ultimate tensile strength defined as the highest stress recorded before substantial necking of specimen

Effect of Layer Height on Density of FFF Nylon

Pearson correlation coefficients were calculated in JMP to show what correlation layer height has on the density of FFF nylon. The correlation coefficient is the measure of the linear relationship between two variables *x* and *y* and can be in the range from -1 to 1 (McClave, Benson, and Sincich, 2014). A correlation coefficient of -1 or 1 indicates a perfect linear relationship, while a coefficient of 0 indicates little or no relationship. Table 8 below shows that the correlation coefficient for density and layer height is -0.7450. This means that from the experimental data for a 0.01 mm decrease in layer height the density will increase by 0.00745 g/cm^3.

Table 8. Pairwise Correlations Table for Ultimate Tensile Strength, Tensile Modulus, Layer Height, and Density

Multivariate

Correlations

	Tensile Modulus (GPa)	Ultimate Tensile Strength (MPa)	Layer height (mm)	Density (g/cm^3)
Tensile Modulus (GPa)	1.0000	0.5692	-0.5739	0.5172
Ultimate Tensile Strength (MPa)	0.5692	1.0000	-0.8024	0.6197
Layer height (mm)	-0.5739	-0.8024	1.0000	-0.7450
Density (g/cm^3)	0.5172	0.6197	-0.7450	1.0000

Pairwise Correlations

Variable	by Variable	Correlation	Count	Lower 95%	Upper 95%	Signif Prob	-.8 -.6 -.4 -.2 0 .2 .4 .6 .8
Ultimate Tensile Strength (MPa)	Tensile Modulus (GPa)	0.5692	18	0.1393	0.8185	0.0137*	
Layer height (mm)	Tensile Modulus (GPa)	-0.5739	18	-0.8208	-0.1462	0.0128*	
Layer height (mm)	Ultimate Tensile Strength (MPa)	-0.8024	18	-0.9234	-0.5366	<.0001*	
Density (g/cm^3)	Tensile Modulus (GPa)	0.5172	18	0.0664	0.7927	0.0279*	
Density (g/cm^3)	Ultimate Tensile Strength (MPa)	0.6197	18	0.2150	0.8427	0.0061*	
Density (g/cm^3)	Layer height (mm)	-0.7450	18	-0.8992	-0.4266	0.0004*	

A one-way ANOVA was performed on density by layer height in JMP. The one-way ANOVA table to include mean density and mean density confidence intervals for each layer can be found in Table 11 of Appendix E. Figure 15 shows a scatter plot of density by layer height from the one-way ANOVA table. The green diamonds in Figure 15 represent the 95% confidence interval of the mean density for each layer height group. The mean density for layer heights 0.1 mm and 0.15 mm are nearly equal at 1.11 g/cm^3 and 1.10 g/cm^3 respectively, but the mean density decreases to 1.085 g/cm3 for layer height 0.2 mm. Looking at the scatter-plot of density by layer height, it appears that with decreasing layer height, density approaches an upper bound where the density remains nearly constant. Additional experiments are needed with additional layer heights to better understand the relationship between density and layer height.

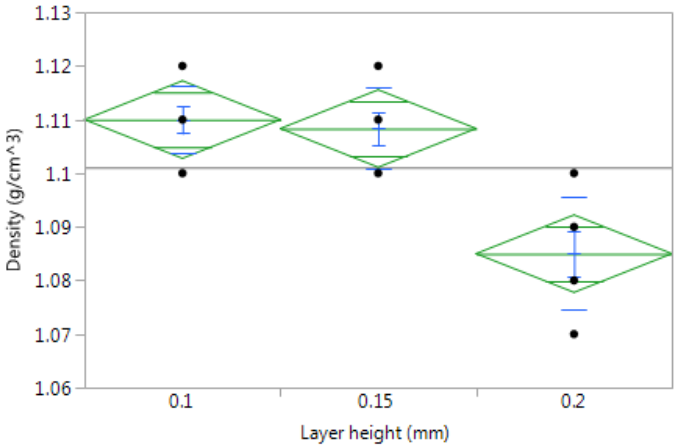

Figure 15. Scatter Plot of Density by Layer Height with 95% Mean Confidence Intervals

Effect of Density on Mechanical Properties of FFF Nylon

A one-way ANOVA was performed for a cohort density variable and for each of the mechanical properties measured to determine if density influences the mechanical properties of FFF nylon specimens made by the Mark One. The cohort variable for density was defined with two levels: "low density" and "high density." Low density was defined as being less than 1.095 (g/cm^3) and high density was defined as being greater than 1.095 (g/cm^3). The density value between "low" and "high" density was determined by visually evaluating the scatter plots of the mechanical properties and density to see if the data formed groups. Figure 16 shows the scatter plot of tensile modulus by density

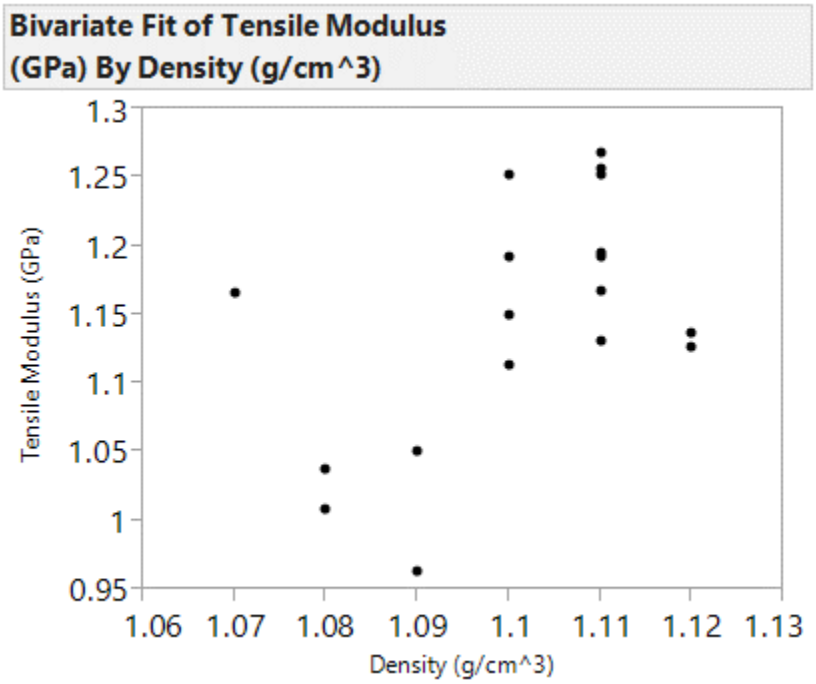

Figure 16. Scatter-Plot of Tensile Modulus by Density for FFF Nylon

for the FFF nylon specimens. It is visually apparent from Figure 16 that the data forms a "low density" group and a "high density" group. The density number between these two groups is 1.095 (g/cm3). A one-way ANOVA was performed for the cohort density variable and for each of the mechanical properties measured. The ANOVA tables can be found in Table 12 through Table 16 of Appendix F. The differences between the means for low density and high density groups were statistically significant for tensile modulus, percent strain at yield, ultimate tensile strength, and percent strain at break. The mean yield stress between the low density and high density groups was found not to be statistically different.

Table 8 shows the Pearson correlation coefficients for ultimate tensile strength, tensile modulus, layer height, and density. Layer height shows a greater correlation for

both tensile modulus and ultimate tensile strength compared to density. This may mean, there are other contributing factors that influence tensile modulus and ultimate tensile strength then density alone.

Results from Continuous Carbon Fiber Composite (CCFC) Testing

Several continuous carbon fiber composites (CCFC) were printed using the same layup pattern in attempt to determine the mechanical properties of the CCFCs. The Mark One defaults to a pre-set layer height when printing with fiber. The layer height when using carbon fiber is 0.125mm. Figure 17 shows the layup pattern used for this test; light gray layers are nylon and black layers are carbon fiber.

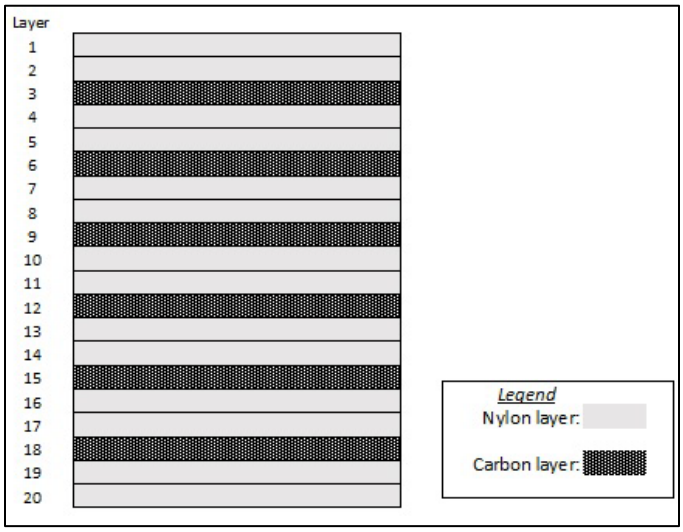

Figure 17. Layup Sequence for the Continuous Carbon Fiber Reinforced Composite

Figure 18 shows a drawing from Eiger. Eiger is the slicing software provided with the Mark One 3D printer. The drawing shows how the carbon fiber was applied to

each layer. At this time, the only fill pattern available for carbon fiber is “concentric” fill. The concentric fill creates concentric rings bordering the outer perimeter of the part. Any part of the carbon fiber layer that does not receive carbon fiber is backfilled with nylon. Figure 19 shows a close-up view of the continuous carbon fiber nylon composite still on the print-bed after printing. The nylon support rim borders the perimeter of the nylon composite. The dimensions of the CAD model for the composite specimen were: length, 254 mm (10 in); width, 12.7mm (0.5 in); and thickness, 2.5 mm (0.098 in).

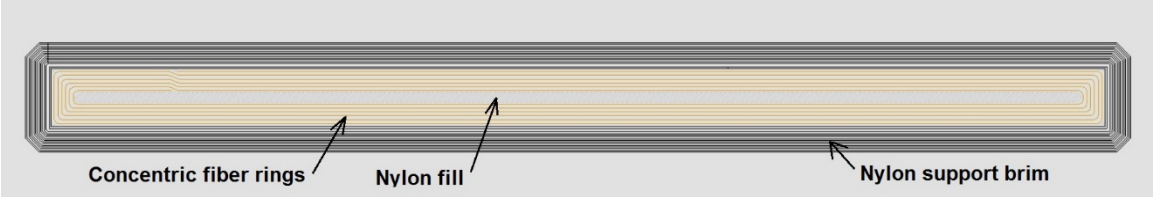

Figure 18. Eiger Screen Shot Showing the Fill Pattern for the Continuous Carbon Fiber Composite


Figure 19. A Close-Up View of the Continuous Carbon Fiber Composite Still on the Print-Bed after Printing

Problems arose during the testing of the composite specimens. Many of the specimens either broke in the grips or there was slippage in the grips during tensile testing, consequently voiding the results of the test. There was only one good test specimen that did not break in the grips during testing. Figure 20 shows this specimen after testing. Figure 21 shows the stress-strain curve for this test. The ultimate tensile strength was 121.1 MPa and the tensile modulus was 9.9 GPa.

Figure 20. Continuous Carbon Fiber Composite Specimen After Testing

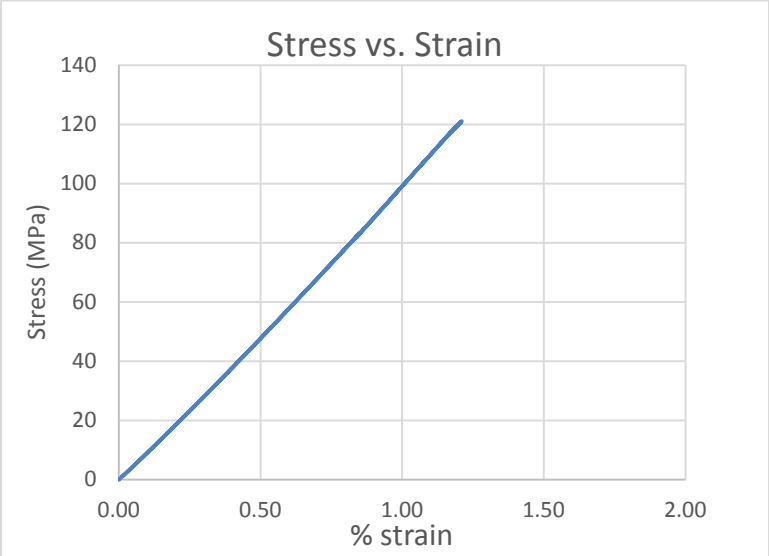

Figure 21. Stress-Strain Curve for the Continuous Carbon Fiber Composite Made on the Mark One 3D printer, Specimen Dimensions: Width, 0.5267 in; Thickness, 0.1567 in; Gage Length, 6 in; Room Temp (71.6F), Relative Humidity (41%)

Scanning Electron Microscope (SEM) Photographs

SEM photographs were taken of the failure surface from one of the CCFC tensile specimens. Figure 22 shows the fracture surface of a carbon fiber reinforced nylon composite. The approximate thickness of the fracture is 2.331 mm. The layup sequence for the specimen in Figure 22 is shown in Figure 17.

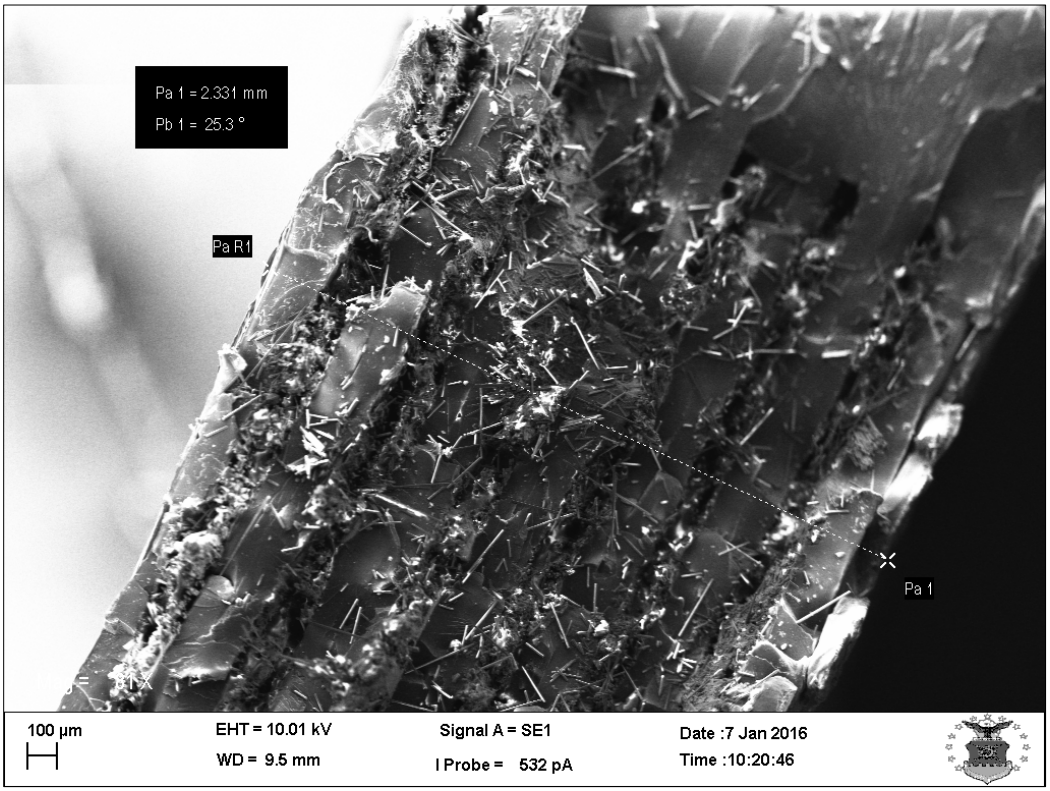

Figure 22. Fracture Surface of a Continuous Carbon Fiber Reinforced Nylon Composite

Figure 23 shows an alternative view of the fracture surface. In this image, discontinuities are visible between each nylon layer but not between rasters. This shows that the

coalescence of the nylon is not complete between layers but is nearly homogeneous between rasters. Additional SEM photographs of the fracture surface are in Appendix G.

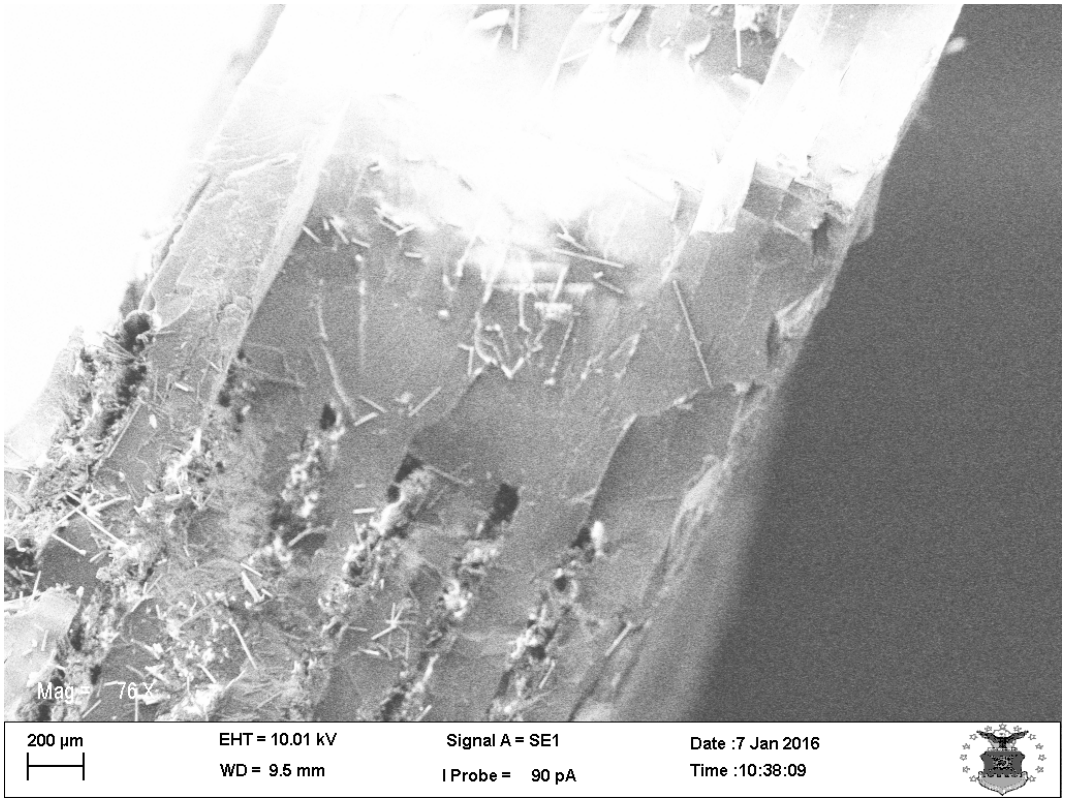

Figure 23. Fracture Surface of a Continuous Carbon Fiber Reinforced Nylon Composite Showing Differentiation Between Layers

V. Discussion and Conclusion

Chapter Overview

This chapter will first include a discussion on how the results of this research answered each of the research questions established in Chapter I. Next, possible future research will be discussed. In conclusion, the implications of this research for engineering and material science will be discussed.

Research Questions Answered

The purpose of this research was to determine how varying Fused Filament Fabrication (FFF) process parameters affect the mechanical properties of PA6 nylon dog-bone specimens produced on the Mark One 3D Printer. A design of experiment (DOE) was conducted using the factors of layer height and raster angle orientation. The mechanical properties measured in the experiment were tensile modulus, yield stress, percent strain at yield, ultimate tensile strength and percent strain at break. An analysis of variance (ANOVA) was performed to identify which factors were statistically significant in influencing mechanical properties. Results of the ANOVA showed that layer height was significant in influencing tensile modulus, ultimate tensile strength and percent strain at break; raster angle orientation was significant in influencing tensile modulus, yield stress, percent strain at yield, and percent strain at break.

Research Question 1.

- What are the mean and confidence intervals for material properties of FFF parts made with varying process parameters?

The mean and 95% confidence intervals for the measured material properties were calculated for each level of layer height and raster angle orientation. This information was included in Table 4.

Research Question 2.

- Can certain FFF process factors be used to optimize the mechanical properties of FFF parts?

The results of the ANOVA show that both layer height and raster angle orientation influence the mechanical properties of FFF part. By reviewing the results discussed in Chapter IV, the optimal treatment for each mechanical property measured can be determined. The optimal condition that maximizes tensile modulus and ultimate tensile strength is a layer height of 0.1 mm and a (±45) raster angle orientation. The optimal condition that maximizes percent strain at break is a layer height of 0.1 mm and a (±45) raster angle orientation. The optimal condition that maximizes yield stress is a layer height of 0.1 mm and a (0/90) raster angle orientation. The optimal condition that maximizes percent strain at yield is a layer height of 0.2 mm and (0/90) raster angle orientation.

Research Question 3.

- How do nylon parts produced by FFF compare with compression molded nylon parts?

As discussed in Chapter IV, the DOE experimental values of the FFF were compared with compression molded nylon parts. The experimental data from the FFF nylon DOE showed lower ultimate tensile strength and tensile modulus then compression-molded nylon. The FFF nylon material property that was comparable to compression molded nylon was percent elongation at break.

Research Question 4.

- What are the mechanical properties of carbon fiber reinforced thermoplastic composites made by FFF?

As discussed in Chapter IV, this question was not answered due to lack of time and problems encountered during testing. One composite specimen was tested and the ultimate tensile strength was 121.1 MPa and the tensile modulus was 9.9 GPa.

Research Implications

This research shed light on how FFF process parameters affect the mechanical properties of FFF materials. The research shows that the mechanical properties of FFF parts can be influenced by changing the process parameters of layer height and raster angle orientation. In the future it is likely that engineers will be able use additive manufacturing to create materials that meet certain performance requirements by specifying a unique treatment of additive manufacturing process parameters.

Measuring the density of additively manufactured parts could be a non-destructive method of quality assurance. The results from the density investigation revealed that different levels of density showed differences in the mean mechanical properties. The

FFF nylon specimens with a “high” level of density showed greater ultimate tensile strength and tensile modulus compared to the FFF nylon specimens with a “low” level of density.

Future Research

A possible future experiment is to see how different nylon and fiber layup sequences influence mechanical properties. Two possible layup sequences that could be tested are shown in Figure 24. Each sequence has the same number of nylon and carbon fiber layers, with 10 carbon fiber layers, and 12 nylon layers. Each layup is also symmetric about the center of the layup to prevent moment forces from influencing testing results. For layup A, each carbon layer is sandwiched between two layers of nylon. For layup B, the layers alternate between two nylon layers and two carbon fiber layers.

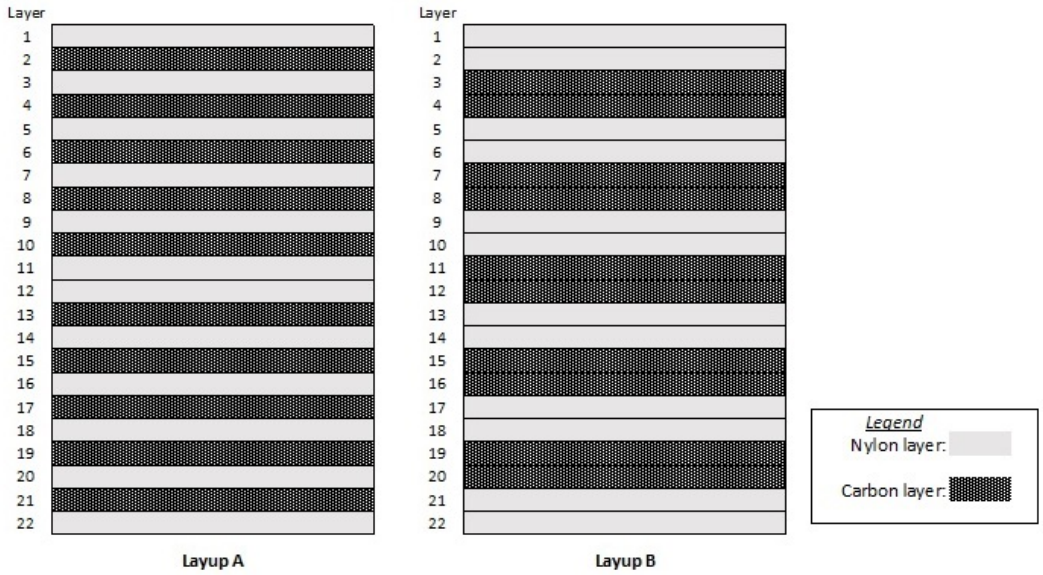

Figure 24. Two Possible Layup Sequences for a Future DOE Experiment

A future investigation can lead to better understanding of the relationship between carbon fiber volume fraction and tensile modulus of continuous carbon fiber composites (CCFC) made through additive manufacturing. The tensile modulus of a single carbon fiber towpreg on a printed nylon layer can be determined through tensile testing. A duplicate CCFC specimen can then be printed to determine the volume fraction of a single carbon towpreg. From this information, a relationship can be made between fiber volume fraction and tensile modulus. This relationship model can be used to predict the tensile modulus of a given carbon fiber fraction. An experiment can then be performed to test the validity of the fiber volume fraction-tensile modulus relationship model.

Appendix A: Mean Gage Dimensions, Testing Load Rate, Mass, and Density for Each Tensile Specimen

Table 9. Mean Gage Dimensions, Testing Load Rate, Mass, and Density for Each PA6 Nylon Tensile Specimen

Data Point	Printing Sequence	Testing Order	Treatment	Angle Orientation	Layer Height (mm)	Mean Gage Width (in)	Mean Gage Thickness (in)	Gage Area (in^2)	Load Rate (lb-force/sec)	Mass (g)	Density (g/cm^3)
1	10	16	1	0/90	0.1	0.5248	0.1577	0.0828	3.035	11.42	1.12
2	12	15	1	0/90	0.1	0.5285	0.1573	0.0831	3.048	11.33	1.11
3	17	1	1	0/90	0.1	0.5245	0.1583	0.0830	3.044	11.37	1.11
4	3	8	2	0/90	0.15	0.5263	0.1593	0.0838	3.074	11.20	1.10
5	6	18	2	0/90	0.15	0.5267	0.1567	0.0825	3.026	11.18	1.10
6	13	7	2	0/90	0.15	0.5308	0.1613	0.0856	3.139	11.39	1.12
7	4	12	3	0/90	0.2	0.5267	0.1553	0.0818	2.999	10.84	1.08
8	11	17	3	0/90	0.2	0.5247	0.1570	0.0824	3.021	10.81	1.08
9	16	13	3	0/90	0.2	0.5248	0.1567	0.0822	3.015	10.86	1.09
10	1	4	4	±45	0.1	0.5310	0.1566	0.0832	3.049	11.04	1.10
11	8	9	4	±45	0.1	0.5255	0.1565	0.0822	3.015	11.30	1.11
12	14	14	4	±45	0.1	0.5297	0.1578	0.0836	3.065	11.30	1.11
13	5	5	5	±45	0.15	0.5298	0.1570	0.0832	3.050	11.29	1.11
14	7	2	5	±45	0.15	0.5336	0.1583	0.0845	3.098	11.08	1.11
15	9	11	5	±45	0.15	0.5300	0.1623	0.0860	3.154	11.34	1.11
16	2	10	6	±45	0.2	0.5332	0.1572	0.0838	3.073	10.98	1.10
17	15	3	6	±45	0.2	0.5315	0.1593	0.0847	3.104	10.89	1.09
18	18	6	6	±45	0.2	0.5253	0.1515	0.0796	2.918	10.74	1.07

Appendix B: Recorded Mechanical Properties for Each Tensile Specimen

Table 10. Recorded Mechanical Properties for Each PA6 Nylon Tensile Specimen

Data Point	Printing Sequence	Testing Order	Treatment	Angle Orientation	Layer Height (mm)	Tensile Modulus (GPa)	Strain at Break (%)	Yield Stress (MPa)	Strain at Yield (%)	Ultimate Tensile Strength (MPa)
1	10	16	1	0/90	0.1	1.1368	128.8	13.654	1.4	38.105
2	12	15	1	0/90	0.1	1.1951	29.28	12.959	1.28	39.156
3	17	1	1	0/90	0.1	1.2569	19.88	13.976	1.31	37.213
4	3	8	2	0/90	0.15	1.1495	96.15	12.068	1.25	35.06
5	6	18	2	0/90	0.15	1.1127	53.68	12.124	1.29	36.383
6	13	7	2	0/90	0.15	1.1267	14.53	12.301	1.29	36.035
7	4	12	3	0/90	0.2	1.0369	0.5	12.164	1.37	35.293
8	11	17	3	0/90	0.2	1.0086	22.08	12.276	1.42	35.019
9	16	13	3	0/90	0.2	0.9629	0.66	12.608	1.51	35.478
10	1	4	4	±45	0.1	1.2526	217.07	11.813	1.14	36.708
11	8	9	4	±45	0.1	1.1314	127.95	11.856	1.25	37.501
12	14	14	4	±45	0.1	1.1667	177.59	12.206	1.25	37.727
13	5	5	5	±45	0.15	1.252	109.16	12.91	1.23	37.795
14	7	2	5	±45	0.15	1.2675	86.42	12.138	1.16	37.778
15	9	11	5	±45	0.15	1.1925	109.09	12.271	1.23	36.333
16	2	10	6	±45	0.2	1.1918	115.63	11.722	1.19	34.652
17	15	3	6	±45	0.2	1.0513	14.25	10.725	1.22	34.126
18	18	6	6	±45	0.2	1.1653	61.92	12.005	1.23	36.055

Appendix C: Specimen Photographs

Figure 25. Treatment 1 Test Specimens after Testing

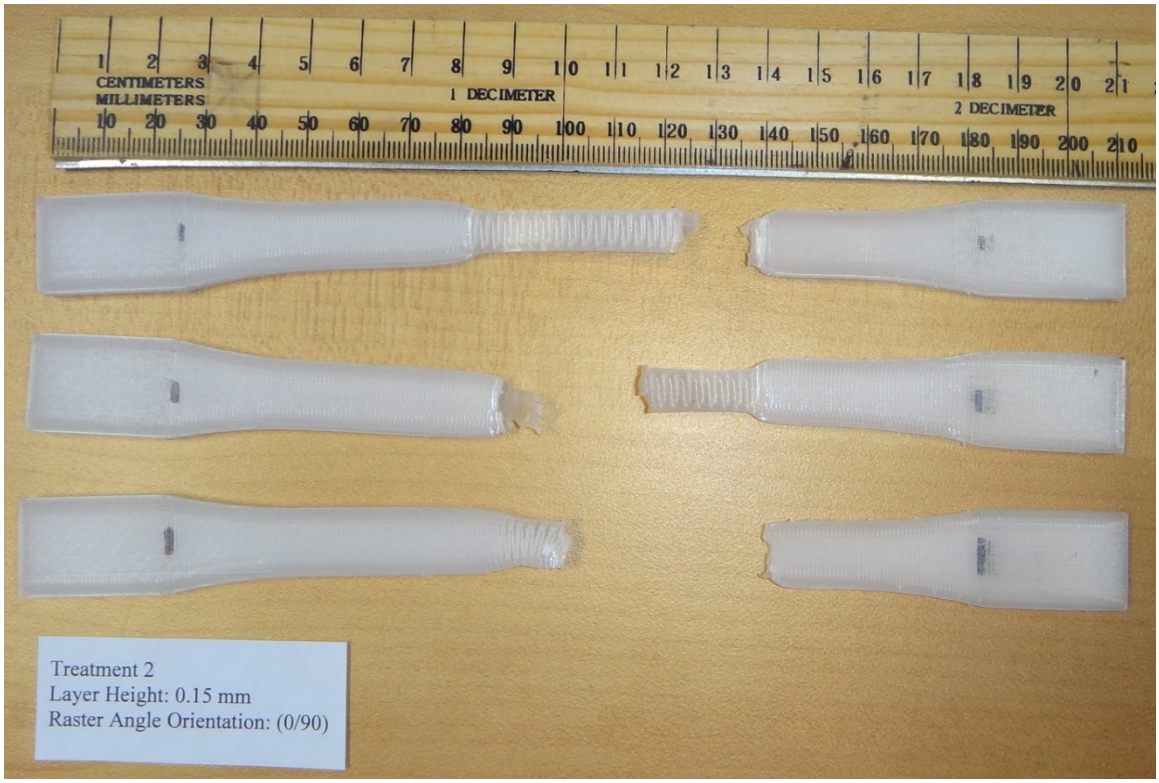

Figure 26. Treatment 2 Test Specimens after Testing

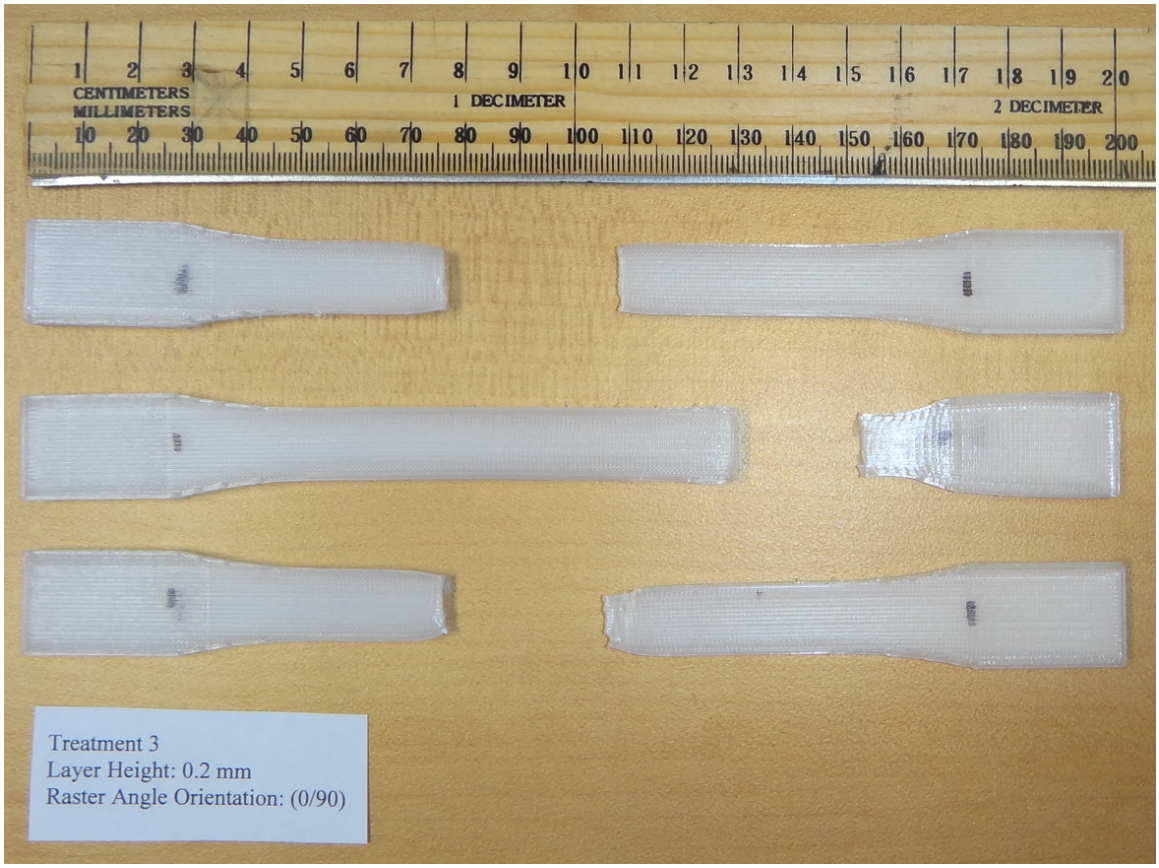

Figure 27. Treatment 3 Test Specimens after Testing

Figure 28. Treatment 4 Test Specimens after Testing

Figure 29. Treatment 5 Test Specimens after Testing

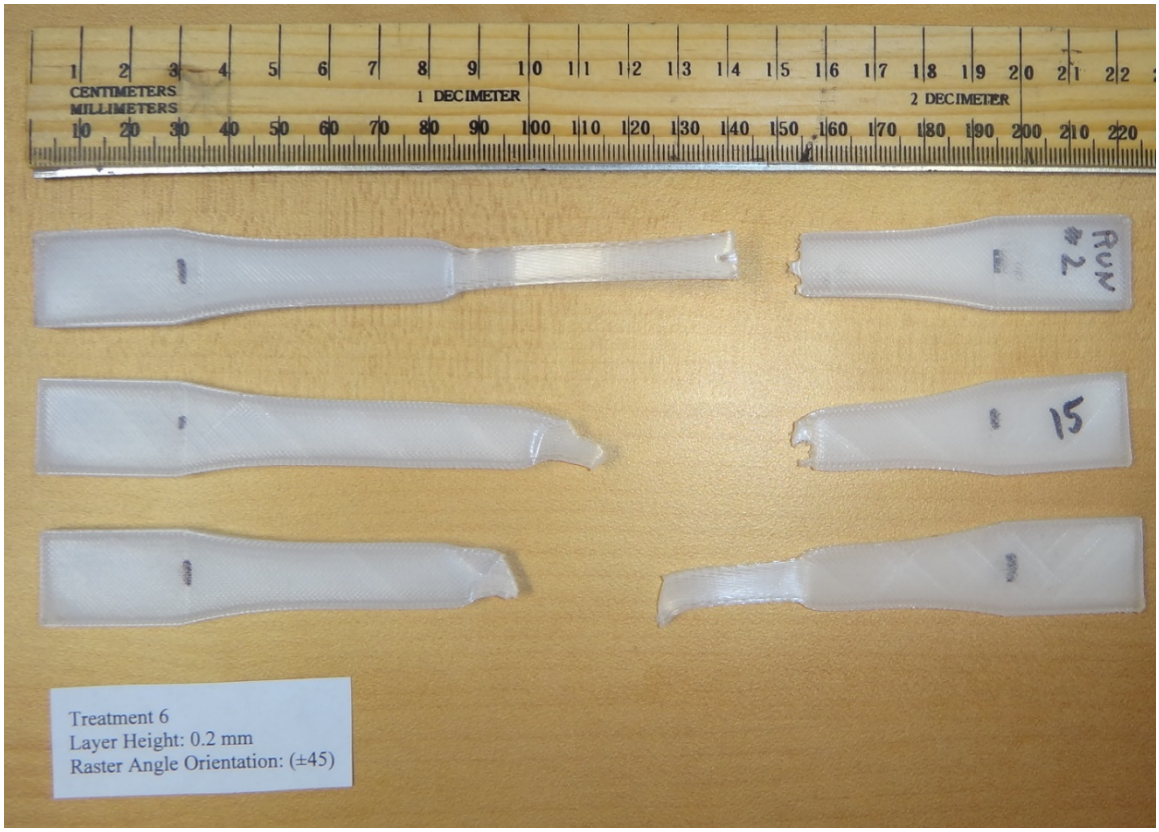

Figure 30. Treatment 6 Test Specimens after Testing

Appendix D: Stress-Strain Curves

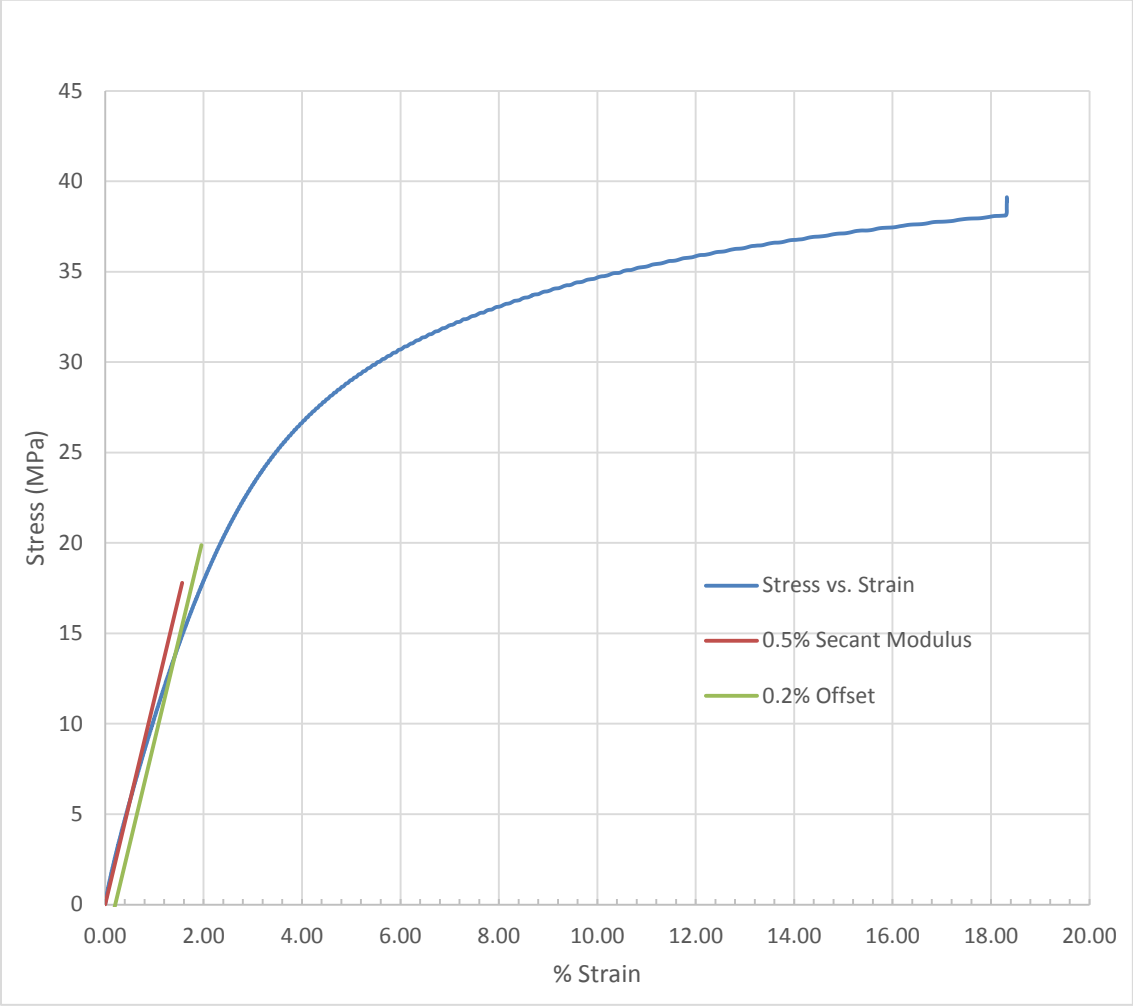

Figure 31. Stress-Strain Curve for FFF PA6 Nylon, Treatment 1; Printing Order, 10; Test Order, 16; Gage Area, 0.0828 in^2; Load Rate, 3.035 lb-force/sec; Testing Room Temperature, 72.3 Degrees Fahrenheit; Testing Room Relative Humidity, 45%

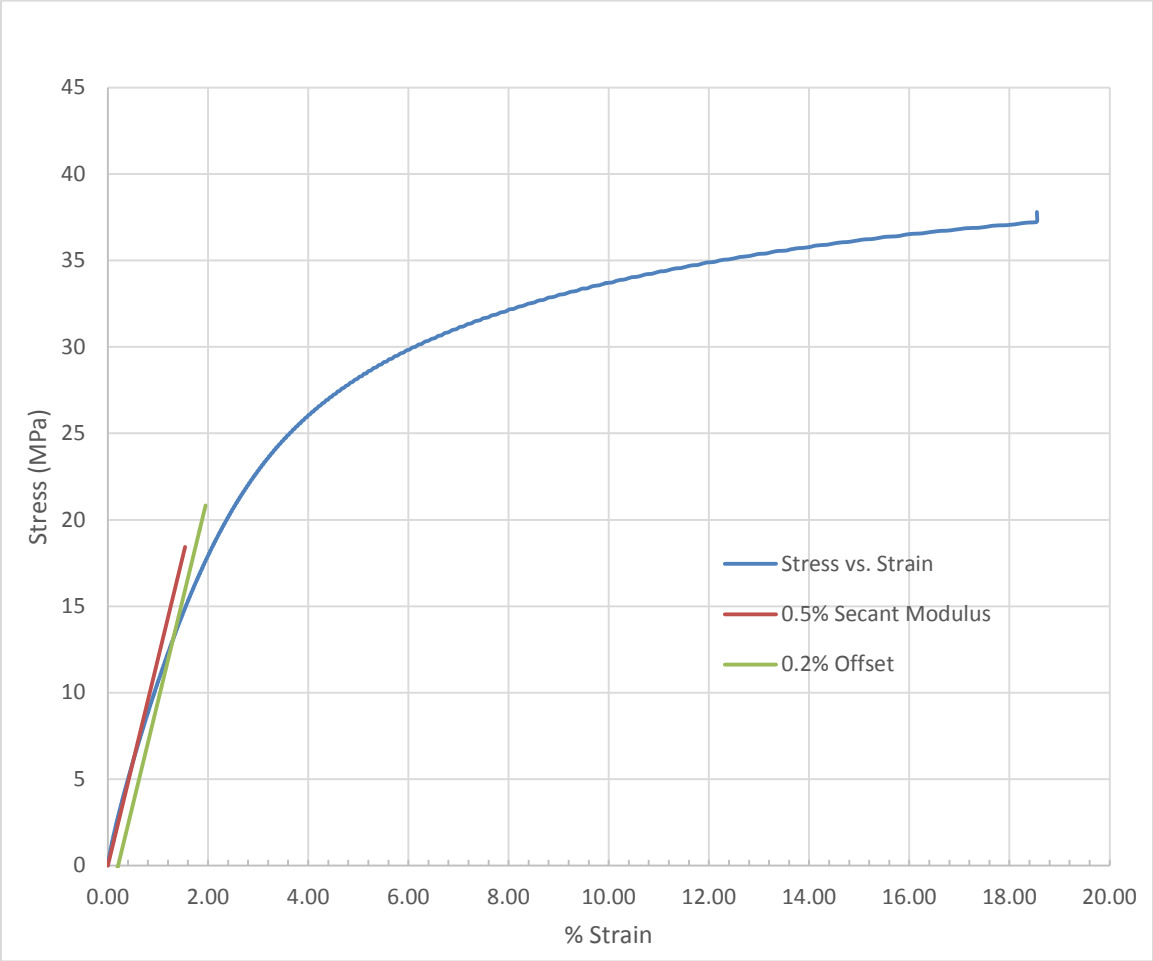

Figure 32. Stress-Strain Curve for FFF PA6 Nylon, Treatment 1; Printing Order, 12; Test Order, 15; Gage Area, 0.0831 in^2; Load Rate, 3.048 lb-force/sec; Testing Room Temperature, 72.3 Degrees Fahrenheit; Testing Room Relative Humidity, 45%

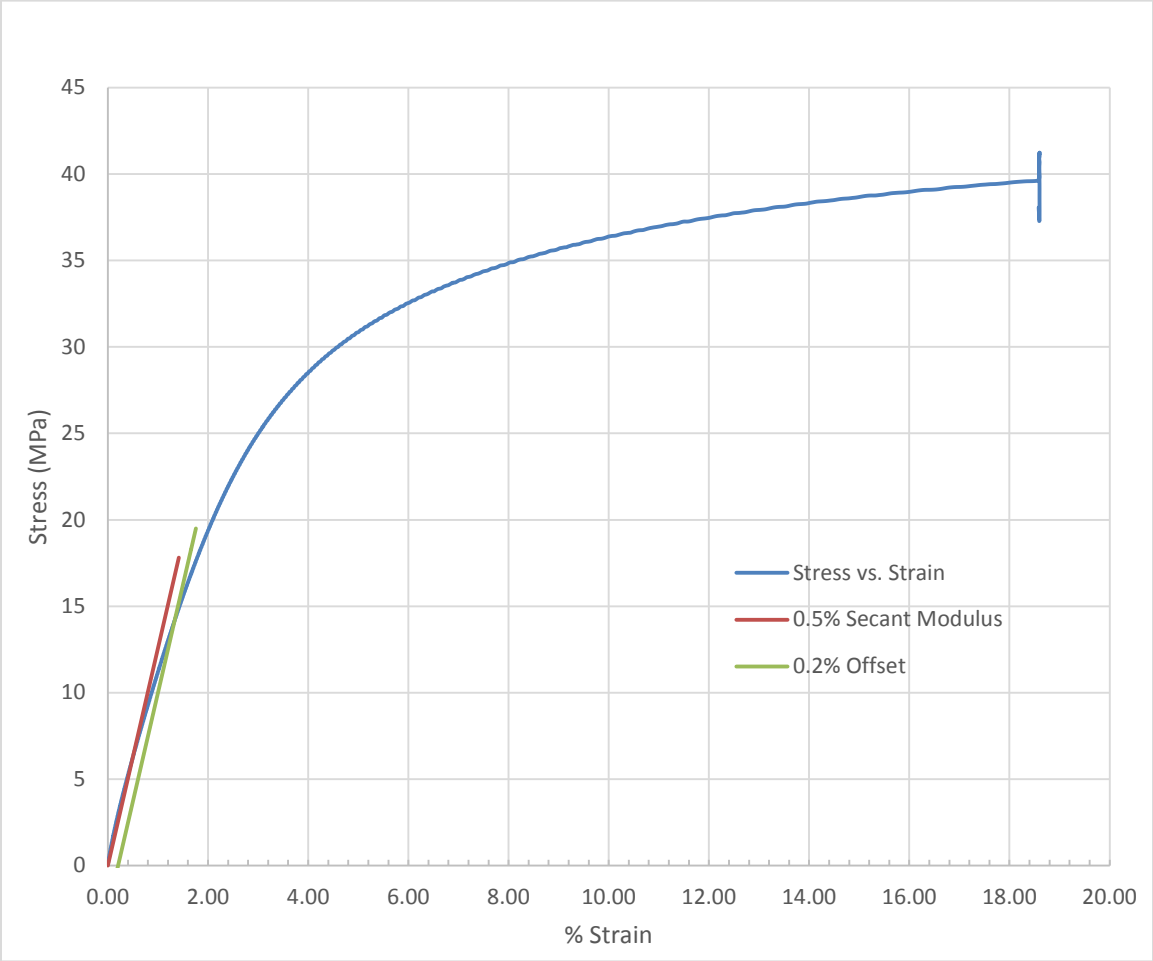

Figure 33. Stress-Strain Curve FFF PA6 Nylon, Treatment 1; Printing Order, 17; Test Order, 1; Gage Area, 0.0830 in^2; Load Rate, 3.044 lb-force/sec; Testing Room Temperature, 72.3 Degrees Fahrenheit; Testing Room Relative Humidity, 45%

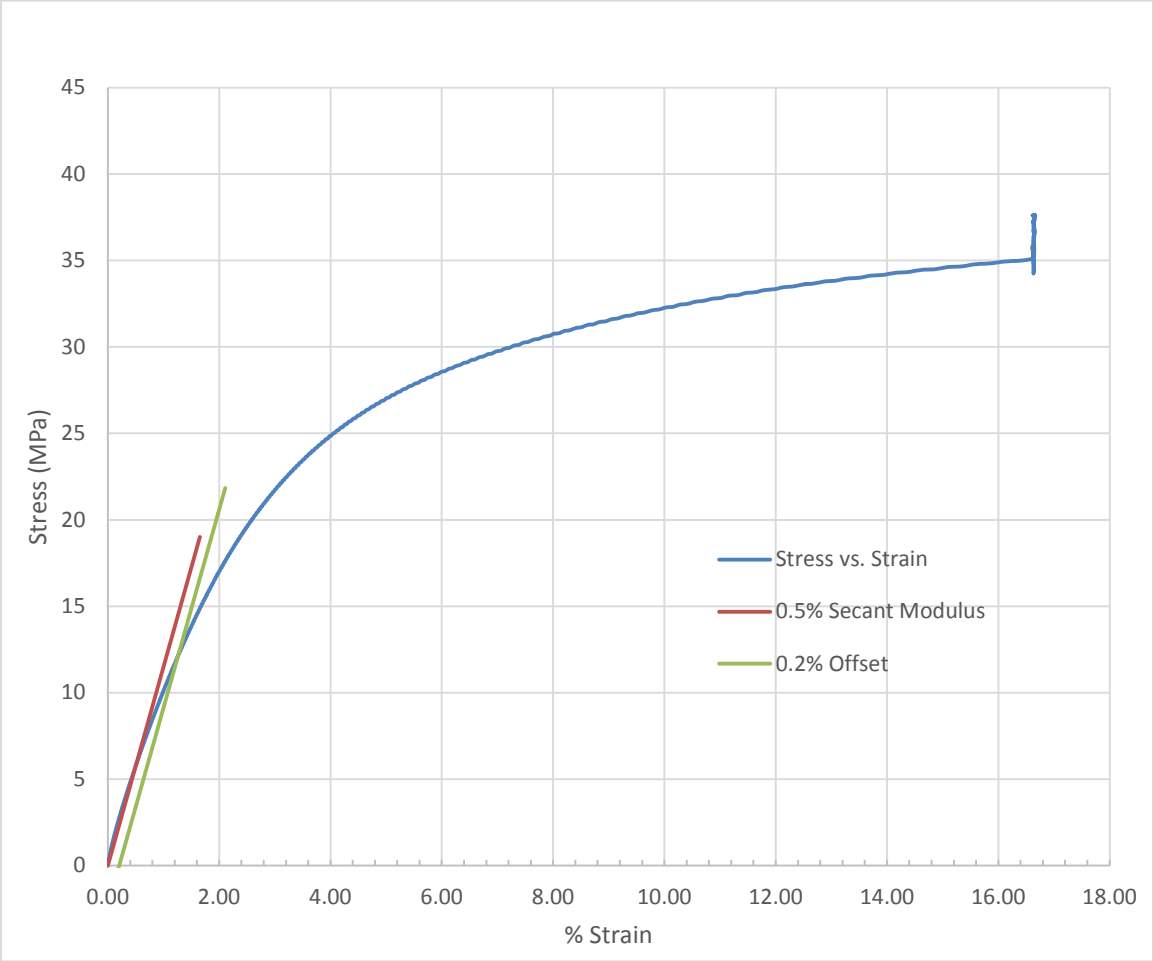

Figure 34. Stress-Strain Curve for FFF PA6 Nylon, Treatment 2; Printing Order, 3; Test Order, 8; Gage Area, 0.0838 in^2; Load Rate, 3.074 lb-force/sec; Testing Room Temperature, 72.3 Degrees Fahrenheit; Testing Room Relative Humidity, 45%

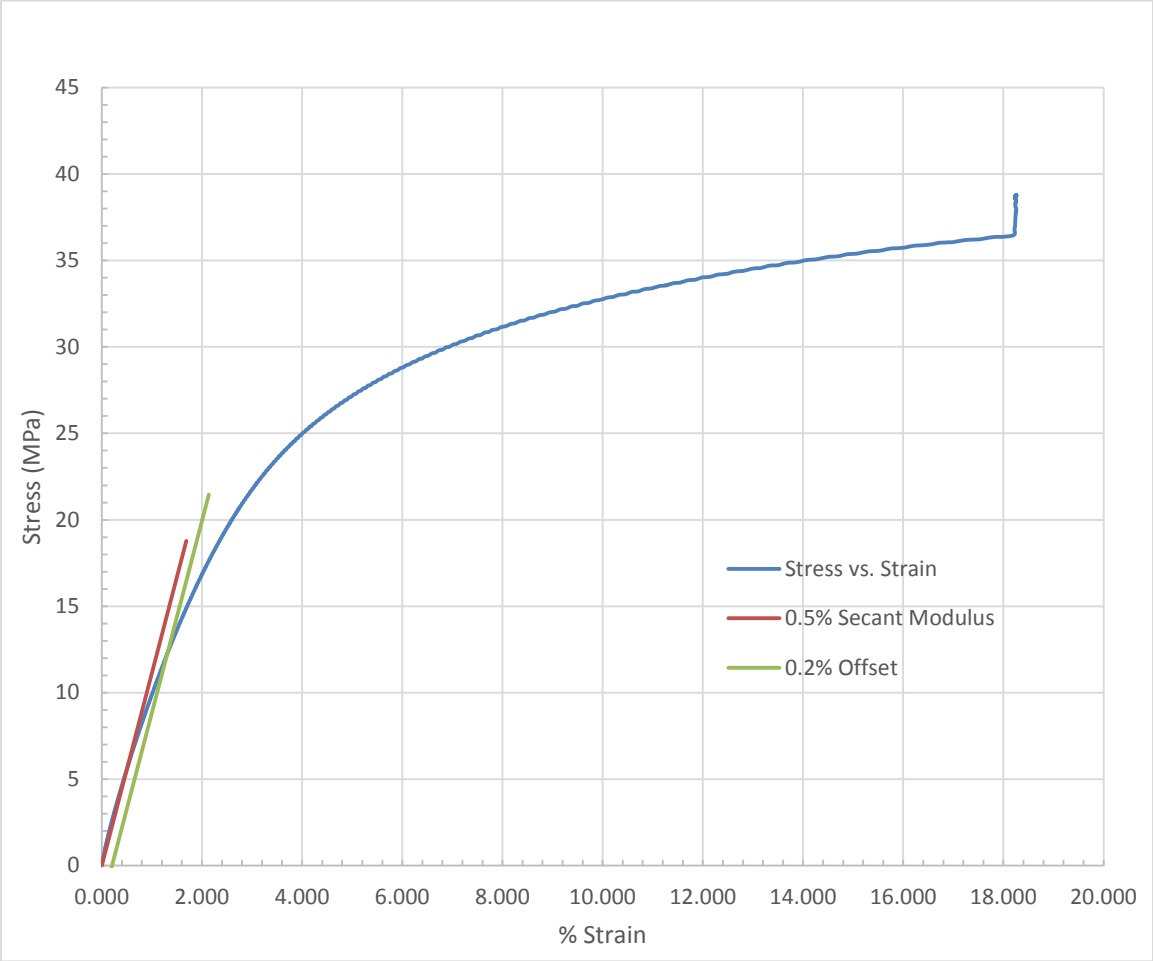

Figure 35. Stress-Strain Curve for FFF PA6 Nylon, Treatment 2; Printing Order, 6; Test Order, 18; Gage Area, 0.0825 in^2; Load Rate, 3.026 lb-force/sec; Testing Room Temperature, 72.3 Degrees Fahrenheit; Testing Room Relative Humidity, 45%

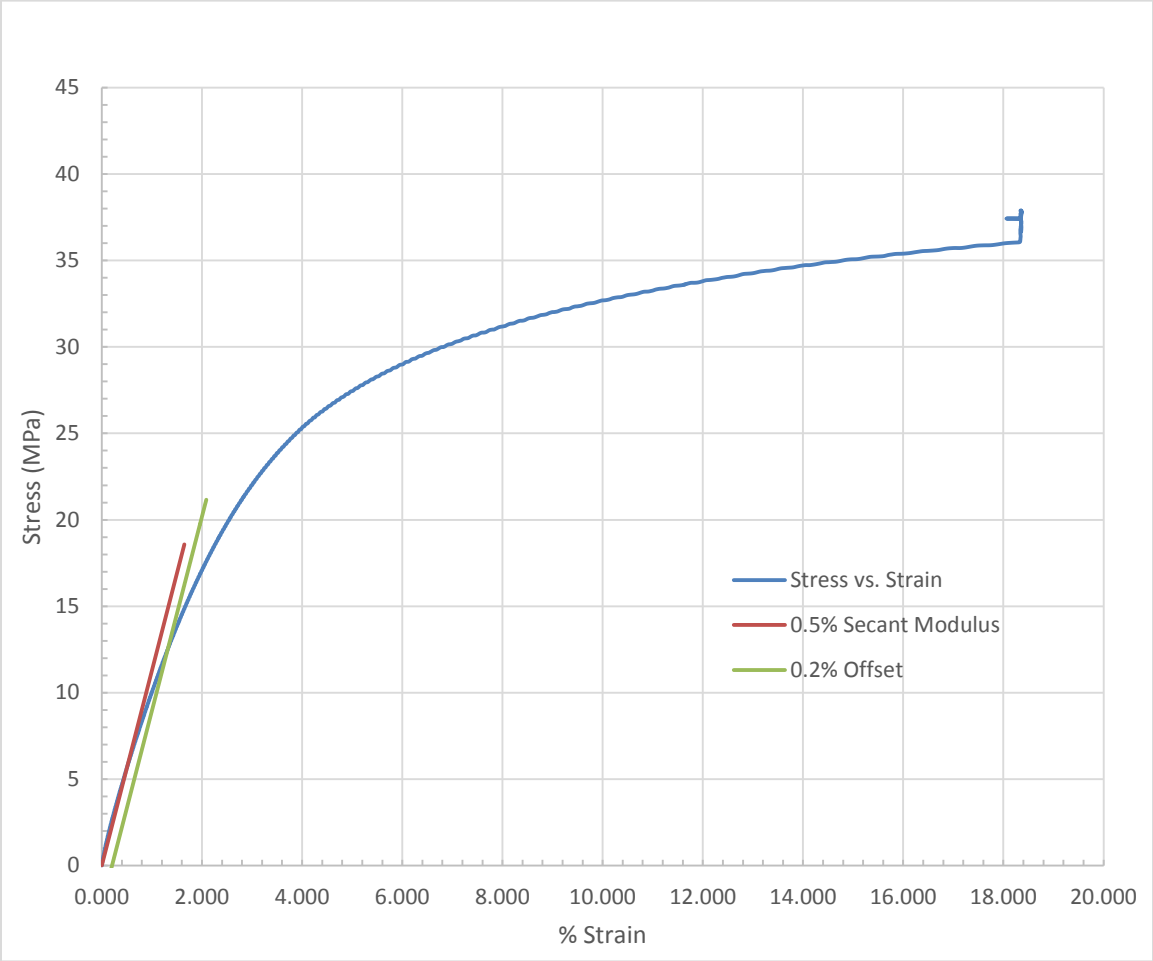

Figure 36. Stress-Strain Curve for FFF PA6 Nylon, Treatment 2; Printing Order, 13; Test Order, 7; Gage Area, 0.0856 in^2; Load Rate, 3.139 lb-force/sec; Testing Room Temperature, 72.3 Degrees Fahrenheit; Testing Room Relative Humidity, 45%

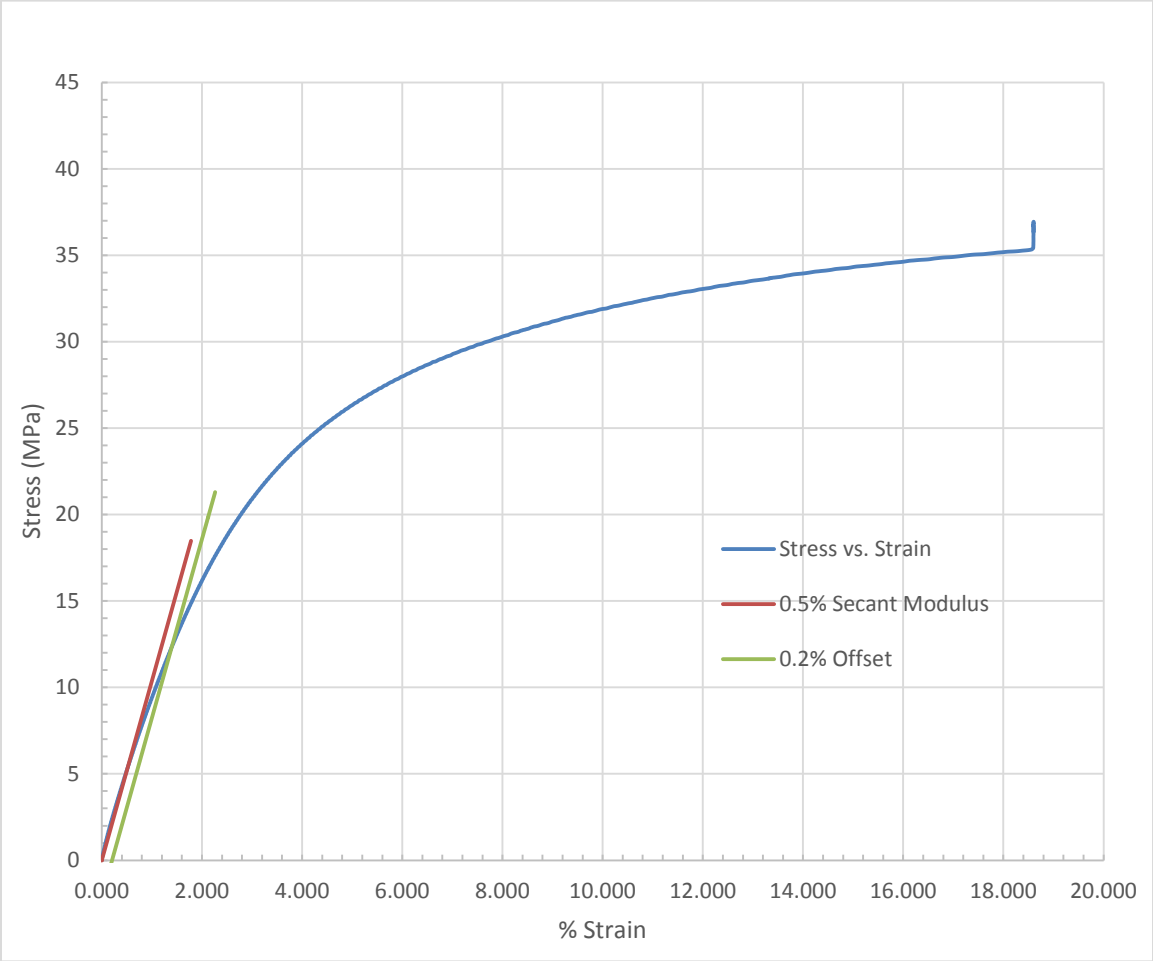

Figure 37. Stress-Strain Curve for FFF PA6 Nylon, Treatment 3; Printing Order, 4; Test Order, 12; Gage Area, 0.0818 in^2; Load Rate, 2.999 lb-force/sec; Testing Room Temperature, 72.3 Degrees Fahrenheit; Testing Room Relative Humidity, 45%

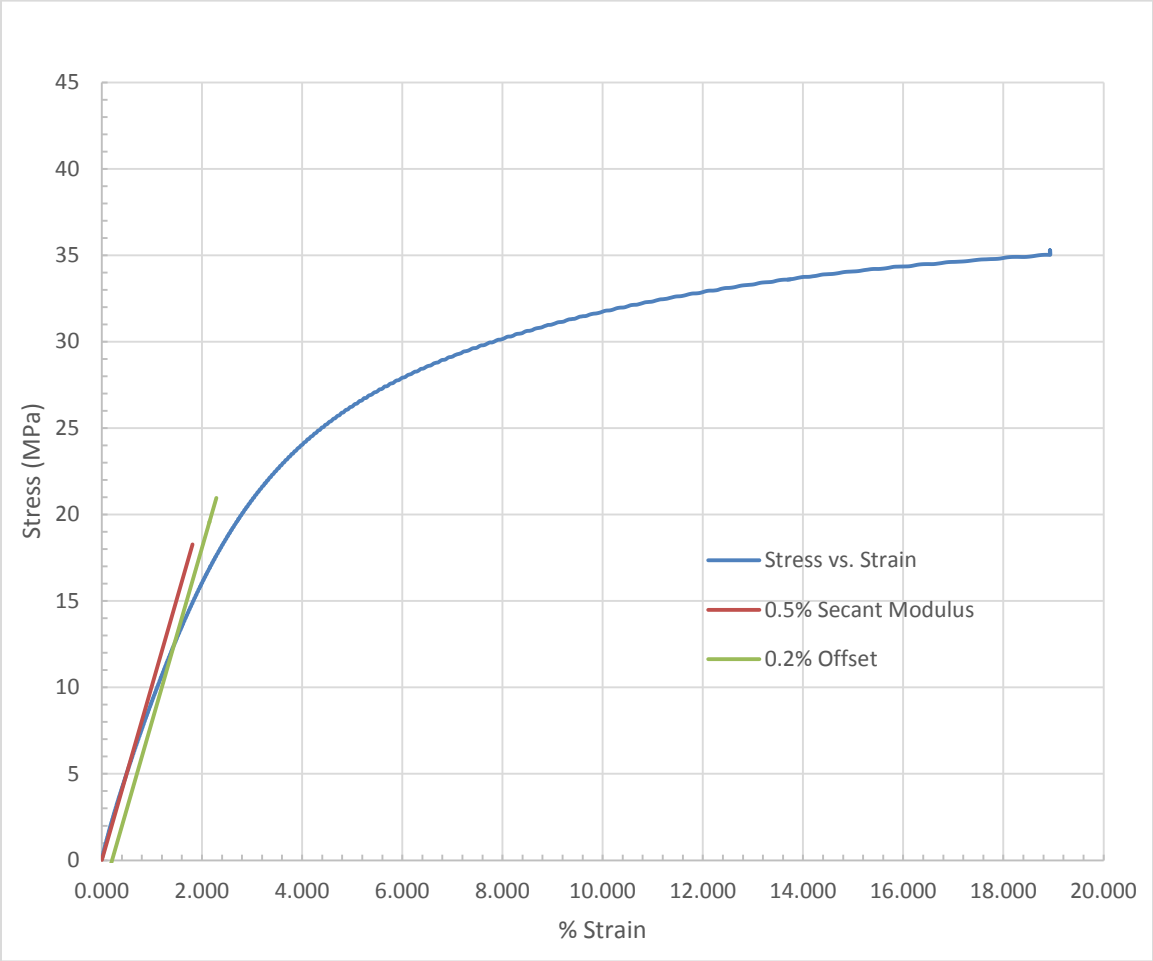

Figure 38. Stress-Strain Curve for FFF PA6 Nylon, Treatment 3; Printing Order, 11; Test Order, 17; Gage Area, 0.0824 in^2; Load Rate, 3.021 lb-force/sec; Testing Room Temperature, 72.3 Degrees Fahrenheit; Testing Room Relative Humidity, 45%

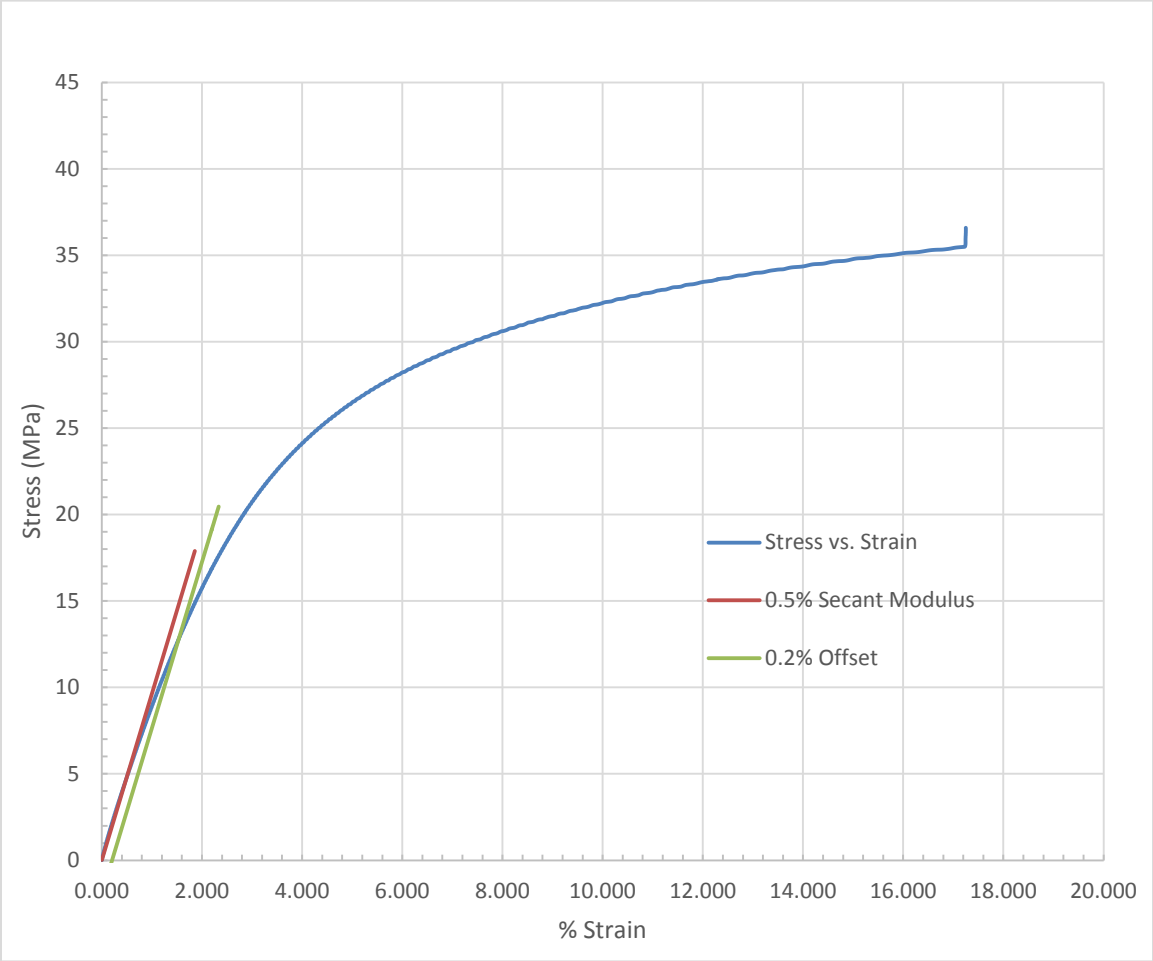

Figure 39. Stress-Strain Curve for FFF PA6 Nylon, Treatment 3; Printing Order, 16; Test Order, 13; Gage Area, 0.0822 in^2; Load Rate, 3.015 lb-force/sec; Testing Room Temperature, 72.3 Degrees Fahrenheit; Testing Room Relative Humidity, 45%

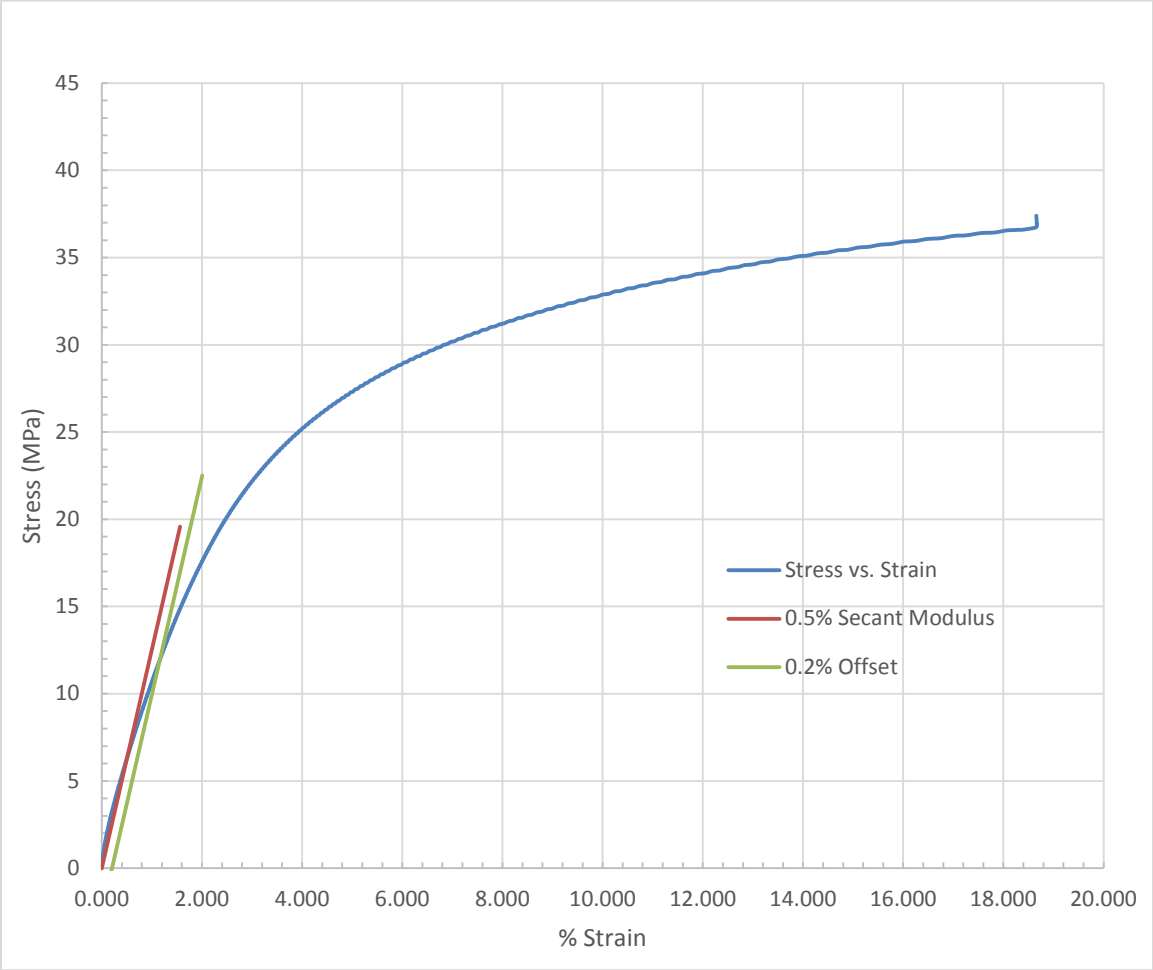

Figure 40. Stress-Strain Curve for FFF PA6 Nylon, Treatment 4; Printing Order, 1; Test Order, 4; Gage Area, 0.0832 in^2; Load Rate, 3.049 lb-force/sec; Testing Room Temperature, 72.3 Degrees Fahrenheit; Testing Room Relative Humidity, 45%

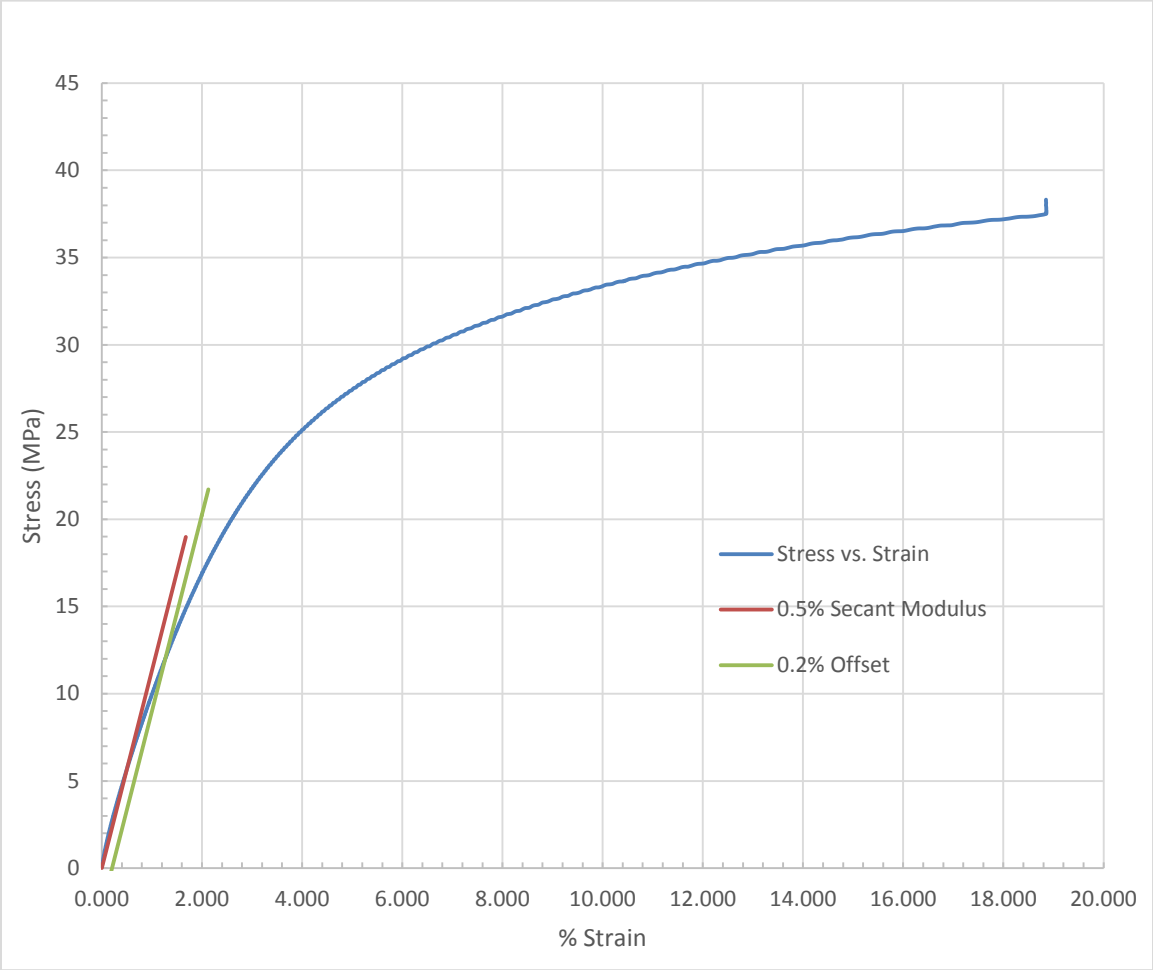

Figure 41. Stress-Strain Curve for FFF PA6 Nylon, Treatment 4; Printing Order, 8; Test Order, 9; Gage Area, 0.0822 in^2; Load Rate, 3.015 lb-force/sec; Testing Room Temperature, 72.3 Degrees Fahrenheit; Testing Room Relative Humidity, 45%

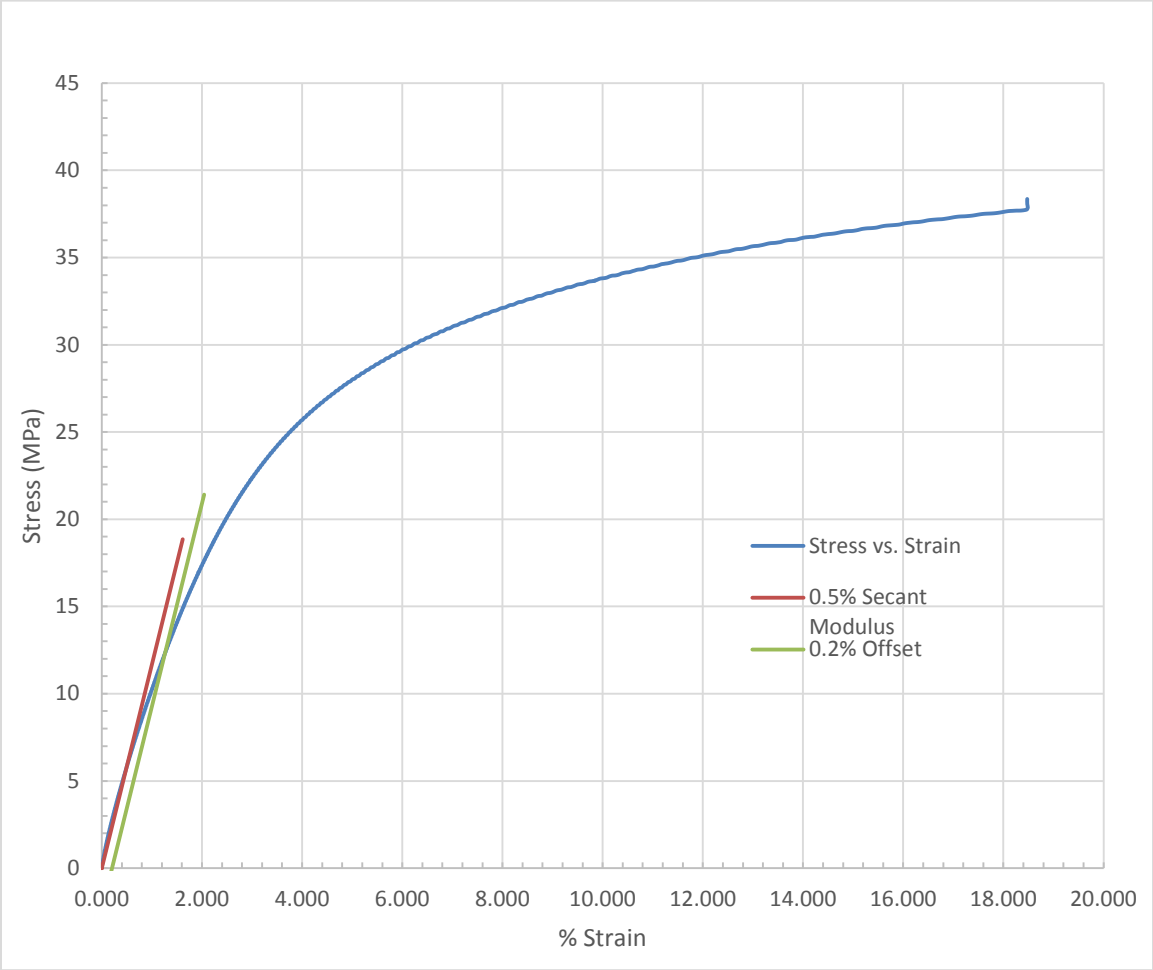

Figure 42. Stress-Strain Curve for FFF PA6 Nylon, Treatment 4; Printing Order, 14; Test Order, 14; Gage Area, 0.0836 in^2; Load Rate, 3.065 lb-force/sec; Testing Room Temperature, 72.3 Degrees Fahrenheit; Testing Room Relative Humidity, 45%

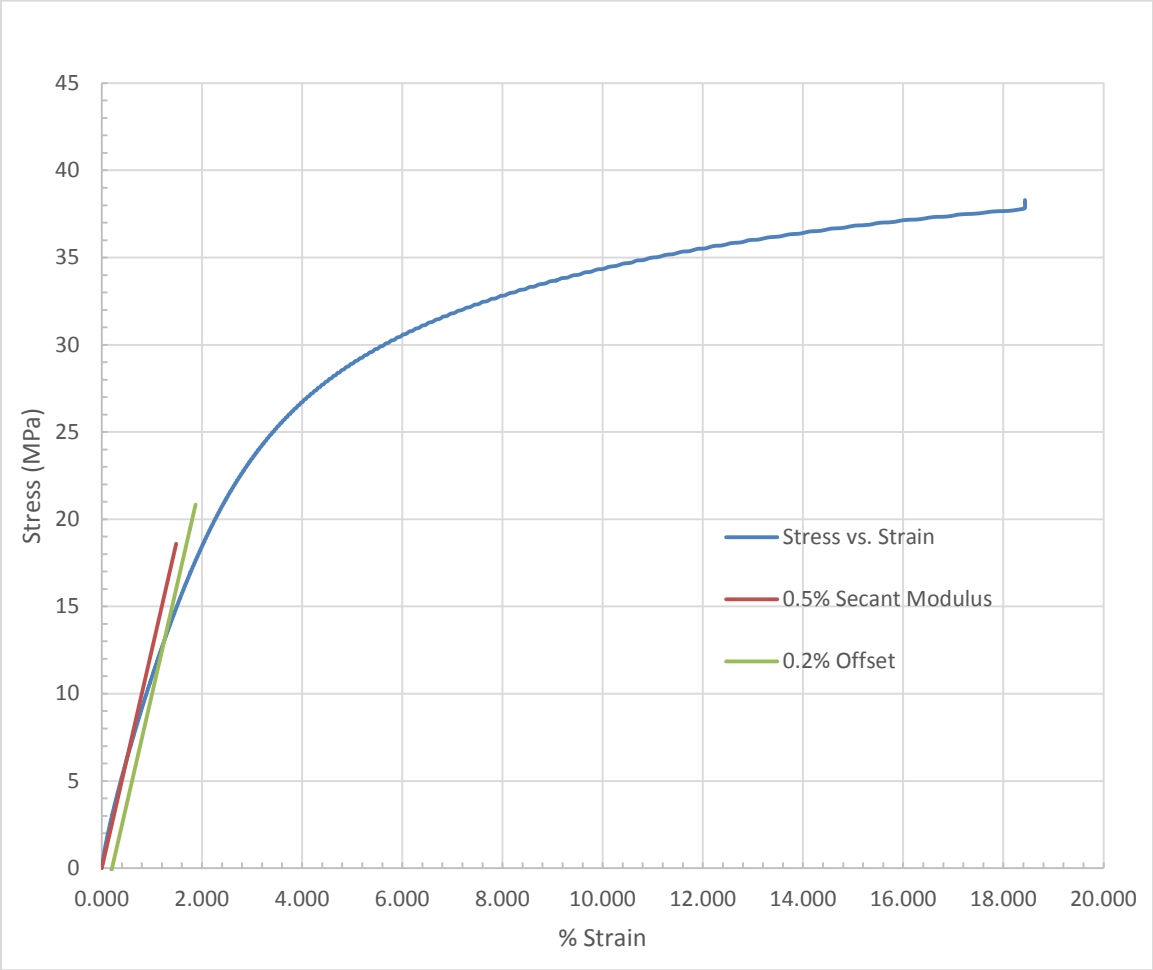

Figure 43. Stress-Strain Curve for FFF PA6 Nylon, Treatment 5; Printing Order, 5; Test Order, 5; Gage Area, 0.0832 in^2; Load Rate, 3.050 lb-force/sec; Testing Room Temperature, 72.3 Degrees Fahrenheit; Testing Room Relative Humidity, 45%

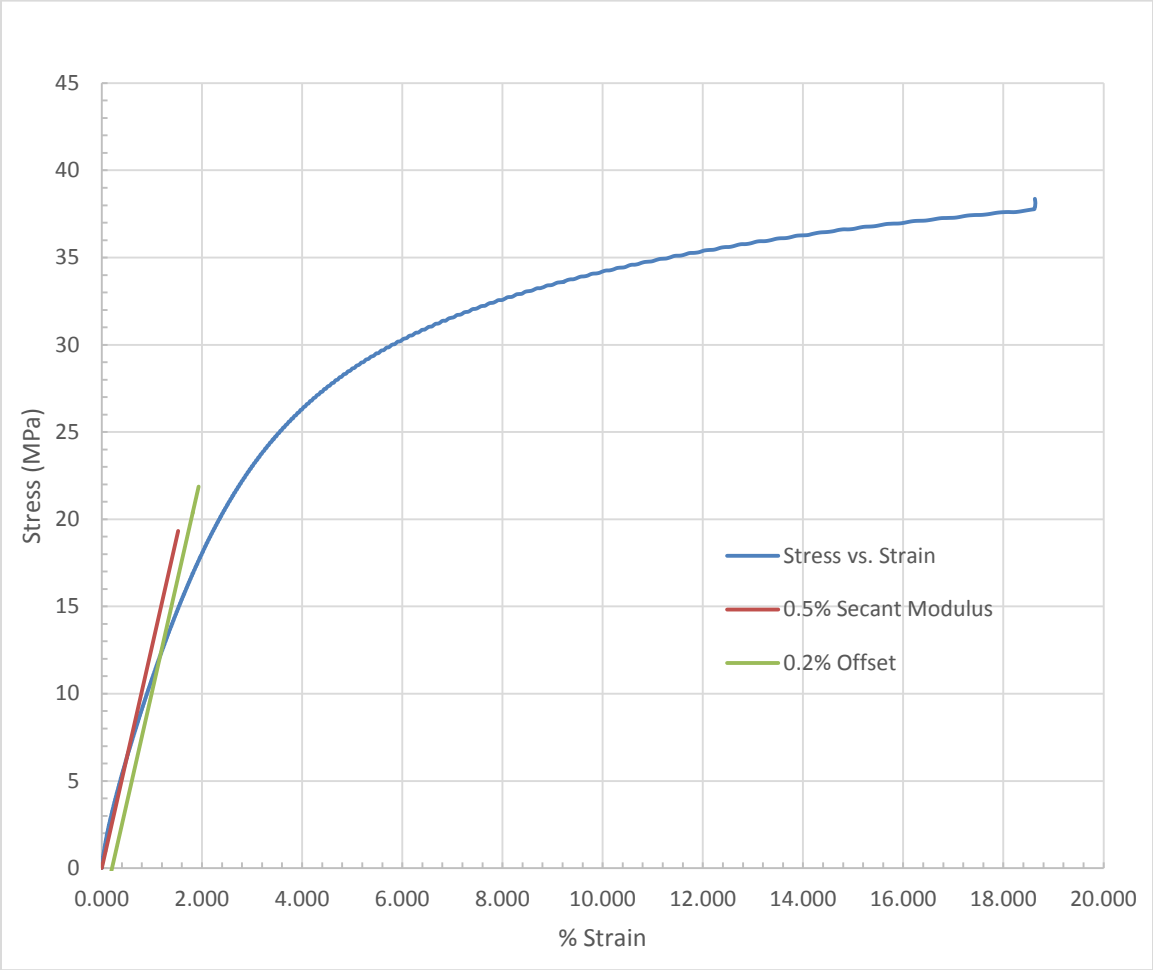

Figure 44. Stress-Strain Curve for FFF PA6 Nylon, Treatment 5; Printing Order, 7; Test Order, 2; Gage Area, 0.0845 in^2; Load Rate, 3.098 lb-force/sec; Testing Room Temperature, 72.3 Degrees Fahrenheit; Testing Room Relative Humidity, 45%

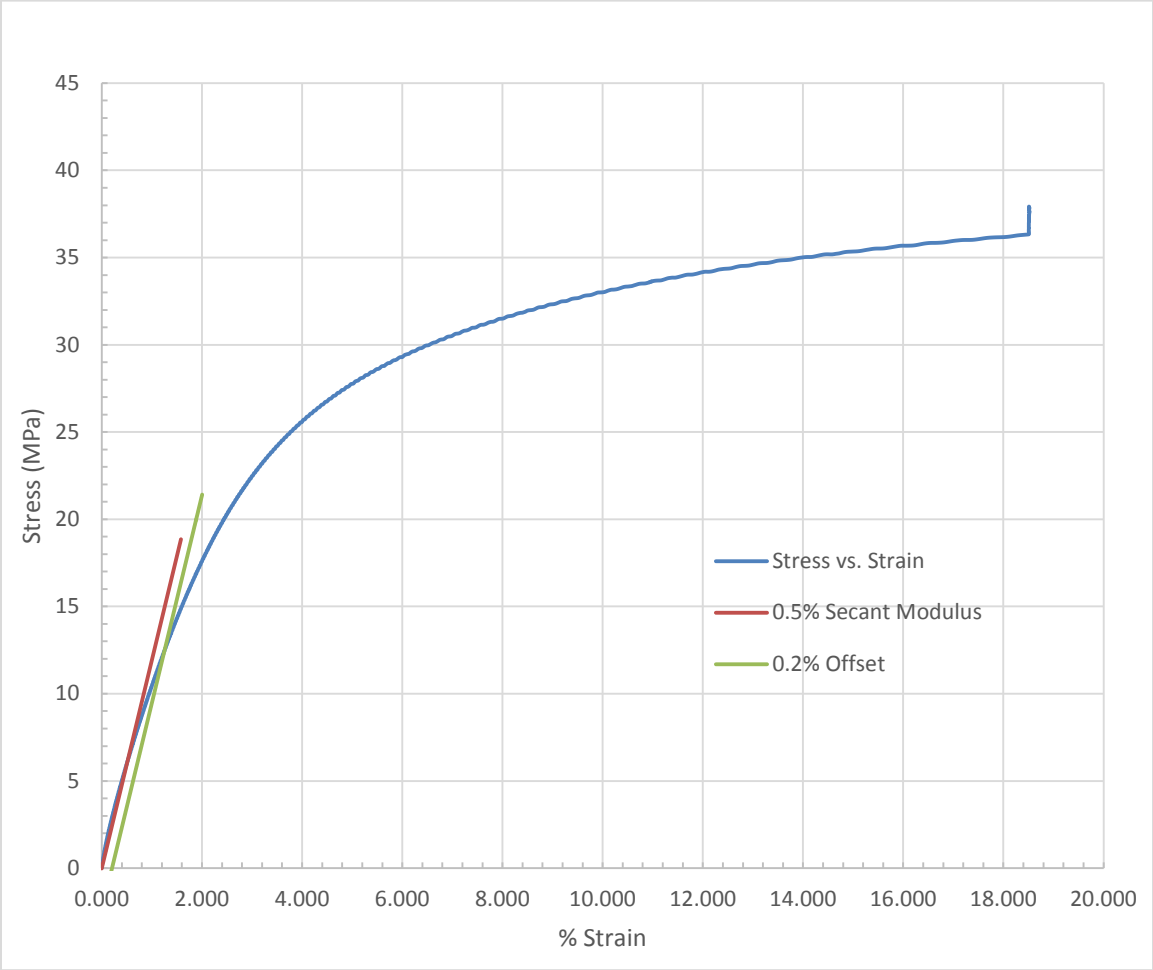

Figure 45. Stress-Strain Curve for FFF PA6 Nylon, Treatment 5; Printing Order, 9; Test Order, 11; Gage Area, 0.0860 in^2; Load Rate, 3.154 lb-force/sec; Testing Room Temperature, 72.3 Degrees Fahrenheit; Testing Room Relative Humidity, 45%

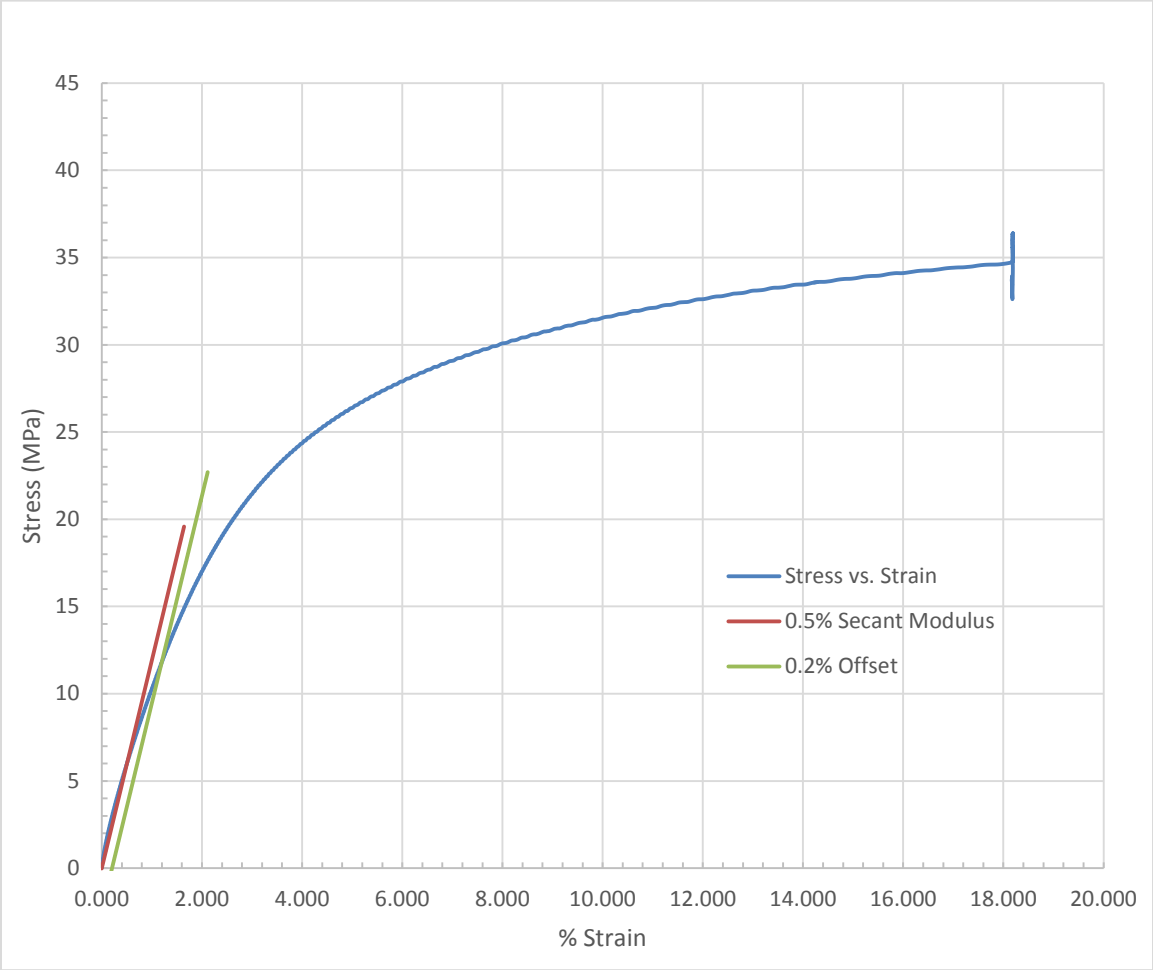

Figure 46. Stress-Strain Curve for FFF PA6 Nylon, Treatment 6; Printing Order, 2; Test Order, 10; Gage Area, 0.0838 in^2; Load Rate, 3.073 lb-force/sec; Testing Room Temperature, 72.3 Degrees Fahrenheit; Testing Room Relative Humidity, 45%

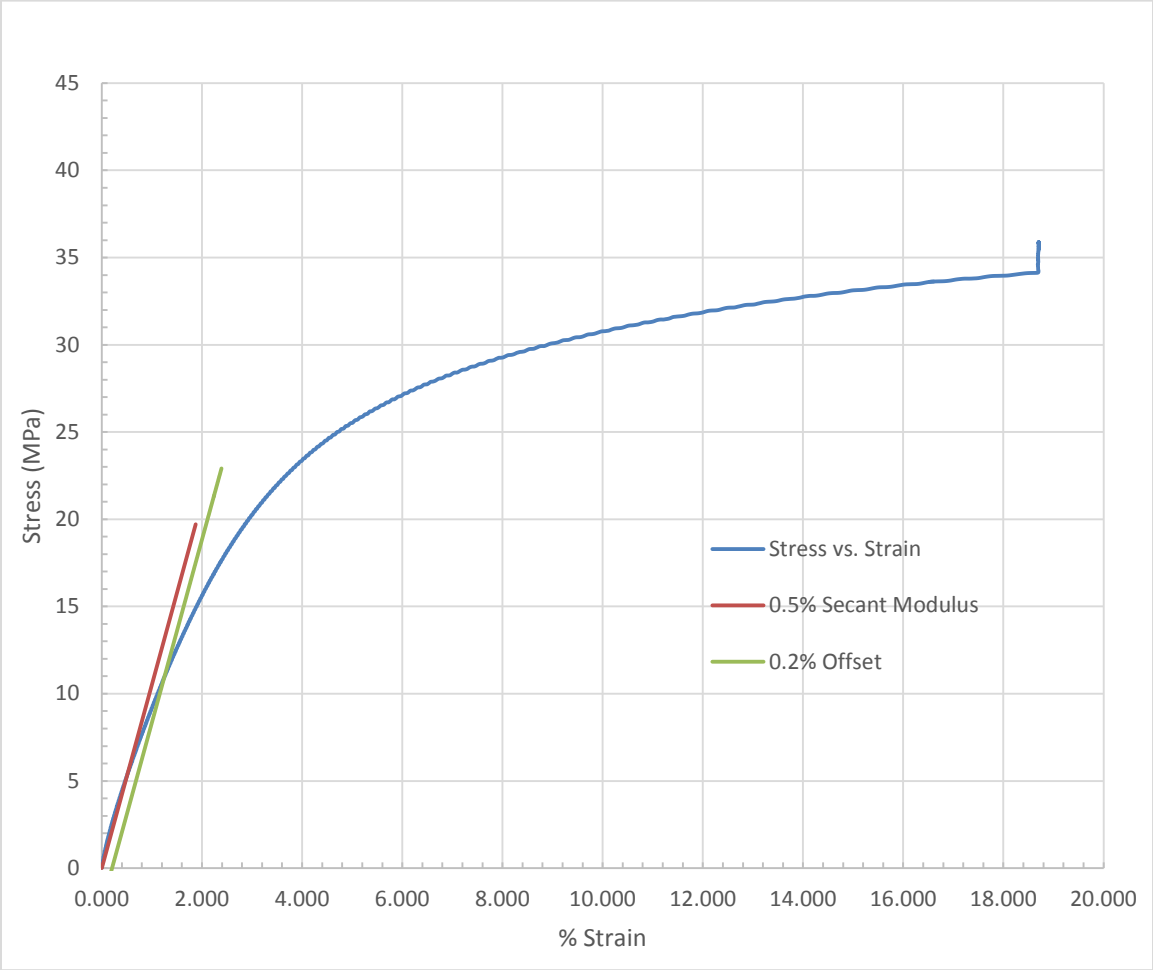

Figure 47. Stress-Strain Curve for FFF PA6 Nylon, Treatment 6; Printing Order, 15; Test Order, 3; Gage Area, 0.0847 in^2; Load Rate, 3.104 lb-force/sec; Testing Room Temperature, 72.3 Degrees Fahrenheit; Testing Room Relative Humidity, 45%

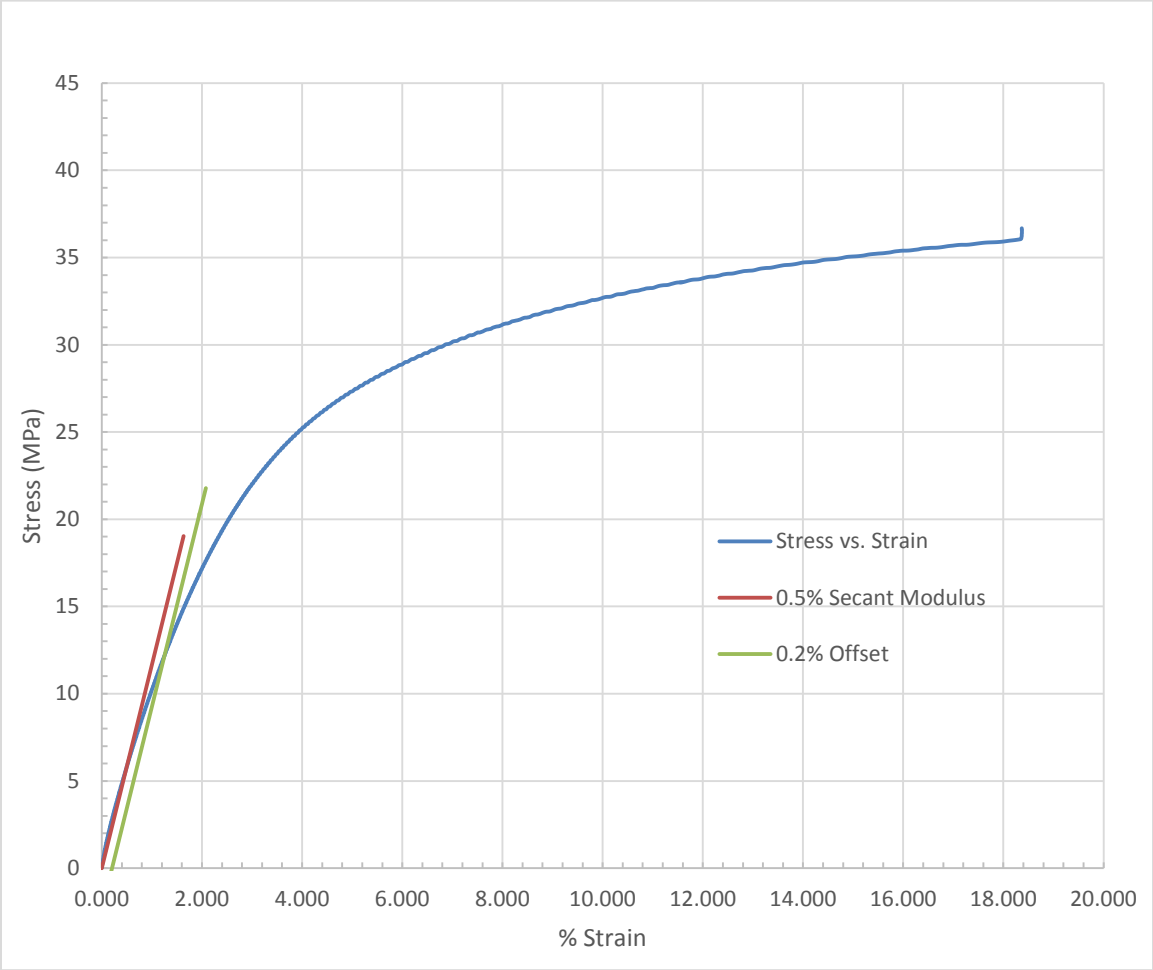

Figure 48. Stress-Strain Curve for FFF PA6 Nylon, Treatment 6; Printing Order, 18; Test Order, 6; Gage Area, 0.0796 in^2; Load Rate, 2.918 lb-force/sec; Testing Room Temperature, 72.3 Degrees Fahrenheit; Testing Room Relative Humidity, 45%

Appendix E: One-Way ANOVA Table for Density by Layer Height

Table 11. One-Way ANOVA Table for Density by Layer Height

Oneway Analysis of Density (g/cm^3) By Layer height (mm)

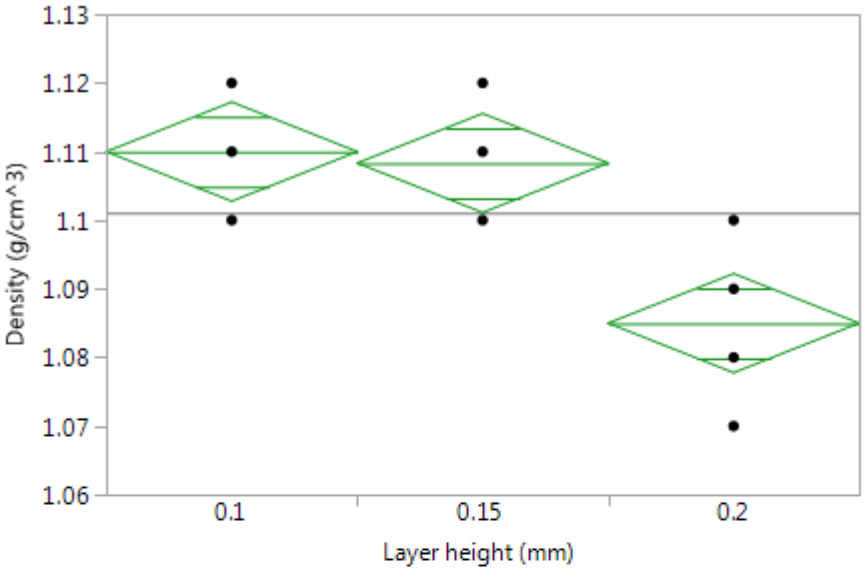

Oneway Anova

Summary of Fit

Rsquare	0.694079
Adj Rsquare	0.653289
Root Mean Square Error	0.0083
Mean of Response	1.101111
Observations (or Sum Wgts)	18

Analysis of Variance

Source	DF	Sum of Squares	Mean Square	F Ratio	Prob > F
Layer height (mm)	2	0.00234444	0.001172	17.0161	0.0001*
Error	15	0.00103333	0.000069		
C. Total	17	0.00337778			

Means for Oneway Anova

Level	Number	Mean	Std Error	Lower 95%	Upper 95%
0.1	6	1.11000	0.00339	1.1028	1.1172
0.15	6	1.10833	0.00339	1.1011	1.1156
0.2	6	1.08500	0.00339	1.0778	1.0922

Std Error uses a pooled estimate of error variance

Appendix F: One-Way ANOVA Tables for Mechanical Properties by Density

Table 12. One-Way ANOVA Table of Tensile Modulus by Density

Oneway Analysis of Tensile Modulus (GPa) By Density

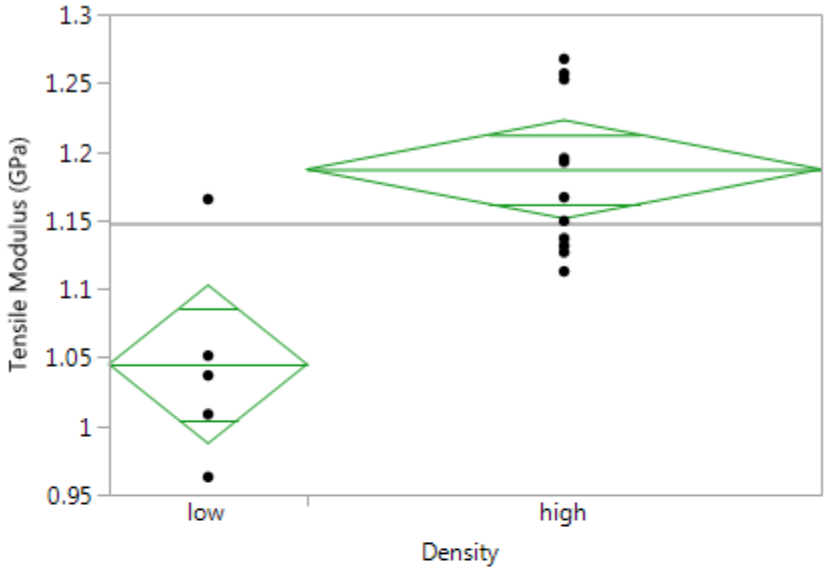

Oneway Anova

Summary of Fit

Rsquare	0.551708
Adj Rsquare	0.52369
Root Mean Square Error	0.060849
Mean of Response	1.147622
Observations (or Sum Wgts)	18

Analysis of Variance

Source	DF	Sum of Squares	Mean Square	F Ratio	Prob > F
Density	1	0.07290914	0.072909	19.6910	0.0004*
Error	16	0.05924249	0.003703		
C. Total	17	0.13215163			

Means for Oneway Anova

Level	Number	Mean	Std Error	Lower 95%	Upper 95%
low	5	1.04500	0.02721	0.9873	1.1027
high	13	1.18709	0.01688	1.1513	1.2229

Std Error uses a pooled estimate of error variance

Table 13. One-Way ANOVA table of Yield Stress by Density

Oneway Analysis of Yield Stress (MPa) (.2% strain offset) By Density

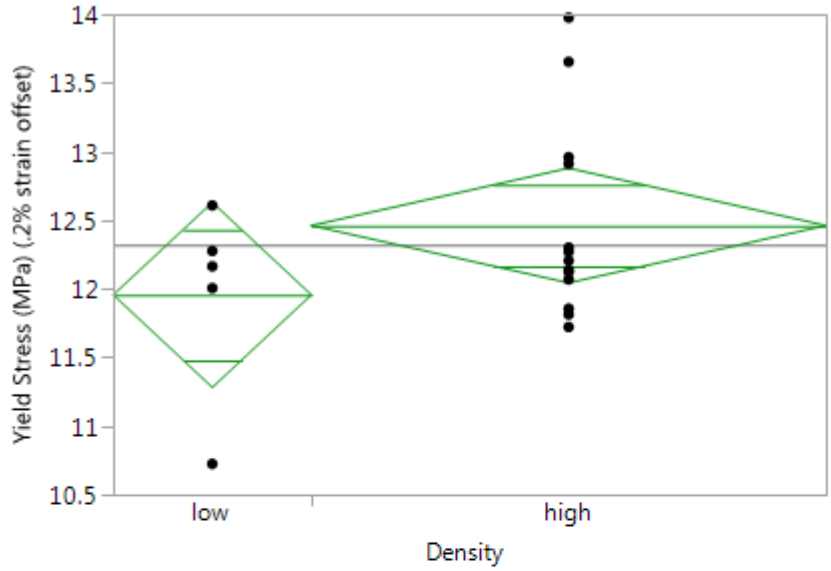

Oneway Anova

Summary of Fit

Rsquare	0.102512
Adj Rsquare	0.046419
Root Mean Square Error	0.710973
Mean of Response	12.32089
Observations (or Sum Wgts)	18

Analysis of Variance

Source	DF	Sum of Squares	Mean Square	F Ratio	Prob > F
Density	1	0.9237875	0.923788	1.8275	0.1952
Error	16	8.0877283	0.505483		
C. Total	17	9.0115158			

Means for Oneway Anova

Level	Number	Mean	Std Error	Lower 95%	Upper 95%
low	5	11.9556	0.31796	11.282	12.630
high	13	12.4614	0.19719	12.043	12.879

Std Error uses a pooled estimate of error variance

Table 14. One-Way ANOVA Table of Percent Strain at Yield by Density

Oneway Analysis of % Strain at Yield By Density

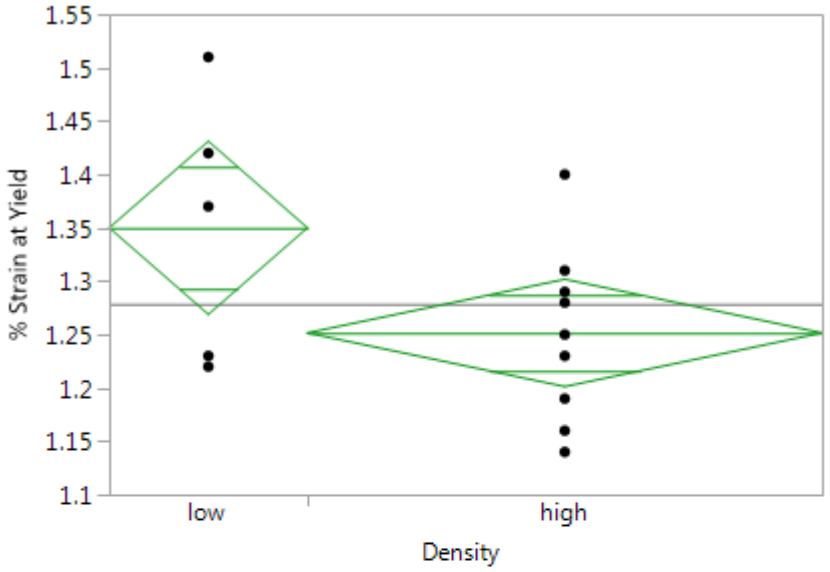

Oneway Anova

Summary of Fit

Rsquare	0.230353
Adj Rsquare	0.18225
Root Mean Square Error	0.085502
Mean of Response	1.278889
Observations (or Sum Wgts)	18

Analysis of Variance

Source	DF	Sum of Squares	Mean Square	F Ratio	Prob > F
Density	1	0.03500855	0.035009	4.7888	0.0438*
Error	16	0.11696923	0.007311		
C. Total	17	0.15197778			

Means for Oneway Anova

Level	Number	Mean	Std Error	Lower 95%	Upper 95%
low	5	1.35000	0.03824	1.2689	1.4311
high	13	1.25154	0.02371	1.2013	1.3018

Std Error uses a pooled estimate of error variance

Table 15. One-Way ANOVA Table of Ultimate Tensile Strength by Density

Oneway Analysis of Ultimate Tensile Strength (MPa) By Density

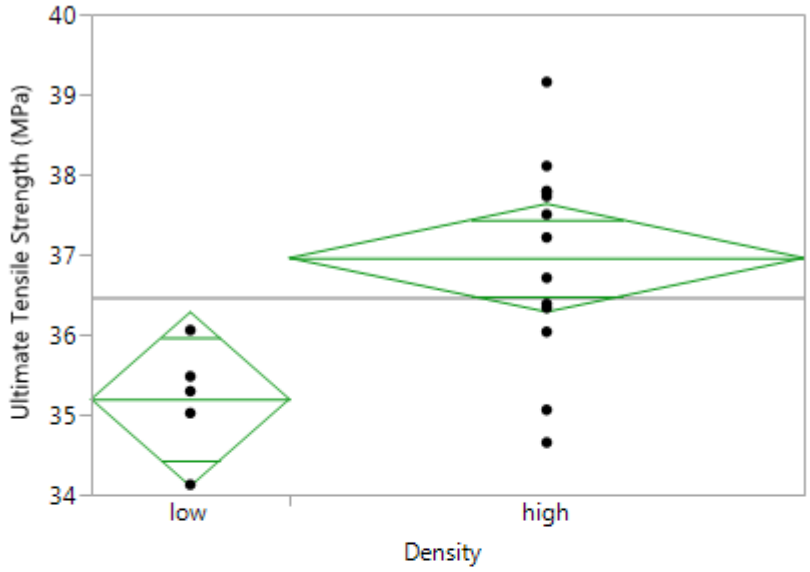

Oneway Anova

Summary of Fit

Rsquare	0.348037
Adj Rsquare	0.307289
Root Mean Square Error	1.146455
Mean of Response	36.46761
Observations (or Sum Wgts)	18

Analysis of Variance

Source	DF	Sum of Squares	Mean Square	F Ratio	Prob > F
Density	1	11.226294	11.2263	8.5413	0.0100*
Error	16	21.029758	1.3144		
C. Total	17	32.256052			

Means for Oneway Anova

Level	Number	Mean	Std Error	Lower 95%	Upper 95%
low	5	35.1942	0.51271	34.107	36.281
high	13	36.9574	0.31797	36.283	37.631

Std Error uses a pooled estimate of error variance

Table 16. One-Way ANOVA Table of Percent Strain at Break by Density

Oneway Analysis of Strain at break (%) By Density

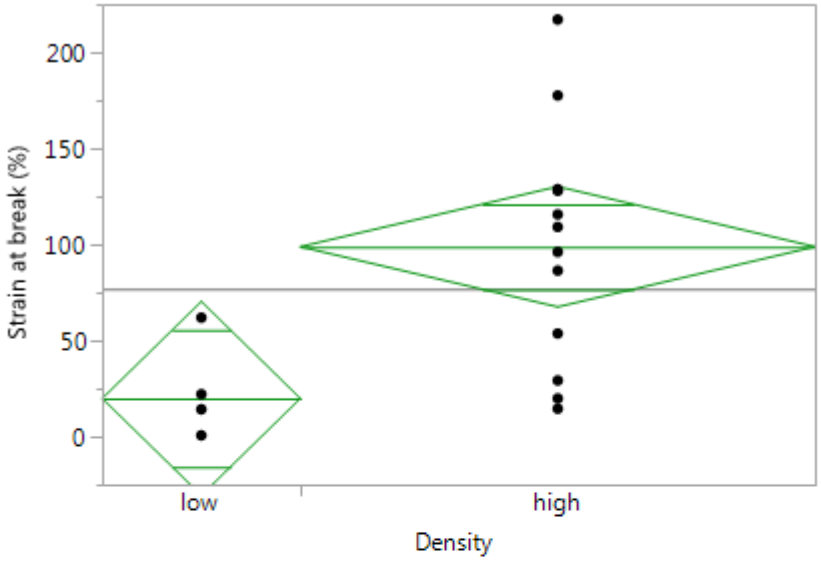

Oneway Anova

Summary of Fit

Rsquare	0.331878
Adj Rsquare	0.29012
Root Mean Square Error	53.23862
Mean of Response	76.92444
Observations (or Sum Wgts)	18

Analysis of Variance

Source	DF	Sum of Squares	Mean Square	F Ratio	Prob > F
Density	1	22526.588	22526.6	7.9477	0.0123*
Error	16	45349.611	2834.4		
C. Total	17	67876.199			

Means for Oneway Anova

Level	Number	Mean	Std Error	Lower 95%	Upper 95%
low	5	19.8820	23.809	-30.59	70.35
high	13	98.8638	14.766	67.56	130.17

Std Error uses a pooled estimate of error variance

Appendix G: Scanning Electron Microscope Photographs

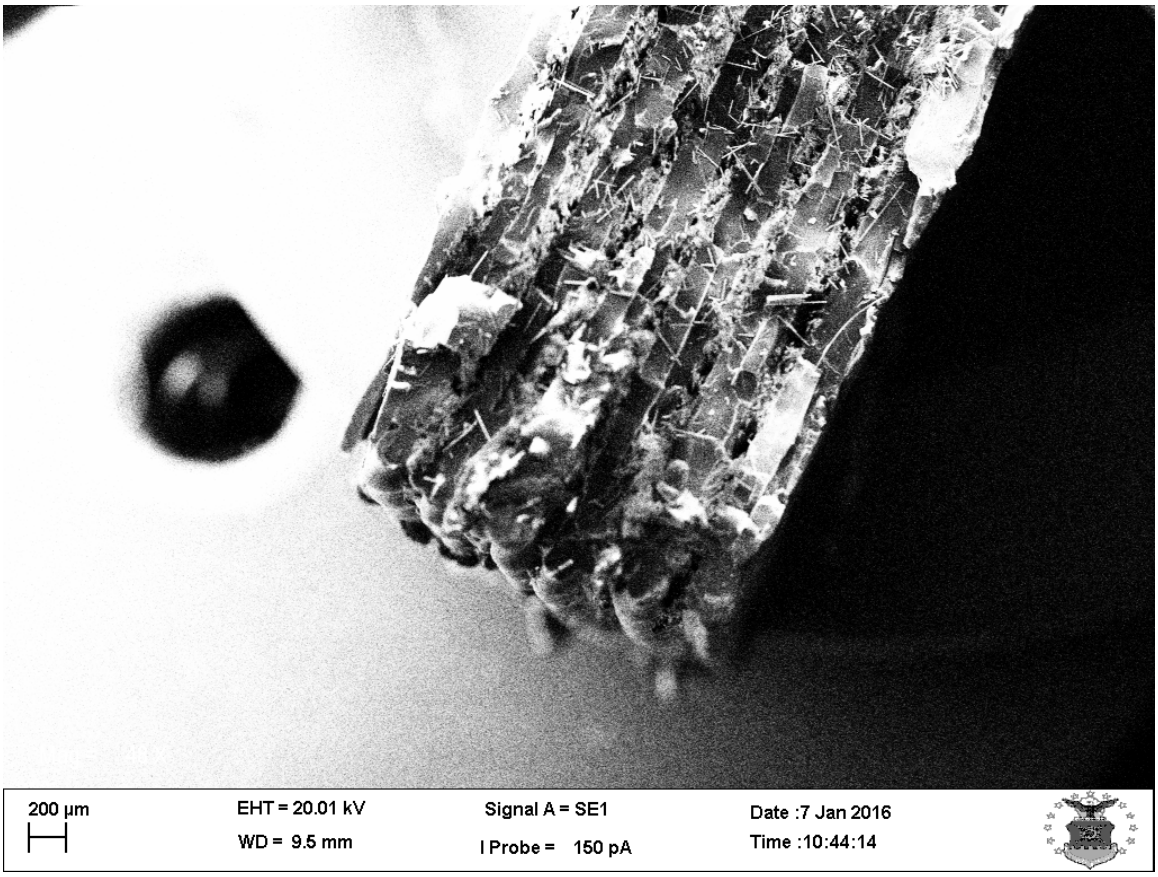

Figure 49. Fracture Surface of Continuous Carbon Fiber Nylon Composite Focusing on Edge of Specimen

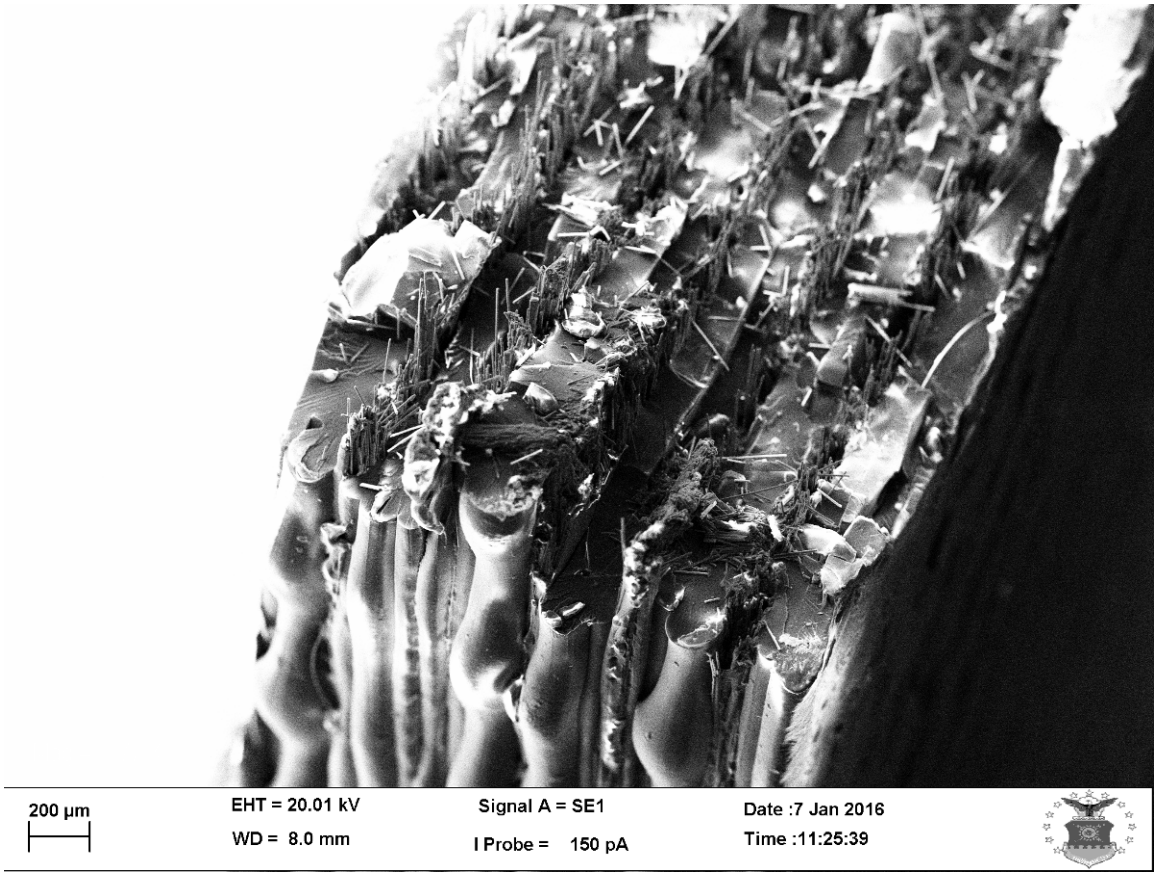

Figure 50. Fracture Surface of Continuous Carbon Fiber Nylon Composite Focusing on Side Edge of Specimen

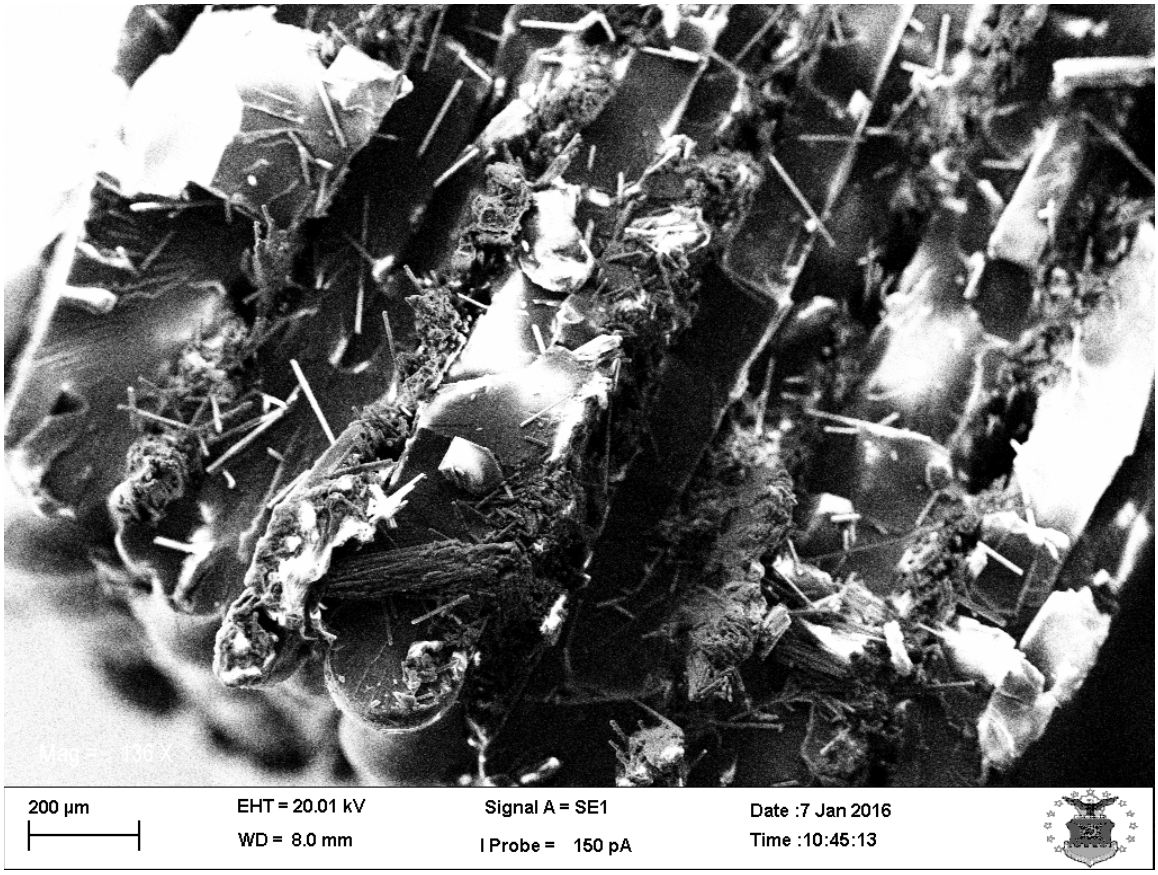

Figure 51. Close-Up View of Fracture Surface of Continuous Carbon Fiber Nylon Composite

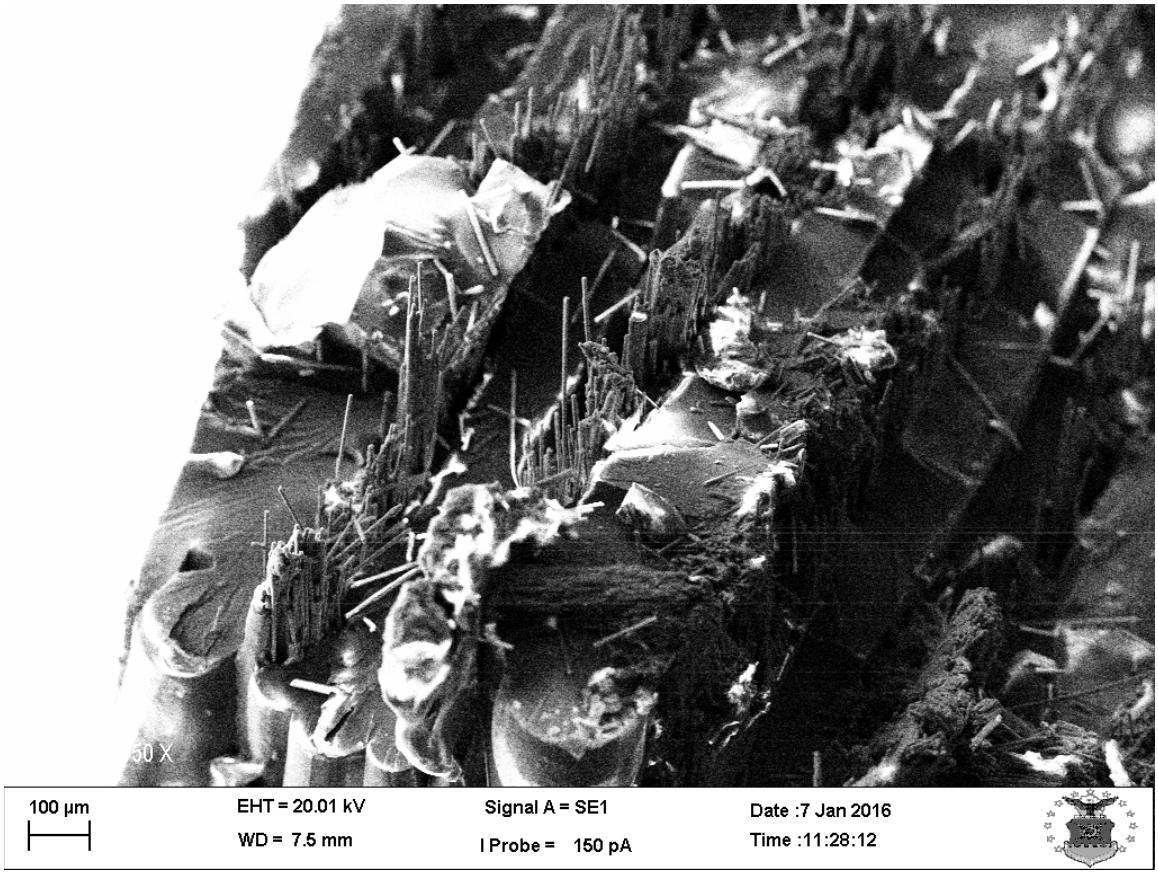

Figure 52. Fracture Surface of Continuous Carbon Fiber Nylon Composite Focusing on Carbon Fibers Between Nylon Layers

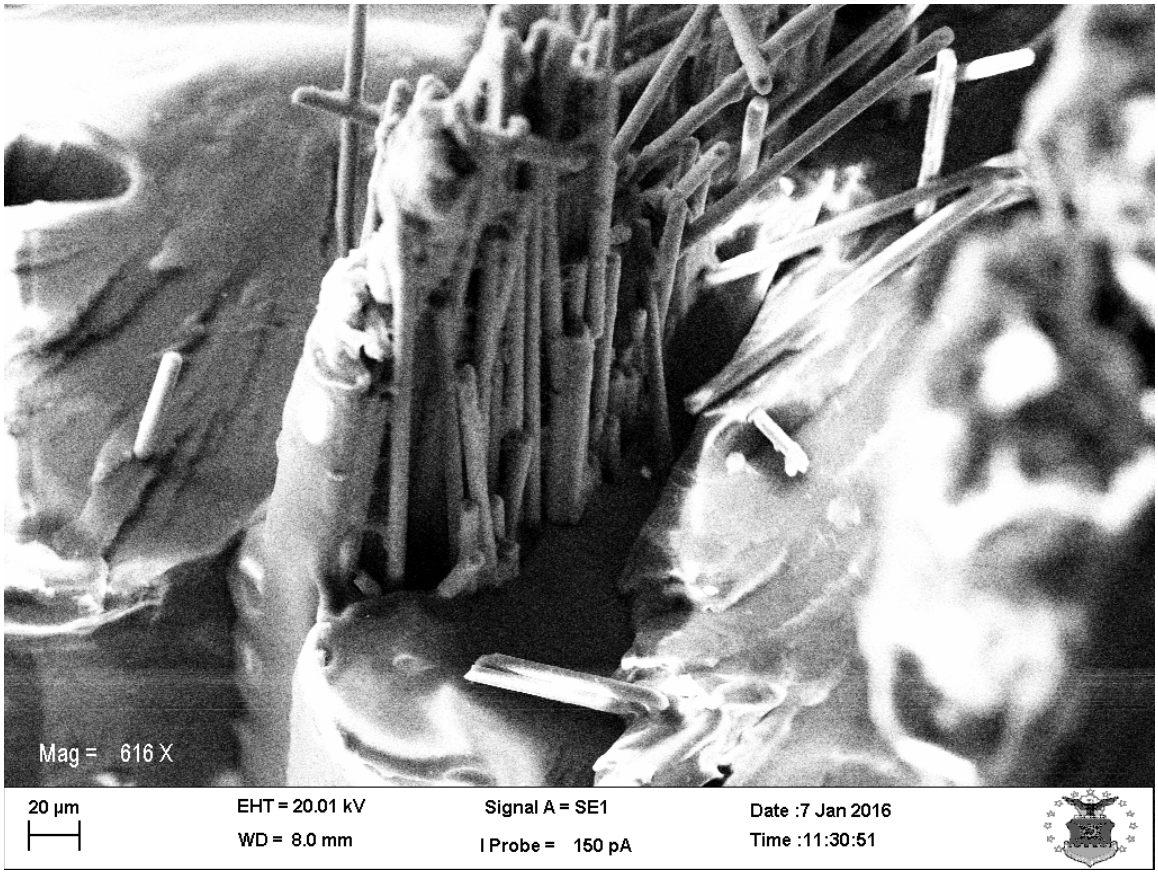

Figure 53. Close-Up View of Individual Carbon Fibers Between Nylon Layers

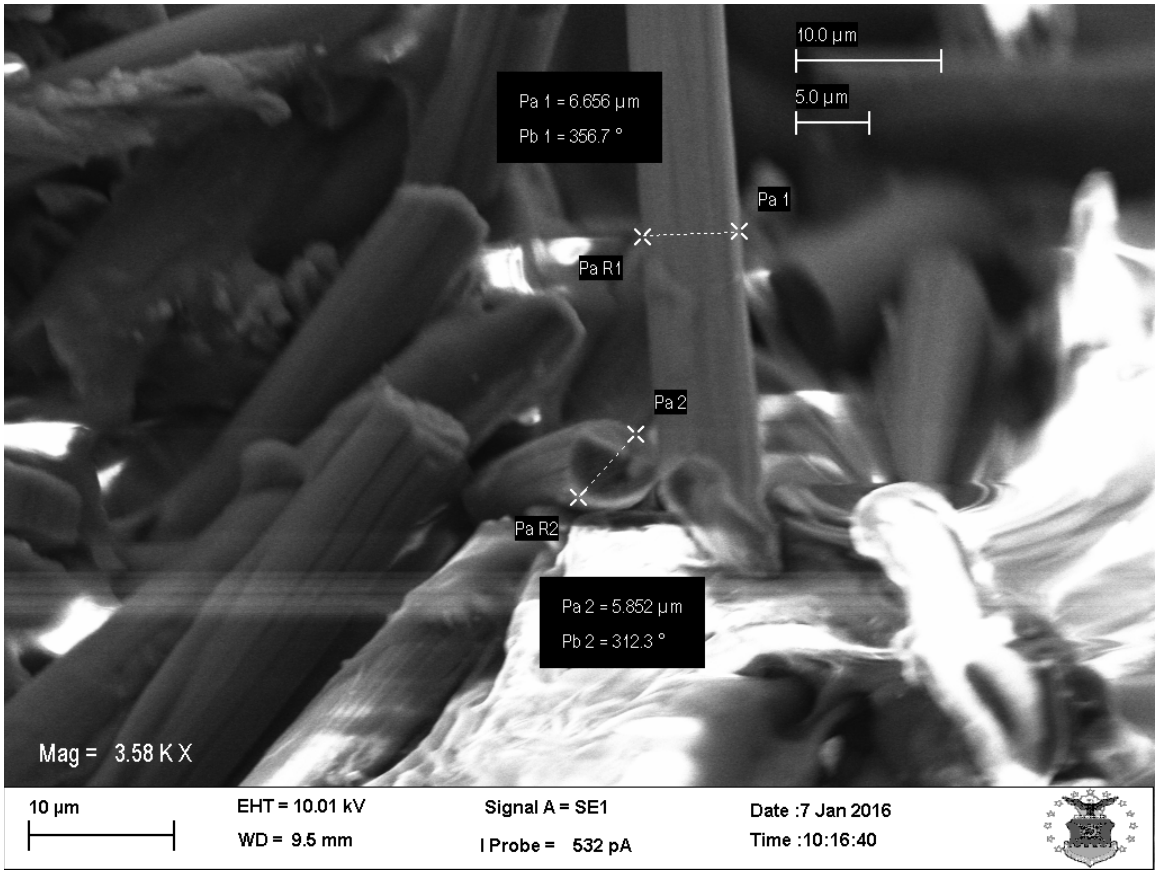

Figure 54. Dimensions of Individual Carbon Fibers from Scanning Electron Microscope

Bibliography

Ahn, S. H., Montero, M., Odell, D., Roundy, S., and Wright, P. K. (2002). Anisotropic material properties of fused deposition modeling ABS. *Rapid Prototyping Journal, 8*(4), 248-257.

Ang, K. C., Leong, K. F., and Chua, C. K. (2006). Investigation of the mechanical properties and porosity relationships in fused deposition modeling-fabricated porous structures. *Rapid Prototyping Journal, 12*(2), 100-105.

Anitha, R., Arunachalam, S., and Radhakrishnan, P. (2001). Critical parameters influencing the quality of prototypes in fused deposition modelling. *Journal of Materials Processing Technology*, 385-388.

ASTM Standard F2792. (2012). *Standard Terminology for Additive Manufacturing Technologies.* ASTM.

Barclift, M. W., and Williams, C. B. (2012). Examining variability in the mechanical properties of parts manufactured via polyjet direct 3D printing. *International Solid Freeform Fabrication Symposium,* (pp. 876-890).

Barnatt, C. (2013). *3D Printing: The Next Industrial Revolution.* Lexington, KY: ExplainingTheFuture.com.

Bertoldi, M., Yardimci, M. A., Pistor, C. M., Guceri, S. I., and Sala, G. (1998). Mechanical characterization of parts processed via fused deposition. *Proc. 9th Solid Freeform Fabrication Symposium,* (pp. 557-565). The University of Texas at Austin, Austin, TX.

Black, S. (2014, May). 3D Printing continuous carbon fiber composites? *High-Performance Composites*.

Brown, R., Davis, J., Dobson, M., and Mallicoat, D. (2014, May-June). 3D Printing, How Much Will It Improve the DoD Supply Chain of the Future? *Defense Acquisition, Technology and Logistics,* 6-10.

Callister, W. D., and Rethwisch, D. G. (2012). *Fundamentals of Materials Science and Engineering: An Integrated Approach.* John Wiley & Sons.

Daniel, I. M., and Ishai, O. (2003). *Engineering Mechanics of Composite Materials* (2nd. ed.). New York: Oxford University Press.

Durgun, I., and Ertan, R. (2014). Experimental investigation of FDM process for improvement of mechanical properties and production cost. *Rapid Prototyping Journal, 20*(3).

Forster, A. M. (2015). *NISTIR 8059: Materials Testing Standards for Additive Manufacturing of Polymer Materials: State of the Art and Standards Applicability.* Gaithersburg, Maryland: National Institute of Standards and Technology.

Gibson, I., Rosen, D. W., and Stucker, B. (2010). Extrusion-based Systems. In *Additive Manufacturing Technologies: Rapid Prototyping to Direct Digital Manufacturing* (pp. 160-186). Springer US.

Griehl, W., and Ruestem, D. (1970). Nylon-12, Preparation, Properties, and Applications. *Industrial and Engineering Chemistry*, *62*(3), 16-22.

Grimm, T. (2004). *User's Guide to Rapid Prototyping.* Society of Manufacturing Engineers.

Hoekstra, N. L., Kraft, B. P., and Newcomer, J. L. (2001). Effect of layer orientation on the mechancial properties of acrylonitrile-butadiene-styrene test specimens produced by fused deposition modeling. *Journal of Injection Molding Technology, 5*(3), 193-199.

Lanzotti, A., Grasso, M., Stainano, G., and Martorelli, M. (2015). The impact of process parameters on mechanical properties of parts fabricated in PLA with an open-source 3-D printer. *Rapid Prototyping Journal*, 604-617.

Lipson, H., and Kurman, M. (2013). *Fabricated: The New World of 3D Printing.* Indianapolis, IN: John Wiley & Sons.

Love, L. J., Kunc, V., Elliot, A., and Blue, C. (2014). The importance of carbon fiber to polymer additive manufacturing. *Journal of Materials Research, 29*(17), 1893-1898.

Martínez, J., Diéguez, J. L., Ares, J. E., Pereira, A., and Pérez, J. A. (2012). Modelization and Structural Analysis of FDM Parts. *The 4th Manufacturing Engineering Society International Conference (MESIC 2011). 1431*, pp. 842-848. American Institute of Physics.

MatWeb, LLC. (2015, Aug 28). Retrieved from MatWeb: Material Property Data: www.matweb.com

McClave, J. T., Benson, G. P., and Sincich, T. (2014). *Statistics for Business and Economics* (12 ed.). Pearson.

Namiki, M., Ueda, M., Todoroki, A., Hirano, Y., and Matsuzaki, R. (2014). 3D printing of continuous fiber reinforced plastic. *Proceedings of SAMPE Seattle.* Seattle, Washington.

Ning, F. D., Cong, W. L., Qiu, J. J., Wei, J. H., and Wang, S. R. (2015). Additive Manufacturing of Carbon Fiber Reinforced Thermoplastic Composites using Fused Deposition Modeling. *Composites Part B: engineering*.

Parsons, D. (2013, May). 3D Printing Provides Fast, Practical Fixes. *National Defense*.

Perry Johnson, Inc. (1987). *Design of Experiments I: A Workbook Based on The Taguchi Method.* Southfield, Michigan.

Rodriguez, J. F., Thomas, J. P., and Renaud, J. E. (2000). Characterization of the mesostructure of the fused-deposition acrylonitrile-butadiene-styrene materials. *Rapid Prototyping Journal, 6*(3), 175-185.

Rodriguez, J. F., Thomas, J. P., and Renaud, J. E. (2003). Design of fused-deposition ABS components for stiffness and strength. *Journal of Mechanical Design, 125*(3), 545-51.

Rodriguez, J. F., Thomas, J. P., and Renaud, J. E. (2003). Mechanical behavior of acrylonitrile butadiene styrene fused deposition materials modeling. *Rapid Prototyping Journal, 9*(4), 219-230.

Roylance, D. (2001, August 23). 3.11 Mechanics of Materials Fall 1999. BY-NC-SA, Creative Commons. Retrieved December 15, 2015, from Massachusetts Institute of Technology: MIT OpenCourseWare: http://ocw.mit.edu/

Rubin, I. I. (Ed.). (1990). *Handbook of Plastic Materials and Technology.* John Wiley & Sons.

Shipp, C. E., and Lafler, K. P. (2012). Proficiency in JMP® Visualization. *SAS Global Forum.* Orlando.

SPI. (1991). *Plastics Engineering Handbook of the Society of the Plastics Industry.* (M. L. Berins, Ed.) New York: Van Nostran Reinhold.

Tadjdeh, Y. (2014). 3D Printing Promises to Revolutionize Defense, Aerospace Industries. *National Defense,* 20-23.

Tadjdeh, Y. (2014, October). Navy Beefs Up 3D Printing Efforts. *National Defense,* 24-26.

Tekinalp, H. L., Kunc, V., Velez-Garcia, G. M., Duty, C. E., Love, L. J., Naskar, A. K., et al. (2014). Highly oriented carbon fiber-polymer composites via additive manufacturing. *Composites Science and Technology, 105,* 144-150.

Tymrak, B. M., Kreiger, M., and Pearce, J. M. (2014). Mechanical properties of components fabricated with open-source 3-D printers under realistic environmental conditions. *Materials and Design, 58,* 242-246.

Ziemian, C., Sharma, M., and Ziemian, S. (2012). Anisotropic Mechanical Properties of ABS Parts Fabricated by Fused Deposition Modelling. In D. M. Gokcek (Ed.), *Mechanical Engineering.* InTech.

REPORT DOCUMENTATION PAGE		*Form Approved OMB No. 0704–0188*
The public reporting burden for this collection of information is estimated to average 1 hour per response, including the time for reviewing instructions, searching existing data sources, gathering and maintaining the data needed, and completing and reviewing the collection of information. Send comments regarding this burden estimate or any other aspect of this collection of information, including suggestions for reducing this burden to Department of Defense, Washington Headquarters Services, Directorate for Information Operations and Reports (0704–0188), 1215 Jefferson Davis Highway, Suite 1204, Arlington, VA 22202–4302. Respondents should be aware that notwithstanding any other provision of law, no person shall be subject to any penalty for failing to comply with a collection of information if it does not display a currently valid OMB control number. PLEASE DO NOT RETURN YOUR FORM TO THE ABOVE ADDRESS.		
1. REPORT DATE (DD–MM–YYYY) 24-03-2016	2. REPORT TYPE Master's Thesis	3. DATES COVERED *(From — To)* Aug 2014 – Mar 2016
4. TITLE AND SUBTITLE Additive Manufacturing Process Parameter Effects on the Mechanical Properties of Fused Filament Fabrication Nylon		5a. CONTRACT NUMBER 5b. GRANT NUMBER 5c. PROGRAM ELEMENT NUMBER
6. AUTHOR(S) Holm, Eric S., Captain, USAF		5d. PROJECT NUMBER 5e. TASK NUMBER 5f. WORK UNIT NUMBER
7. PERFORMING ORGANIZATION NAME(S) AND ADDRESS(ES) Air Force Institute of Technology Graduate School of Engineering and Management 2950 Hobson Way WPAFB OH 45433-7765		8. PERFORMING ORGANIZATION REPORT NUMBER AFIT-ENV-MS-16-M-159
9. SPONSORING / MONITORING AGENCY NAME(S) AND ADDRESS(ES) Naval Postgraduate School 1 University Circle Monterey, CA 93943 Attn: Dr. Keith F. Snider 831-656-3621		10. SPONSOR/MONITOR'S ACRONYM(S) 11. SPONSOR/MONITOR'S REPORT NUMBER(S) NPS-BAA-14-002
12. DISTRIBUTION / AVAILABILITY STATEMENT Distribution Statement A. Approved for Public Release; Distribution Unlimited		
13. SUPPLEMENTARY NOTES This work is declared a work of the U.S. Government and is not subject to copyright protection in the United States.		
14. ABSTRACT The purpose of this research was to determine how varying Fused Filament Fabrication (FFF) process parameters affect the mechanical properties of PA6 nylon dog-bone specimens produced on the Mark One 3D Printer. A design of experiment (DOE) was conducted using the factors of layer height and raster angle orientation. The mechanical properties measured in the experiment were tensile modulus, yield stress, percent strain at yield, ultimate tensile strength and percent strain at break. An analysis of variance (ANOVA) was performed to identify which factors were statistically significant in influencing mechanical properties. Results of the ANOVA showed that layer height was significant in influencing tensile modulus, ultimate tensile strength and percent strain at break; raster angle orientation was significant in influencing tensile modulus, yield stress, percent strain at yield, and percent strain at break. Both tensile modulus and ultimate tensile strength increased with decreasing layer height. The optimal condition that maximizes stiffness and strength is a layer height of 0.1 mm and a (±45) raster angle orientation.		
15. SUBJECT TERMS Additive Manufacturing, Design of Experiment, Fused Filament Fabrication, Mechanical Properties, Nylon		

16. SECURITY CLASSIFICATION OF:			17. LIMITATION OF ABSTRACT	18. NUMBER OF PAGES	19a. NAME OF RESPONSIBLE PERSON
a. REPORT	b. ABSTRACT	c. THIS PAGE			Major Vhance V. Valencia, PhD, USAF
U	U	U	UU	119	19b. TELEPHONE NUMBER (Include Area Code) (937) 255-3636 x4823 (vhance.valencia@afit.edu)

Standard Form 298 (Rev. 8–98)
Prescribed by ANSI Std. Z39.18